

**SOFT ANALYZER FOR NO_x EMISSIONS APPLICATION
ON CGTG IN COGENERATION PLANT**

BY

ALI A. AL-MALAK

A Thesis Presented to the
DEANSHIP OF GRADUATE STUDIES

KING FAHD UNIVERSITY OF PETROLEUM & MINERALS

DHAHRAN, SAUDI ARABIA

In Partial Fulfillment of the
Requirements for the Degree of

MASTER OF SCIENCE

In

SYSTEMS ENGINEERING

May 2014

KING FAHD UNIVERSITY OF PETROLEUM & MINERALS

DHAHRAN- 31261, SAUDI ARABIA

DEANSHIP OF GRADUATE STUDIES

This thesis, written by Ali A. Al-Malak under the direction of his thesis advisor and approved by his thesis committee, has been presented and accepted by the Dean of Graduate Studies, in partial fulfillment of the requirements for the degree of **MASTER OF SCIENCE IN SYSTEMS ENGINEERING**.

Thesis Committee:



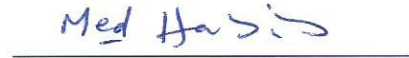
Dr. Fouad M. Al-Sunni
Department Chairman



Dr. Moustafa Elshafei
(Advisor)



Dr. Salam A. Zummo
Dean of Graduate Studies



Dr. Mohamed A. Habib
(Member)

29/5/14
Date



Dr. Fouad M. Al-Sunni
(Member)

© Ali A. Al-Malak

2014

I dedicate this work in memory to the soul of my dear father for his sincere love and unlimited support that paved the roads towards success in life

ACKNOWLEDGMENTS

In the name of Allah, the Most Beneficent, the Most Merciful

All praise and glory goes to Almighty Allah (the Powerful and Exalted in Might) who gave me the courage and patience to carry out this work. Peace and blessings of Allah be upon his last prophet Mohammad (PBUH), his family and his companions.

My heartfelt appreciation and gratitude goes to my parents who were, after Allah, the source of success in my life. I was carried through the most difficult moments in my life by my mother continuous prayers, love, and support. Also, I would like to extend my heartfelt appreciation to my wife and children who shared with me all the difficult moments before the nice ones, the one whose unlimited support, keen understanding, patience, and love enabled me to complete this work.

I would like to express special thanks and appreciation to my thesis advisor, Dr. Mustafa Elshafei, for his invaluable help and advice. I acknowledge his efforts, encouragement, support, valuable time, patience, and guidance, and particularly his critical review of the thesis at every stage.

I extend gratitude to my thesis committee members, Dr. Mohamed Habib and Dr. Fouad Al-Sunni for their interest, cooperation, guidance, and insightful feedback.

I am also thankful to all the Systems Engineering faculty and staff members for their kind support and cooperation. The support and facilities provided by King Fahed University of Petroleum and Minerals for completing this work are highly appreciated.

Finally, thanks are due to all of my friends and colleagues for their moral support, good wishes and the memorable days shared together; special thanks are extended to my friend Khalid E. Al-Khater.

TABLE OF CONTENTS

ACKNOWLEDGMENTS	V
TABLE OF CONTENTS.....	VII
LIST OF TABLES.....	X
LIST OF FIGURES.....	XI
LIST OF ABBREVIATIONS.....	XIII
ABSTRACT.....	XVI
ملخص الرسالة.....	XVIII
CHAPTER 1 INTRODUCTION.....	1
1.1 Cogeneration technology	3
1.1.1 Steam turbine cogeneration	6
1.1.2 Gas turbine cogeneration system	8
1.1.3 Combined steam/gas based cogeneration system.....	12
1.1.4 Reciprocating engine based cogeneration system.....	14
1.2 NO _x Formation process	16
1.2.1 Zeldovich Mechanism.....	16
1.2.2 Prompt Mechanism	17
1.2.3 Nitrous Oxide Mechanism	17
1.2.4 Fuel-Bound Nitrogen Mechanism	18
1.3 Environmental & Health Impact of NO _x	18
1.3.1 Environmental acidification.....	18
1.3.2 Stratospheric ozone depletion.....	19

1.3.3	Health problems	19
1.4	NO _x Measurement techniques	20
CHAPTER 2 LITERATURE REVIEW		22
CHAPTER 3 COGENERATION PLANT UNDER STUDY		46
3.1	Process description	46
3.2	Combustion Gas Turbine Generator (CGTG)	47
3.3	GE DLN-2.6 Combustion system	49
3.3.1	DLN-2 Fuel system	53
3.3.2	DLN-2.6 Combustion modes	55
3.3.3	DLN-2.6 Combustor NO _x emissions	60
CHAPTER 4 ARTIFICIAL NEURAL NETWORKS		62
4.1	ANN Applications	63
4.2	ANN Characteristics	65
4.3	Biological and artificial neurons	66
4.4	Feed Forward Back Propagation Neural Network (FFBPNN)	68
4.5	Adaptive Neuro Fuzzy Inference System (ANFIS)	75
CHAPTER 5 NO_x EMISSION MODELING		80
5.1	Process data analysis	80
5.1.1	Sensitivity analysis	81
5.1.2	Process data correlation with NO _x	84
5.2	ANFIS Modelling	86
5.2.1	ANFIS model with six inputs (X*X*X*X*X*X)	88
5.2.2	ANFIS with five inputs (X*X*X*X*X):	93
5.2.3	ANFIS with four inputs (X*X*X*X):	104

5.3	FFBPNN Modelling	109
5.3.1	FFBPNN with ten inputs.....	109
5.3.2	FFBPNN with six inputs.....	113
5.3.3	FFBPNN with five inputs	117
5.3.4	FFBPNN with four inputs	121
5.4	Results and Discussion	126
CHAPTER 6 CONCLUSION.....		144
REFERENCES.....		146
VITAE.....		150

LIST OF TABLES

Table 1	Literature Modeling Approach and Application.....	41
Table 2	Process data ranges during start up.	80
Table 3	Strength of relationship corresponding to correlation coefficient ρ	84
Table 4	Correlation coefficient for process variables	85
Table 5	FFBPNN (10 inputs) modeling results.	110
Table 6	FFBPNN (10-42-1) modeling results	111
Table 7	FFBPNN (6 inputs) modeling results	114
Table 8	FFBPNN (6-42-1) modeling results	115
Table 9	FFBPNN (5 inputs) modeling results	118
Table 10	FFBPNN (5-26-1) modeling results	119
Table 11	FFBPNN (4 inputs) modeling results	122
Table 12	FFBPNN (4-45-1) modeling results	123
Table 13	ANFIS modeling for Designing NO _x PEMS	126
Table 14	FFBPANN modeling for Designing NO _x PEMS	129
Table 15	Performance Comparison between FFBPNN & ANFIS models.....	132
Table 16	Comparison between FFBPNN & ANFIS modeling.....	133

LIST OF FIGURES

Figure 1	Backpressure steam turbine based cogeneration system	6
Figure 2	Extraction-cum-condensing steam turbine based cogeneration system.....	7
Figure 3	Gas turbine based cogeneration system with supplementary fired WHRB ..	10
Figure 4	Reciprocating engine based cogeneration system with unfired WHRB	15
Figure 5	NOX Analyzer (Sick-Maihak model GM31)	21
Figure 6	Gas turbine generator assembly	48
Figure 7	DLN-2.6 Combustor fuel nozzles.....	49
Figure 8	Cap assembly-view from downstream	50
Figure 9	DLN-2.6 Combustor.....	51
Figure 10	DLN-2 Fuel nozzle cross-section	52
Figure 11	DLN-2 Combustor fuel streams	53
Figure 12	DLN-2.6 Fuel system control valves.....	55
Figure 13	DLN-2.6 Fuel flow scheduling.....	55
Figure 14	DLN-2.6 Fuel nozzles arrangement	58
Figure 15	DLN-2.6 Loading sequence.....	60
Figure 16	Temperature profile in CGTG	61
Figure 17	Biological neuron	67
Figure 18	Artificial neuron	68
Figure 19	Multi-layer Feed Forward Neural Network.....	69
Figure 20	Information processing in a neural network.....	69
Figure 21	Feed Forward with multiple hidden slabs architecture.....	73
Figure 22	ANFIS architecture.....	77
Figure 23	Process data in direct proportionality with NO _x formation	81
Figure 24	Inverse proportionality of Air/Fuel Ratio with NO _x formation	82
Figure 25	Constant process data with no clear influence on NO _x formation	83
Figure 26	Process data with no clear correlation with NO _x	84
Figure 27	ANFIS (2*2*2*2*2*2) model.....	89
Figure 28	ANFIS (3*3*3*3*3*3) model.....	89
Figure 29	ANFIS (2*2*2*2*12*2) model.....	90
Figure 30	ANFIS (2*3*2*2*3*2) model.....	92
Figure 31	ANFIS (2*4*2*2*4*2) model.....	92
Figure 32	ANFIS (2*2*2*2*2) model with O ₂	94
Figure 33	ANFIS (3*3*3*3*3) model with O ₂	95
Figure 34	ANFIS (2*2*2*2*12) model with O ₂	96
Figure 35	ANFIS (2*3*2*2*3) model with O ₂	97
Figure 36	ANFIS (2*4*2*2*4) model with O ₂	98
Figure 37	ANFIS (2*2*2*2*2) model with relative humidity.	99
Figure 38	ANFIS (3*3*3*3*3) model with relative humidity.	100
Figure 39	ANFIS (2*2*2*12*2) model with relative humidity.	101

Figure 40	ANFIS (2*3*2*3*2) model with relative humidity.	102
Figure 41	ANFIS (2*4*2*4*2) model with relative humidity.	103
Figure 42	ANFIS (2*2*2*2) model.	105
Figure 43	ANFIS (3*3*3*3) model.	105
Figure 44	ANFIS (4*4*4*4) model.	106
Figure 45	ANFIS (2*2*2*12) model.	107
Figure 46	ANFIS (2*8*2*8) model.	108
Figure 47	FFBPNN (10-42-1) Performance at different epochs number.	111
Figure 48	FFBPNN (10-42-1) Error Histogram.	112
Figure 49	FFBPNN (10-42-1) Regression test.	113
Figure 50	FFBPNN (6-42-1) Performance at different epochs number.	116
Figure 51	FFBPNN (6-42-1) Error Histogram.	116
Figure 52	FFBPNN (6-42-1) Regression test.	117
Figure 53	FFBPNN (5-26-1) Performance at different epochs number.	120
Figure 54	FFBPNN (5-26-1) Error Histogram.	120
Figure 55	FFBPNN (5-26-1) Regression test.	121
Figure 56	FFBPNN (4-45-1) Performance at different epochs number.	124
Figure 57	FFBPNN (4-45-1) Error Histogram.	124
Figure 58	FFBPNN (4-45-1) Regression test.	125
Figure 59	ANFIS models performance in reference to target output.	127
Figure 60	FFBPNN models performance in reference to target output.	130
Figure 61	ANFIS (4 inputs-2*2*2*12) Regression test.	134
Figure 62	ANFIS (5 inputs-2*2*2*2*2) Regression test.	135
Figure 63	ANFIS (6 inputs-2*2*2*2*2*2) Regression test.	136
Figure 64	FFBPNN (4-45-1) Regression test.	138
Figure 65	FFBPNN (5-26-1) Regression test.	139
Figure 66	FFBPNN (6-42-1) Regression test.	140
Figure 67	FFBPNN (10-42-1) Regression test.	142

LIST OF ABBREVIATIONS

ABC	:	Artificial Bee Colony
AI	:	Artificial Intelligence
ANFIS	:	Adaptive Neuro Fuzzy Inference System
ANN	:	Artificial Neural Network
BPNN	:	Back Propagation Neural Network
CAAA	:	Clean Air Act Amendment
CEMS	:	Continues Emission Monitoring System
CFD	:	Computational Fluid Dynamics
CGTG	:	Combustion Gas Turbine Generator
CHP	:	Combined Heat & Power
CNN	:	Cascading Neural Network
DLN	:	Dry Low NO _x
DLP	:	Distributed Logic Process
DRNN	:	Dynamic Recurrent Neural Network
DS	:	Dynamic Systems
ELM	:	Extreme Learning Machine

EPA	:	Environmental Protection Agency
FBN	:	Fuel Bounded Nitrogen
FCRNN	:	Fully Connected Recurrent Neural Network
FL	:	Fuzzy Logic
FFBPNN	:	Feed Forward Back Propagation Neural Network
FFMLPNN	:	Feed Forward Multi-Layer Perceptron Neural Network
GA	:	Genetic Algorithm
GE	:	General Electric
GRNN	:	General Regression Neural Network
HRSG	:	Heat Recovery Steam Generator
IGV	:	Inlet Guide Vanes
LS-SVM	:	Least Square-Support Vector Machine
MFNN	:	Multilayer Feed Forward Neural Network
MGT	:	Micro Gas Turbine
NIEHS	:	National Institute of Environmental Health Sciences
NLPCA	:	Non Linear Principle Component Analysis
NNPLS	:	Neural Network Partial Least Square

NO _x	:	Nitrogen Oxides
NSGA	:	Non-dominated Sorting Genetic Algorithm
PEMS	:	Predictive Emissions Monitoring System
PM	:	Pre-Mix
PPMVD	:	Parts Per Million Volumetric Dry
RATA	:	Relative Accuracy Test Audit
WHRB	:	Waste Heat Recovery Boiler

ABSTRACT

Full Name : Ali A. Al-Malak
Thesis Title : Soft Analyzer for NO_x Emissions Applications on CGTG in
Cogeneration Plant
Major Field : Systems and Control Engineering
Date of Degree : May 2014

Many industrial sectors built cogeneration plants to reliably secure their power supplies, and efficiently produce the plant demand of steam through the associated heat. Due to the rise of fuel cost and tightening environmental regulations, the number of cogeneration plants is increasing in lieu to individual boilers and steam turbine generators. Most of the recent cogeneration plants are equipped with hardware-based analyzer which is a Continuous Emission Monitoring System (CEMS) to monitor the NO_x emissions from the plant stack as per EPA regulations. The CEMS is unreliable and subjected to high failure rates, require high capital cost, high maintenance cost, high operational cost, subject to long lag time, and slow response. In this work a software-based analyzer was designed which is the Predictive Emission Monitoring System (PEMS) by applying Artificial Neural Networks (ANN) on process data collected from a cogeneration plant (156 MW X 2 CGTGs) equipped with CEMS for NO_x monitoring. The developed PEMS can be used as a reliable tool to monitor the NO_x emissions and verify the existing CEMS readings that will be eventually demolished. By providing a relationship between the process variables and the emissions, PEMS will also assist in understanding the NO_x behavior in reference to the process variations and thus enables better emission control.

In fact two approaches in NN were tested to develop and decide the final model based on the obtained performance. Both ANFIS and FFBPNN approaches went through many experiments at different number of process inputs and structural design parameters. Throughout the entire course of experiments it was found that the FFBPNN model outperforms the ANFIS model. Also, it was found increasing the number of inputs to ANFIS model will degrade its performance in addition to complicating the model structure and increasing the computational time. However, in FFBPNN model, the performance enhanced slightly. Based on that, it was concluded that FFBPNN model with four inputs (Load, Steam flow, Firing temperature, and A/F) shall be selected as the final PEMS model with the consideration of decreasing the number of inputs decreases the points of failure of the model.

ملخص الرسالة

الاسم الكامل: علي عبدالله علي الملك

عنوان الرسالة: محلل حاسوبي لقياس تركيز إنبعاثات أكاسيد النيتروجين من المولدات التوربينية في محطة التوليد المزدوج للطاقة

التخصص: هندسة النظم و التحكم

تاريخ الدرجة العلمية: رجب 1435 هجرية

أنشأت العديد من القطاعات الصناعية محطات التوليد المزدوج للطاقة لتأمين امدادات الطاقة بموثوقية وإنتاج البخار المطلوب للمصنع بكفاءة من خلال الحرارة المرافقة. وبسبب إرتفاع تكلفة الوقود وتشديد الأنظمة البيئية ، فإن عدد محطات التوليد المزدوج للطاقة في إزدیاد على حساب الغلايات والمولدات التوربينية البخارية المفردة. إن معظم محطات التوليد المشترك للطاقة الحديثة مزودة بجهاز تحليل للغازات الذي يعرف بنظام مراقبة الانبعاثات المستمر (CEMS) لمراقبة انبعاثات أكاسيد النيتروجين من مدخنة المصنع وفقا للوائح وكالة حماية البيئة . ونظام (CEMS) غير موثوق وعرضة لمعدلات فشل عالية، تتطلب تكلفة رأس مال مرتفعة وتكلفة صيانة و تشغيل عالية، و تخضع لتأخر العينات لوقت طويل، و بطء الإستجابة. في هذا العمل تم تصميم محلل حاسوبي يعرف بنظام مراقبة الإنبعاثات التنبؤي (PEMS) من خلال تطبيق الشبكات العصبية الاصطناعية (ANN) على بيانات العمليات التي تم جمعها من محطة توليد مزدوج للطاقة (156 ميغاواط في 2 مولدة توربينية) المزودة بنظام (CEMS) لمراقبة أكاسيد النيتروجين. سيتم استخدام نظام (PEMS) كأداة موثوقة لمراقبة انبعاثات أكاسيد النيتروجين ولتحقق من قراءات جهاز (CEMS) القائم الذي سيتم الإستغناء عنه في نهاية المطاف. و من خلال إيجاد علاقة بين متغيرات العمليات التشغيلية و الانبعاثات، نظام (PEMS) سيساعد أيضا في فهم سلوك أكاسيد النيتروجين للمتغيرات في العمليات التشغيلية، وبالتالي يمكن التحكم

بالأنبعاثات بشكل أفضل. في الواقع تم اختبار نهجين في الشبكات العصبية (NN) لتطوير و تقرير النموذج النهائي استنادا إلى الأداء التي تم الحصول عليه. تم إجراء العديد من التجارب لكلا النهجين (ANFIS) و (FFBPNN) باستخدام مدخلات عملية بأعداد مختلفة وتصاميم هيكلية متعددة. من خلال جميع التجارب، تبين أن أداء النموذج (FFBPNN) يتفوق على نموذج (ANFIS). أيضا ، نجد أن زيادة عدد المدخلات إلى نموذج (ANFIS) يضعف أدائها بالإضافة إلى تعقيد هيكل النموذج وزيادة الوقت الحسابي. وعلى عكس ذلك، في نموذج (FFBPNN) تعزز الأداء قليلا. بناء على ذلك ، تم الأستنتاج أن نموذج (FFBPNN) مع أربعة مدخلات (الحمولة ، وتدفق البخار، درجة حرارة الإحتراق، و معدل الهواء للوقود) ينبغي اختياره كنموذج (PEMS) النهائي مع الإعتبار أن خفض عدد المدخلات يقلل من نقاط فشل النظام.

CHAPTER 1

INTRODUCTION

Many industrial sectors built cogeneration plants to secure their power supplies reliably and efficiently produce the plant demand of steam through the associated heat. Due to the rise of fuel cost and tightening environmental regulations, the number of cogeneration plants will increase in lieu to individual boilers and steam turbine generators. Most of the recent cogeneration plants are equipped with hardware-based analyzer which is the Continuous Emission Monitoring System (CEMS) to monitor the NO_x emissions from the plant stack as per EPA regulations. The CEMS is unreliable and subjected to high failure rates, require high capital cost, high maintenance cost, high operational cost, subject to long lag time, and slow response. In this work a software-based analyzer was designed which is the Predictive Emission Monitoring System (PEMS) by applying Artificial Neural Networks (ANN) on process data collected from cogeneration plant (156 MW X 2 CGTGs) equipped with CEMS for NO_x monitoring. Two ANNs approaches were evaluated; the Feed Forward Back Propagation Neural Network (FFBPNN) and the Adaptive Neuro Fuzzy Inference System (ANFIS). The developed PEMS can be used to verify the existing CEMS readings and used as reliable tool to monitor the NO_x emissions. By providing a relationship between the process and the emissions, PEMS will also assist in understanding the NO_x behavior in reference to the process variations and thus enables better emission control.

The main objective of this thesis is to develop a PEMS for NO_x generated from Combustion Gas Turbine Generators. The modeling approach is through applying ANFIS and FFBPNN systems. The specific objectives are:

- Critical review of the past research in the field of combustion NO_x modeling.
- Develop NO_x prediction model by ANFIS using industrial process data.
- Develop NO_x prediction model by FFBPNN using industrial process data.
- Compare the results obtained from the developed models and recommend the best model structure for NO_x prediction.

In the next sections under this introductory chapter the cogeneration technology is discussed. Followed by a significant discussion on the NO_x formation in combustion processes, highlights on the impact of NO_x on environment and health, and the NO_x measurement techniques. In chapter 2, a literature review in the area of PEMS is presented at which it was found no much work have been done in developing NO_x PEMS system in the cogeneration plants and the focus was in the boilers and furnaces.

The cogeneration plant under study is discussed under chapter 3; at which brief process description is provided followed by detailed description of the Dry Low NO_x burner (GE DLN-2.6). In chapter 4, the Artificial Neural Networks is discussed with focus on FFBPNN and ANFIS. Detailed NO_x modeling and comparison are presented in chapter 5. Finally, the conclusion and future work is addressed in chapter 6.

1.1 Cogeneration technology

Cogeneration first appeared in late 1880s in Europe and in the U.S.A. during the early years of the 20th century, when most industrial plants generated their own electricity using coal-fired boilers and steam-turbine generators. Many of the plants used the exhaust steam for industrial processes.

When central electric power plants and reliable utility grids were constructed and the costs of electricity decreased, many industrial plants began purchasing electricity and stopped producing their own. Other factors that contributed to the decline of industrial cogeneration were the increasing regulation of electric generation, low energy costs which represent a small percentage of industrial costs, advances in technology such as packaged boilers, availability of liquid or gaseous fuels at low prices, and tightening environmental restrictions.

The utilization of cogeneration started to increase after the first dramatic rise of fuel costs in 1973. Systems that are efficient and can utilize alternative fuels have become more important in the face of price rises and uncertainty of fuel supplies. In addition to decreased fuel consumption, cogeneration results in a decrease of pollutant emissions. For these reasons, governments in Europe, U.S.A., South East Asia and Japan are taking an active role in the increased use of cogeneration.

Cogeneration is the simultaneous generation and utilization of fuel energy in different forms at optimum efficiency through cost-effective and environmental-friendly operational process. Cogeneration systems primarily generate electricity and utilize the associated heat to support the operation of facility processes such as steam generation.

All continuous process plants such as fertilizers, petrochemicals, hydrocarbon refineries, paper and pulp manufacturing units, food processing, dairy plants, pharmaceuticals, sugar mills, etc always require uninterrupted supply of electric power and steam to sustain the critical operational processes.

Small continuous process chemical industrial units generally depend on the grid power, while generating process steam through conventional fired industrial boilers. Large and medium scale chemical industries can implement cogeneration systems to meet their requirement of essential energy inputs (power and steam) and achieve better availability, reliability and economics of the plant operations.

Due to the rise of fuel cost and tightening environmental regulations, the number of cogeneration plants is increasing in lieu to individual boilers and steam turbine generators. Cogeneration technology uses different combinations of power and heat producing equipment, which are numerous.

A proper selection of a cogeneration system configuration, from a few basic system configurations described below, makes it feasible to produce first either electrical energy or thermal energy. (Energy Efficiency Office, 1992)

- a. Steam turbine based cogeneration system
- b. Gas turbine based cogeneration system
- c. Combined steam/gas turbine based cogeneration system
- d. Reciprocating engine based cogeneration system

Most widely used cogeneration systems in the chemical process industrial plants are based on steam turbine, gas turbine or combined steam/gas turbine configurations with installations based on reciprocating engine configuration in moderate number. These configurations are widely accepted by the industries due to their proven track record and easy commercial availability of required equipment.

All combinations of cogeneration systems are based on the First and Second Laws of Thermodynamics. Basic concepts of possible different configurations of cogeneration systems, consisting of a primary energy source, a prime mover driven electric power generator and arrangement to use the waste heat energy rejected from the prime mover, are briefly described along with the system schematic diagrams.

1.1.1 Steam turbine cogeneration

This system works on the principle of Rankine cycle of heat balance. In Rankine cycle, the fuel is first fired in a suitable boiler to generate high-pressure steam at predetermined parameters. The produced steam is then expanded through a steam turbine to produce mechanical power, electricity and a low-pressure steam. The steam turbine could be of backpressure type, extraction-cum-condensed type or extraction-cum-back pressure type depending on different levels and parameters at which the steam is required by the chemical process in that particular plant. Cogeneration system with backpressure steam turbine is schematically represented in Figure 1.

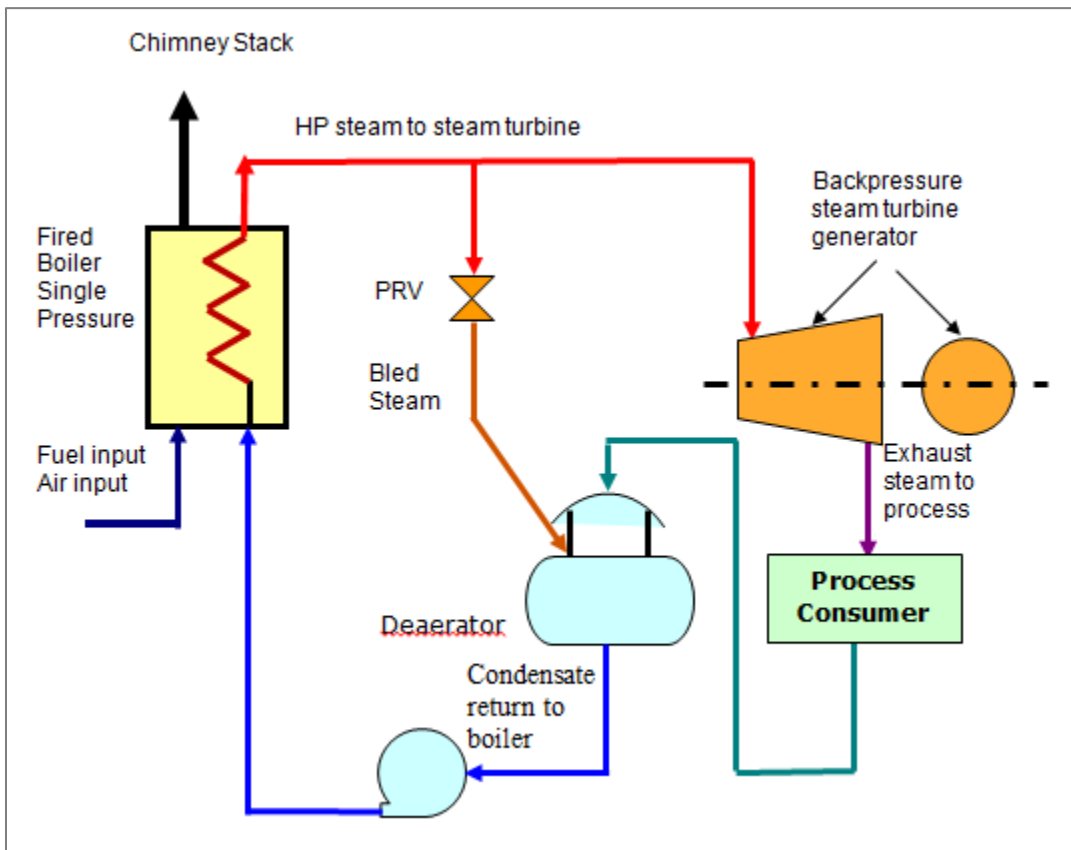


Figure 1 Backpressure steam turbine based cogeneration system

In a conventional fossil fuel fired power plant, maximum fuel efficiency of about 35% is achieved. Maximum heat loss occurs by way of the heat rejection in a steam condenser where a straight condensing steam turbine is used. Some improvement in the efficiency could be attained through extraction-cum-condensing steam turbine instead of straight condensing type as shown in Figure 2. The steam so extracted could be supplied to either process consumer or to heat the feed water before it enters into boiler. As seen from above, the rejected heat energy from the steam turbine is most efficiently used to meet the thermal energy requirement of that particular chemical process by adopting non-condensing steam turbine based cogeneration system. The overall efficiency of around 80-85% is achieved in this type of plant configuration.

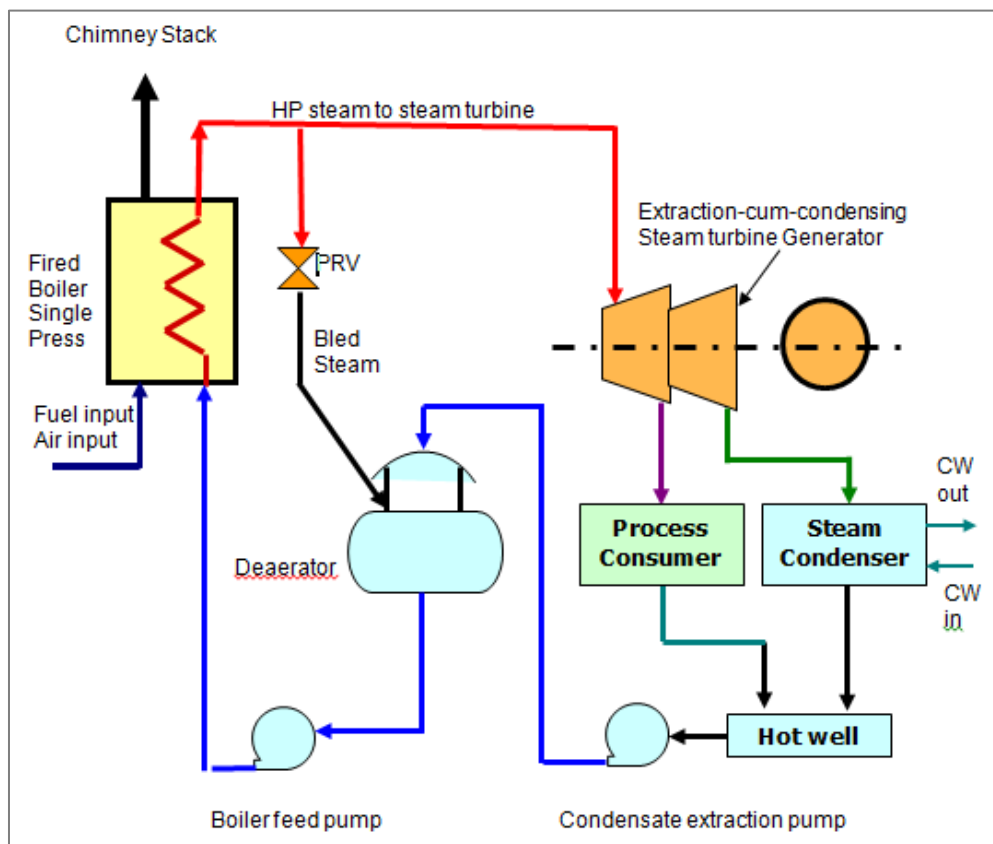


Figure 2 Extraction-cum-condensing steam turbine based cogeneration system

The selection of steam turbine for a particular cogeneration application depends on process steam demand at one or more pressure/temperature levels, the electric load to be driven, power and steam demand variations, essentiality of steam for process, etc. The steam to power ratio also plays a role in selection of the steam turbine. Generation of very high-pressure steam and low back pressure at steam turbine exhaust would result into small steam to power ratio. Smaller value of ratio would indicate the lower utilization value of steam for heating or process purpose. The flexibility in steam to power ratio can be obtained by using steam turbines with regulated extraction.

Steam turbine based cogeneration systems can be fired with variety of fossil fuels like coal, lignite, furnace oil, residual fuel oil, natural gas or non-conventional fuels like biogas, bagasse, municipal waste, husk, etc. Hence, the fuel flexibility for this type of system is excellent. However, this configuration is not recommended for smaller installations as it is more expensive and maintenance oriented. It is also not feasible to adopt this system if the chemical industry is located nearer to a populated area, as it becomes a major source of environmental pollution depending upon type of fuel used, i.e. coal, lignite or furnace oil.

1.1.2 Gas turbine cogeneration system

This type of system works on the basic principle of Bryton cycle of thermodynamics. Air drawn from the atmosphere is compressed and mixed in a predetermined proportion with the fuel in a combustor, in which the combustion takes place. The flue gases with a very

high temperature from the combustor are expanded through a gas turbine, which drives electric generator and air compressor. A portion of mechanical power is used for compression of the combustion air: the balance is converted into electric power. The exhaust flue gases from the gas turbine, typically at a high temperature of 480-540 °C, acts as a heat source from which the heat is recovered in the form of steam or hot air for any desired industrial application.

Industrial gas turbine based power plants installed to generate only electric power operate at the thermal efficiency of 25-35% only depending of type and size of gas turbine. Aero derivative gas turbines operate at marginal higher efficiency than the conventional industrial heavy-duty machines. With recovery of heat in exhaust flue gases in a waste heat recovery boiler (WHRB) or heat recovery steam generator (HRSG) to generate the steam, overall plant efficiency of around 85-90% is easily achieved. As an alternative, the heat of exhaust flue gases can also be diverted to heat exchanger to generate hot water or hot air. Figure 3 shows a schematic of Gas Turbine based cogeneration system.

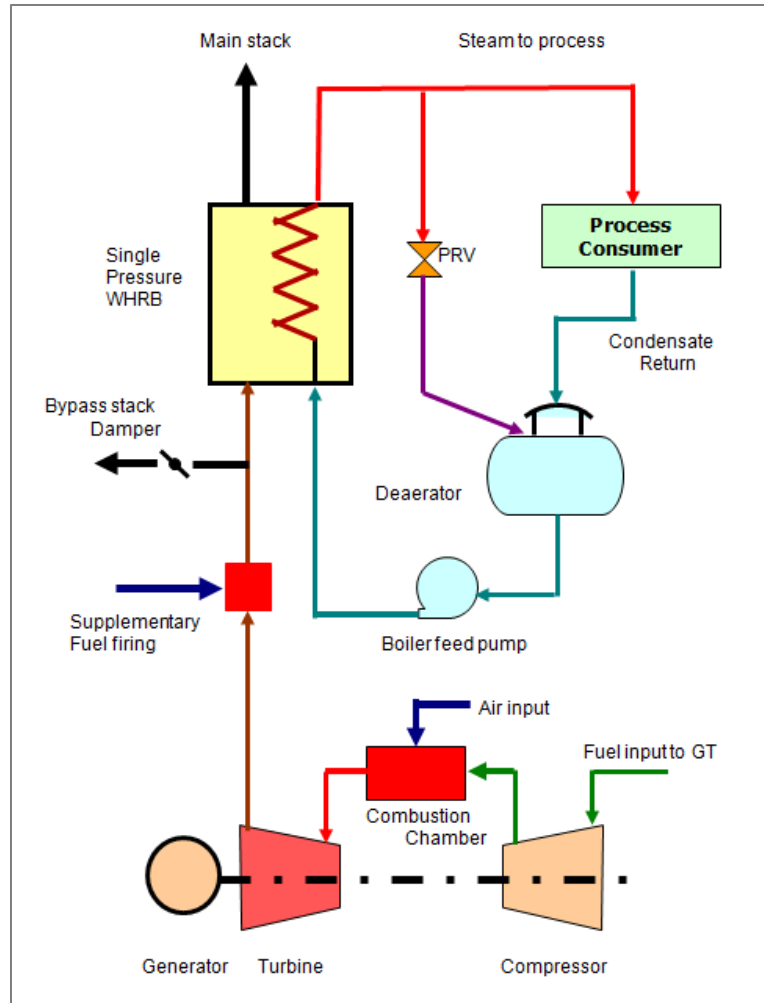


Figure 3 Gas turbine based cogeneration system with supplementary fired WHRB

Compared to steam turbine based cogeneration system, the gas turbine based cogeneration system is ideal for the chemical process industries where the demand of steam is relatively high and fairly constant in comparison to that of power demand.

Gas turbine based cogeneration system gives a better performance with clean fuels like natural gas, or non-ash bearing or low ash bearing liquid hydrocarbon fuels like Naphtha,

High speed diesel, etc. Though high ash bearing hydrocarbon based fuels like fuel oil, crude oil or residual fuel oil can also be fired in the gas turbines, but with some inherent problems like frequent cleaning of gas turbine, more maintenance and spares, etc.

Another major drawback is that when the demand of power drops below 80% of gas turbine capacity, the specific fuel consumption increases and the steam output from WHRB also drops. The steam output can be maintained by resorting to a supplementary fuel firing in WHRB. The burners for supplementary firing are generally installed in the exhaust flue duct provided between the gas turbine and WHRB, and are designed to enable WHRB to maintain full steam output even when the gas turbine is partly loaded. This system ensures a high flexibility in design and operation of the plant, as it is possible to widely vary ratio of steam to power loads without very much affecting the overall plant efficiency. In case of exhaust duct based supplementary firing, the fuel requirement is substantially reduced proportionate to additional steam generated due to presence of about 15% hot unburned Oxygen in exhaust flue gases.

The gas turbine based cogeneration scheme with the supplementary-fired WHRB, with firing in duct between gas turbine and WHRB, is shown in Figure 3. If supplementary firing is not provided, it becomes a simple cogeneration system consisting of gas turbine generator and WHRB.

1.1.3 Combined steam/gas based cogeneration system

It is clear from the title of system itself that it works on the basis of combination of both Rankine and Bryton cycles, and hence it is called combined steam/gas turbine based cogeneration system. In this system, fuel energy is first utilized in operating the gas turbine as described in Gas turbine based cogeneration system. Waste heat of high temperature exhaust flue gases from the gas turbine is recovered in WHRB to generate a high-pressure steam. This high-pressure steam is expanded through a back-pressure steam turbine, or an extraction-cum-back pressure steam turbine, or an extraction-cum-condensing steam turbine to generate some additional electric power. The low-pressure steam available either from the exhaust of back-pressure steam turbine or from extraction is supplied to the process consumer. Such combination of two cycles gives a definite thermodynamic advantage with very high fuel utilization factor under various operating conditions.

When the ratio of electrical power to thermal load is high, the cogeneration plant based on combined cycle principle provides better results than the plant based on only back pressure steam turbine due to availability of additional power from steam turbine, besides low pressure steam, without firing of any extra fuel. If supplementary firing is resorted to in WHRB, as mentioned in case of Gas Turbine based system, to maintain steam supply during low loads on gas turbine, the operational flexibility of such plants can be brought nearer to extraction-cum-condensing steam turbine.

The process in which the demand of electricity remains very high even when the demand of steam is very low, then extraction-cum-condensing steam turbine can be used instead of back pressure steam turbine. The control concept is similar to that as mentioned above, except that the steam turbine generator also participates in control of electrical output. The process steam is controlled by steam turbine bypass valve. In case of zero process steam output, the control range of electrical power output is extended by allowing almost total steam exhaust from steam turbine to go to the condenser for that particular duration.

Process steam requirements at different parameters can also be satisfied in combined cycle system by installing either a condensing steam turbine with double extraction, or a back pressure turbine with one or two extraction.

Combined gas-cum-steam turbine system based cogeneration achieves overall plant efficiency of around 90% with optional fuel utilization. In addition to this, the combined cycle plants are most economical in many cases due to very low heat rates, low specific capital cost of gas turbine plants and availability of power from open cycle operation of gas turbine plant, as it requires lesser time for erection. Major drawback of this system is less fuel flexibility as in case of gas turbine based cogeneration system.

1.1.4 Reciprocating engine based cogeneration system

In this system, the reciprocating engine is fired with fuel to drive the generator to produce electrical power. The process steam is then generated by recovery of waste heat available in engine exhaust in WHRB. The engine jacket cooling water heat exchanger and lube-oil cooler are other sources of waste heat recovery to produce hot water or hot air. The reciprocating engines are available with low, medium or high-speed versions with efficiencies in the range of 35 - 42 %.

Generally, low speed reciprocating engines are available with high efficiencies. The engines having medium and high speeds are widely used for cogeneration applications due to higher exhaust flue gas temperature and quantity. When diesel engines are operated alone for power generation, a large portion of fuel energy is rejected via exhaust flue gases. In cogeneration cycle, practically all the heat energy in engine jacket cooling water and lube-oil cooler, and substantial portion of heat in exhaust gases is recovered to produce steam or hot water. With this, the overall system efficiency of around 65-75% is achieved. The system configuration is shown in Figure 4.

The heat rates of reciprocating engine cycles are high in comparison to that of steam turbine and gas turbine based cogeneration systems. This system is particularly suitable for application requiring a high ratio of electric power to steam.

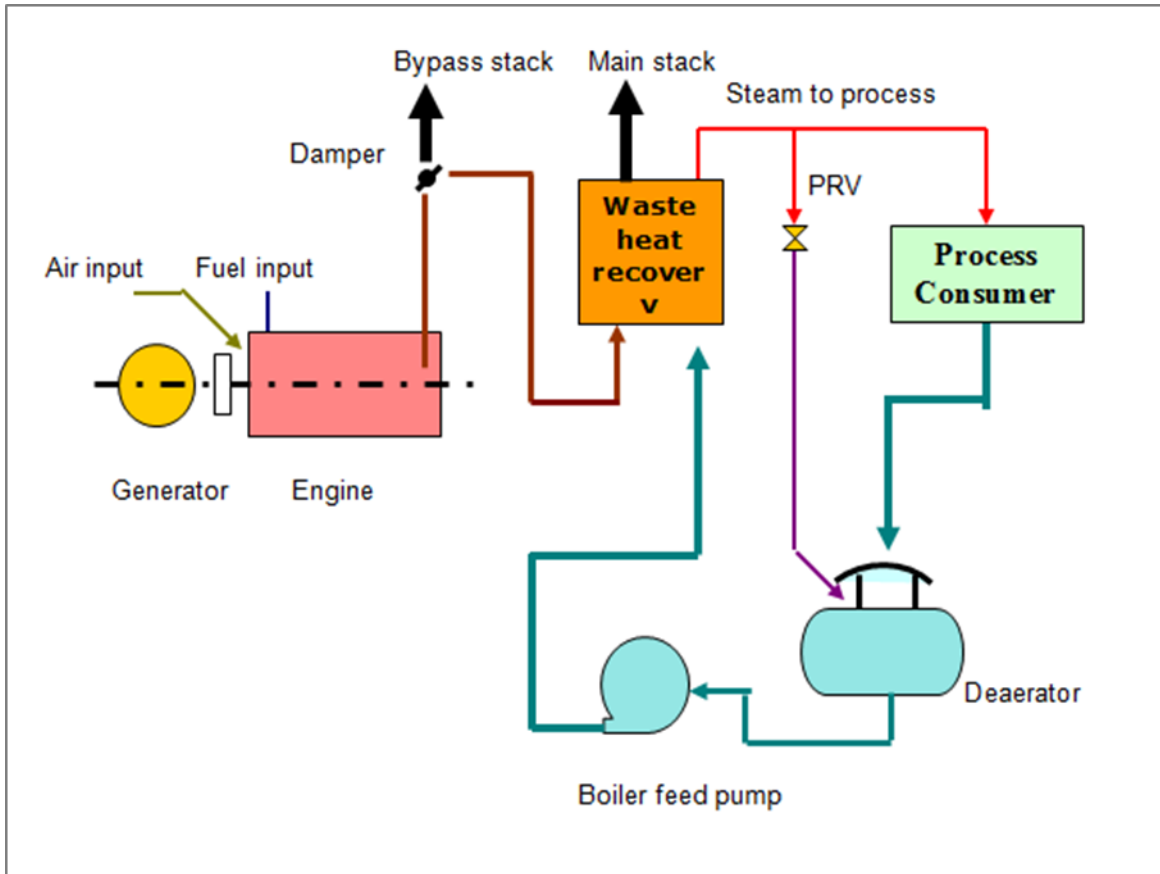


Figure 4 Reciprocating engine based cogeneration system with unfired WHRB

Reciprocating engines can be fired only with hydrocarbon based fuels such as High speed diesel, Light diesel oil, residual fuel oils, Natural gas, etc. The engines are developed in which natural gas is also directly fired. In view of lower overall fuel efficiency as mentioned above, the system is not economically better placed compared to steam turbine or gas turbine based cogeneration systems, particularly where power and steam are continuously in demand. Further to above, diesel engines are more maintenance oriented and hence generally preferred for operating intermittently, or as stand by emergency power source. These are major drawbacks preventing widespread use of diesel engine based cogeneration system.

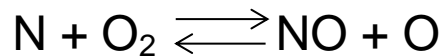
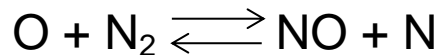
Similar to any other energy generation via combustion process, the cogeneration plants are one of the main contributors of NO_x emissions to atmosphere.

1.2 NO_x Formation process

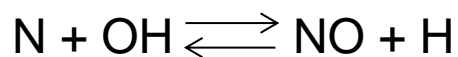
Nitrogen oxides (NO_x) is the total amount of nitric oxide (NO) and nitrogen dioxide (NO₂). The formation of NO₂ results only from the subsequent oxidation of NO and hence the total NO_x (NO + NO₂) is not affected by the amount of NO₂ formed and calculation NO is sufficient to determine the total NO_x (Turns, 2000). The NO formation process is undergoing through four chemical mechanisms.

1.2.1 Zeldovich Mechanism

The Zeldovich mechanism produces NO by the reaction of atmospheric oxygen and nitrogen at elevated temperatures. It consists of two chain reactions:



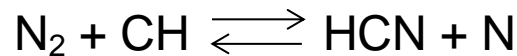
These reactions can further extended by adding the reaction:



These reactions are called extended Zeldovich mechanism and commonly referred to as thermal NO because the formation rates are only significant at high temperatures more than 1600°C (2900°F) such as the combustion chamber in gas turbines and burners in boilers (Turns, 2000).

1.2.2 Prompt Mechanism

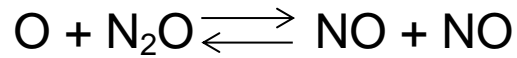
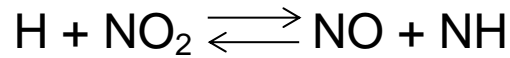
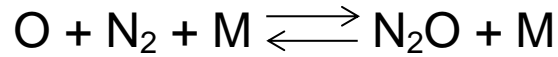
This mechanism takes into account the prompt NO formation in the primary reaction zone of the combustor (Fenimore, 1971). Whereas, the hydrocarbon radicals present during the combustion process reacts with atmospheric nitrogen to initiate the formation of NO that take place through subsequent reactions. The initiating reaction is:



The N atom forms NO through the last two reactions of Zeldovich mechanism. The HCN route to NO is complex. It will undergo through subsequent reactions forming NCO then NH and finally N that will form NO again through the Zeldovich N atom reactions.

1.2.3 Nitrous Oxide Mechanism

This mechanism is significant at low temperature conditions that take place in lean-premixed combustion (Turns, 2000). This mechanism undergoes through three subsequent reactions:



1.2.4 Fuel-Bound Nitrogen Mechanism

This mechanism covers the NO formation due to burning fuel containing nitrogen. It begins with pyrolysis of the nitrogen organically-bounded in the fuel to HCN that will undergo subsequent reactions to form NO as explained in the prompt mechanism (Toof, 1985). This mechanism is significant when burning fuels containing nitrogen such as coal.

1.3 Environmental & Health Impact of NO_x

The NO_x emitted from the stack is in the form of nitric oxide (NO) and nitrogen dioxide (NO₂) which is harmful atmospheric pollutants and poisonous to livings.

1.3.1 Environmental acidification

NO_x mixes with rain water and acidifies it by forming nitrous acid (HNO₂) and nitric acid (HNO₃). This acidic rain after it falls on plats and streams, it can kill fish and vegetation. Also, it accelerates the cracking of buildings. (EPA, 2011)

1.3.2 Stratospheric ozone depletion

NO_x reacts with ozone and free oxygen in the atmosphere that will destroy the upper-level ozone which is required to protect against the sun ultraviolet light. On the other hand, it create undesired ozone in the lower atmosphere that contribute to photochemical smog, visibility reduction, and global warming. (NIEHS, 2011)

1.3.3 Health problems

NO_x is harmful to the respiratory system. Firstly, it can react with ammonia, moisture, and other compounds to form small particles which can penetrate into the lungs and create or worsen respiratory complications including airway inflammation in healthy people or increased symptoms in people with asthma, emphysema, and bronchitis. Secondly, NO_x reacts with atmospheric oxygen to produce ground level ozone that contributes to respiratory problems through the oxidation of lung tissue. Thirdly, NO₂ is a highly reactive gas (strong oxidizing agent) that has a suffocating odor. It is highly toxic and hazardous due to its ability to delay the chemical inflammation of lungs edema. It can lead to headache, eye and throat irritation, chest tightness, and gradual loss of strength. Moreover, it can be fatal in prolonged exposure cases where it can cause violent coughing, difficulty in breathing, and cyanosis. (EPA, 2011)

Because of these harmful effects, various government agencies place restrictions on NO_x emissions. These restrictions are enforced through the Clean Air Act Amendments (CAAA) of atmospheric pollutants, including NO_x. In order to prove compliance with

these standards, combustion turbine operators must implement continuous NO_x monitoring (Hung, 1995). The restriction on NO_x emissions has led to combustion turbine technology enhancement for NO_x control, while the associated requirement for continuous monitoring has led to the demand for less expensive, more efficient emissions monitoring technologies.

1.4 NO_x Measurement techniques

There are two main technologies for monitoring NO_x emissions, the hardware based which is the Continuous Emissions Monitoring System (CEMS) that relies on sampling and analyzing of the exhaust gas. And the other is the software based which is the Predictive Emissions Monitoring System (PEMS) that applies mathematical algorithms and equations on the process parameters available in the control system (DCS) contributing to NO_x formation.

In addition to the initial cost of a CEMS, there are significant annual costs for calibration and maintenance. Also, it is subject to frequent failures. A typical CEMS installation is shown in Figure 5.

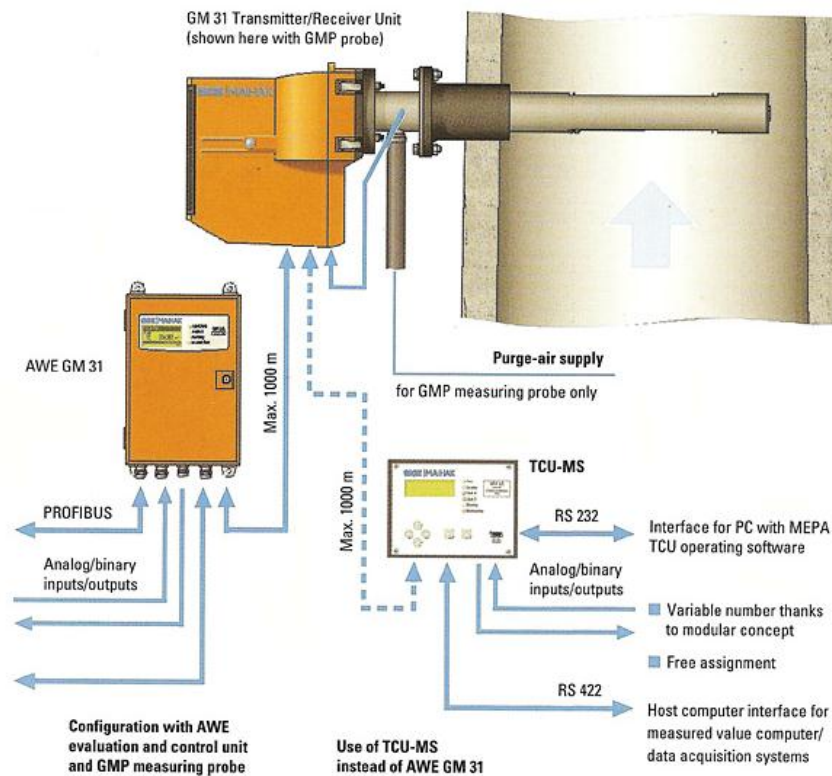


Figure 5 NOx Analyzer (Sick-Maihak model GM31)

A less expensive and thus more desirable approach is to estimate NO_x based on easily measured parameters that contribute to the NO_x formation. These parameters can include ambient conditions, combustion pressure, fuel-air ratio, and gas-generator turbine exit temperature. A package consisting of the appropriate sensors, hardware, and incorporated algorithms used to calculate emissions is referred to as Predictive Emissions Monitoring System (PEMS). A PEMS is lower cost, lower maintenance (less complex), more reliable, allow real time estimation, does not require periodic calibration using costly calibration gases, and can be incorporated into existing gas turbine monitoring system which already measure most of the appropriate parameters. |

CHAPTER 2

LITERATURE REVIEW

This section includes a brief literature review in the area of “Predictive Emission Monitoring Systems” applied in combustion systems. It covers most of the papers that concerned with the PEMS from 1991 to 2013 in chronological order and summarized at the end.

SPECHT (1991) described a memory-based network that provides estimates of continuous variables and converges to the underlying (linear or nonlinear) regression surface. This general regression neural network (GRNN) is a one-pass learning algorithm with a highly parallel structure. Even with sparse data in a multidimensional measurement space, the algorithm provides smooth transitions from one observed value to another. The algorithmic form can be used for any regression problem in which an assumption of linearity is not justified.

DONG and MCAVOY (1995) Discussed using neural network partial least squares (NNPLS) (Qin & McAvoy, 1992), and nonlinear principal components analysis (NLPCA) (Dong & McAvoy, 1993) to build soft sensors for emission monitoring using data from an industrial heater. Several issues which are very important for the soft sensor approach

are discussed, such as variable selection, sensor validation, and missing sensor replacement.

KAMES and KEELER (1995) Discussed the application of Pavilion's Process Insights" for PEMS demonstration projects on two different cement kilns for predicting SO₂ and NO emissions. The example discussed involved predicting NO_x emissions at a 221 MMBtu/hr gas-fired boiler at Arkansas Eastman Company. The predictive model was initially built from data collected on approximately 120 process variables. The final PEMS was reduced to a set of 22 of the most important process variables as inputs and one output (lb NO_x/MMBtu readings). The NO_x emission model was installed at Arkansas Eastman in May, 1993, was certified via passing a Relative Accuracy Test Audit (RATA) one month later (June, 1993), and is now operating continuously under an operating permit with the Arkansas Department of Pollution Control and Ecology. This was the first PEMS installed on a Subpart Db boiler and done with the approval of EPA, Region VI in conjunction with EPA Headquarters.

REIFMAN and FELDMAN (1998) Investigated the applications of two classes of artificial neural networks for the identification and control of discrete-time non-linear dynamical systems. A fully connected recurrent network is used for process identification, and a multilayer feed forward network is used for process control. The two neural networks are arranged in series for closed-loop control of oxides of nitrogen emissions of a simplified representation of a dynamical system. Plant data from one of

Commonwealth Edison's coal-fired power plants was used for testing the approach, with initial results indicating that the method is feasible. However, as the number of state variables and control variables are increased, further work is required to determine whether the method remains feasible.

IKONEN et. al. (2000) Used fuzzy neural networks to model the process. In distributed logic processors (DLP) the rule base is parameterized. The DLP derivatives required by gradient-based training methods are given, and the recursive prediction error method is used to adjust the model parameters. The power of the approach is illustrated with a modeling example where NO_x-emission data from a full-scale fluidized-bed combustion district heating plant are used. The method presented in this paper is general, and can be applied to other complex processes as well.

AZID et. al. (2000) Applied Artificial Neural Networks (ANN) based on feed forward back propagation model on data taken from Lumut Power Plant to predict stack gases from the combustion chamber. The prediction from Neural Network based on training agrees well with the data taken from CEMS.

STEOHEN (2000) Used a cascading neural network to model the NO_x emission in a coal-fired power generation plant. This type of neural network has more connections than that found in the layered feed forward neural network. Algorithm for training this type of

neural network is suggested and then it is used to build a NO_x emission model for a coal fired power generation plant. Simulation results show the merits of this type of neural network.

CHONG et. al. (2001) Presented the application of feed-forward multi-layered perceptron networks as a simplistic means to model the gaseous emissions emanating from the combustion of lump coal on a chain-grate stoker-fired boiler, The resultant 'black-box' models of the oxygen concentration, nitrogen oxides and carbon monoxide in the exhaust flue gas were able to represent the dynamics of the process and delivered accurate one-step-ahead predictions over a wide range of unseen data. This system identification approach is an alternative to the mathematical modeling of the physical process, which although lacking in model transparency and elegance, is able to produce accurate one-step ahead predictions of the derivatives of combustion. This has been demonstrated not only with data sets that were obtained from the same series of experiments (which also demonstrated the repeatability of the model) but also for data with a temporal separation of almost eight months from the training data set.

ZHOU et. al. (2001) Used neural network and genetic algorithms to optimize the low NO_x combustion on pulverized coal burned utility boiler. The NO_x emission characteristic of a 600 MW capacity boiler operated under different conditions is experimentally investigated and on the basis of experimental results, the artificial neural network is used to describe its NO_x emission property to develop a neural network based

model. A genetic algorithm is employed to perform a search to determine the optimum solution of the neural network model, identifying appropriate set points for the current operating conditions and the low NO_x emission of the pulverized coal burned boiler is achieved.

FERRETTI and PIRODDI (2001) proposed a neural network based strategy for the estimation of the NO_x emissions in thermal power plants, fed with both oil and methane fuel. A detailed analysis based on a three-dimensional simulation of the combustion chamber has pointed out the local nature of the NO_x generation process, which takes place mainly in the burners zone. Two different learning procedures have been investigated. Both based on the external inputs to the burners and a suitable mean cell temperature, while using local and global NO_x flow rates as learning signals. The approach has been assessed with respect to both simulated and experimental data.

TRONCI et. al. (2002) addressed the relevant issues associated to the development of neural-based software sensors for monitoring the pollutant emissions coming out from combustion chambers. The objective was to prove the potential of software sensors as alternative monitoring systems to conventional analytical equipment. The preliminary results refer to a 4:8 MW power pilot plant operating at the Enel Santa Gilla Research Center in Cagliari, Italy.

KALOGIROU (2003) illustrated how Artificial Intelligence (AI) techniques might play an important role in modeling and prediction of the performance and control of combustion process. He outlined an understanding of how AI systems operate by way of presenting a number of problems in the different disciplines of combustion engineering. The various applications of AI are presented in a thematic rather than a chronological or any other order. Problems presented include two main areas: combustion systems and internal combustion (IC) engines. Combustion systems include boilers, furnaces and incinerators modeling and emissions prediction, whereas, IC engines include diesel and spark ignition engines and gas engines modeling and control. Results presented in this paper, are testimony to the potential of AI as a design tool in many areas of combustion engineering.

KESGIN (2003) Used Genetic algorithm (GA) and neural network analysis to predict the effects of design and operational parameters on engine efficiency and NO_x emissions of a natural gas engine. A computer program to calculate the amount of NO_x emissions based on a reaction kinetic model is developed. The validity of this program is verified by measurements from a turbocharged, lean-burn, natural gas engine. Using the results from this program, the effects of operational and design parameters of the engine were investigated. Then a wide range of engine parameters are optimised using a simple GA regarding both efficiency and NO_x emissions. Because of the large computation requirements especially for NO_x level determination, an artificial neural network model based on results of these investigations is used to predict the engine efficiency and NO_x

emissions. The results show an increase in efficiency as well as the amount of NO_x emissions being kept under the constraint value of 250 mg/Nm³ for stationary engines.

ZHOU et. al. (2003) Introduces an approach to predict the nitrogen oxides (NO_x) emission characteristics of a large capacity pulverized coal fired boiler with artificial neural networks (ANN). The NO_x emission and carbon burnout characteristics were investigated through parametric field experiments. The effects of over-fire-air (OFA) flow rates, coal properties, boiler load, air distribution scheme and nozzle tilt were studied. On the basis of the experimental results, an ANN was used to model the NO_x emission characteristics and the carbon burnout characteristics. Compared with the other modeling techniques, such as computational fluid dynamics (CFD) approach, the ANN approach is more convenient and direct, and can achieve good prediction effects under various operating conditions. A modified genetic algorithm (GA) using the micro-GA technique was employed to perform a search to determine the optimum solution of the ANN model, determining the optimal set points for the current operating conditions, which can suggest operators' correct actions to decrease NO_x emission.

GRAZIANI et. al. (2004) Proposed a novel strategy to improve the estimation of nitrogen oxides emissions produced by chimneys of refineries. In particular nonlinear models, obtained by using MLPs neural networks, which are being a commonly used tool in processing data acquired in petrochemical processes, are proposed. The performance of

the proposed model with respect to both traditional heuristic models and linear models are described.

CICCONI et. al. (2005) Developed Predictive Emission Monitoring (PEM) systems for four natural gas fired power generating facilities. The systems are based on an artificial neural network (ANN) using the power plant operation variables to predict the nitric oxide (NO) portion of the exhaust emissions. The PEM systems were trained with emission and operation data gathered from the facilities during normal operation. A multi-layer perceptron fully-connected feed forward network with two hidden layers was the best architecture for all of the facilities. The accuracy of the system was determined using the relative accuracy (RA) calculations from the Environment Canada EPS 1/PG/7 report (Environment Canada, 1993).

HABIB et. al. (2007) investigated numerically the problem of NO_x pollution using a model furnace of an industrial boiler utilizing fuel gas. Governing conservation equations of mass, momentum and energy, and equations representing the transport of species concentrations, turbulence, combustion and radiation modeling in addition to NO modeling equations were solved together to present temperature and NO distribution inside the radiation and convection sections of the boiler. The boiler under investigation is a 160 MW, water-tube boiler, gas fired with natural gas and having two vertically aligned burners. The simulation study provided the NO distribution in the combustion chamber and in the exhaust gas at various operating conditions of fuel to air ratio with

varying either the fuel or air mass flow rate, inlet air temperature and combustion primary air swirl angle. In particular, the simulation provided more insight on the correlation between the maximum furnace temperature and furnace average temperatures and the thermal NO concentration. The results have shown that the furnace average temperature and NO concentration decrease as the excess air factor k increases for a given air mass flow rate. When considering a fixed value of mass flow rate of fuel, the results show that increasing k results in a maximum value of thermal NO concentration at the exit of the boiler at $k = 1.2$. As the combustion air temperature increases, furnace temperature increases and the thermal NO concentration increases sharply. The results also show that NO concentration at exit of the boiler exhibits a minimum value at around swirl angle of 45° .

RUSINOWSKI and STANEK (2007) Presented a method and example results of calculations of the neural modeling of steam boilers. Empirical models can be worked out based on the results of specially organized measurements or continuous measurements recorded in the computer system storing the operational performance. The introduction of operational measurement data for material and energy balances required the separation of stationary sub-periods of boiler operations. For each separated sub-period of stationary operation thermal calculations based on DIN 1942 have been carried out. The results of calculations are utilized to estimate the neural model of a steam boiler. This model describes the dependence of the main operational parameters of the boiler upon the flue gas losses and losses due to unburned combustibles. The parameters of the neural model have been estimated by means of the back-propagation method.

LIGANG et. al. (2008) proposed a novel “one-pass” neural network, generalized regression neural network (GRNN) to establish a non-linear model between the parameters of the boiler (300MW steam capacity) and the NO_x emissions. The selection of the GRNN model’s parameter is discussed. The results show that the GRNN model predicted NO_x emissions much more accurate than the widely-used “iterative” BPNN model and the multiple linear regression model. The main advantage of the GRNN model, by comparing with the traditional BPNN model, consists of the certainty of the predictive result, simplicity in network structure, quick convergence rate and much better predictive accuracy, especially for the case with a very large number of training samples.

SHAKIL et. al. (2008) Used dynamic neural networks to develop soft sensors for the NO_x and O₂ emission due to combustion operation in industrial boilers. A simplified structure for the soft sensor is obtained by grouping the input variables, reducing the input data dimension and utilizing the system knowledge. The principal component analysis (PCA) is used to reduce the input data dimension. The genetic algorithm (GA) is used to estimate the system’s time delays by optimizing a linear time-delay model. Real data from a boiler plant is used to validate the models. The performance of the proposed dynamic models is compared with static neural network models. The results demonstrate the effectiveness of the proposed models.

FAST et. al. (2009) Demonstrated different utilities for industrial use of an artificial neural network (ANN) model for a gas turbine. The ANN model was constructed with

the multi-layer feed-forward network type and trained with operational data using back-propagation. The results showed that operational and performance parameters of the gas turbine, including identification of anti-icing mode, can be predicted with good accuracy for varying local ambient conditions. Different possible applications of this ANN model were also demonstrated. These include instantaneous gas turbine performance estimation through a graphical user interface and extrapolation beyond the range of training data.

SMREKAR et. al. (2009) Developed artificial neural network (ANN) models using real plant data for the prediction of fresh steam properties from a brown coal-fired boiler of a Slovenian power plant is reported. Input parameters for this prediction were selected from a large number of available parameters. Initial selection was made on a basis of expert knowledge and previous experience. However, the final set of input parameters was optimized with a compromise between smaller number of parameters and higher level of accuracy through sensitivity analysis. Data for training were selected carefully from the available real plant data. Two models were developed, one including mass flow rate of coal and the other including belt conveyor speed as one of the input parameters. The rest of the input parameters are identical for both models. Both models show good accuracy in prediction of real data not used for their training. Thus both of them are proved suitable for use in real life, either on-line or off-line. Better model out of these two may be decided on a case-to-case basis depending on the objective of their use. The objective of these studies was to examine the feasibility of ANN modeling for coal-based power or combined heat and power (CHP) plants.

LEI-HUA et. al. (2009) Built a soft-sensor modeling on NO_x emission of power station boilers based on least squares support vector machines (LS-SVM). The model can predict NO_x emission in different conditions. The comparative analysis of forecast-results between LS-SVM model and ANN model showed that LS-SVM has more strong generalization ability and higher calculation speed.

FAST et. al. (2009) Used artificial neural network (ANN) to model a gas turbine. The ANN model was constructed with the multi-layer feed-forward network type and trained with operational data using back-propagation. The results showed that operational and performance parameters of the gas turbine, including identification of anti-icing mode, can be predicted with good accuracy for varying local ambient conditions. Different possible applications of this ANN model were also demonstrated. These include instantaneous gas turbine performance estimation through a graphical user interface and extrapolation beyond the range of training data.

DAVIS and BLACK (2010) Reviewed the state-of-the-art emissions control technology for heavy-duty gas turbines with emphasis on the operating characteristics and field experience of Dry Low NO_x (DLN) combustors for E and F technology machines. Lean premixed DLN technology has also been demonstrated on oil fuel and is also discussed.

ZHENG et. al. (2010) studied NO_x emissions modeling for real-time operation and control of a 300MWe coal-fired power generation plant is studied. A least square support vector regression (LS-SVR) model was proposed to establish a non-linear model between the parameters of the boiler and the NO_x emissions. The results show that the LS-SVR model predicted NO_x emissions with good accuracy. LS-SVR model is much more accurate than the GRNN model previously reported by the authors. LS-SVR model will be a good alternative to a neural network based model which is commonly used to implement the predictive emission monitoring system (PEMS).

FICHET et. al. (2010) Addressed the numerical prediction of NO_x emissions from gas turbines. Generated from Computational Fluid Dynamics (CFD), a Reactor Network (RN) is defined to model the NO_x formation with a detailed chemistry. An optimized procedure is proposed to split the reactive flow field into homogeneous zones considered as Perfectly Stirred Reactors (PSR). Once connected together, they result in a Chemical Reactor Network (CRN) that yields a detailed composition regarding species and temperature in the combustion chamber. Sensitivity studies are then performed to estimate the influence of air humidity and gas turbine load on NO_x predictions. The NO_x emissions predicted are in good agreement with the measured data in terms of levels and trends for the case studied (a gas turbine flame tube fed with natural gas and functioning at a pressure of 15 bar). Finally, the RN methodology has shown to be efficient estimating accurately NO_x emissions with a short response time (few minutes) and small CPU requirements.

EDDY and HAINING (2010) Investigated testing a CFD based NO_x model over a variety of coal type, firing configuration and boiler size ranging from 200MWe sub-critical to most modern 1000 MWe ultra supercritical. In most cases, the NO_x estimates based on input data readily available from power plants were found within the range of measured data (with the worst estimate being 22% higher than the maximum measured NO_x level). The CFD results also indicated some sensitivity of the NO_x estimates to the ratio of volatile nitrogen to char nitrogen and the importance of NO reduction by char. However, this study showed that the locations of fuel-bound nitrogen evolution with respect to the stoichiometric condition within the boiler actually governed the overall NO emissions.

FARQUAD et. al. (2010) Proposed hybrid rule extraction procedure has two phases: (1) Obtain the reduced training set in the form of support vectors using SVR (2) Train the machine learning techniques (with explanation capability) using the reduced training set. Machine learning techniques viz., Classification And Regression Tree (CART), Adaptive Network based Fuzzy Inference System (ANFIS) and Dynamic Evolving Fuzzy Inference System (DENFIS) are used in the phase 2. The proposed hybrid rule extraction procedure is compared to stand-alone CART, ANFIS and DENFIS. Extensive experiments are conducted on five benchmark data sets viz. Auto MPG, Body Fat, Boston Housing, Forest Fires and Pollution, to demonstrate the effectiveness of the proposed approach in generating accurate regression rules. The efficiency of these techniques is measured using Root Mean Squared Error (RMSE). From the results obtained, it is concluded that when the support vectors with the corresponding predicted target values are used, the SVR

based hybrids outperform the stand-alone intelligent techniques and also the case when the support vectors with the corresponding actual target values are used.

BARTOLINI et. al. (2010) Applied artificial neural networks (ANNs) to describe the performance of a micro gas turbine (MGT). In particular, they were used (i) to complete performance diagrams for unavailable experimental data; (ii) to assess the influence of ambient parameters on performance; and (iii) to analyze and predict emissions of pollutants in the exhausts. The experimental data used to feed the ANNs were acquired from a manufacturer's test bed. Though large, the data set did not cover the whole working range of the turbine; ANNs and an artificial neural fuzzy interference system (ANFIS) were therefore applied to fill information gaps. The results of this investigation were also used for sensitivity analysis of the machine's behavior in different ambient conditions.

ELANGESHWARAN et. al. (2011) developed intelligent Predictive Monitoring Emission Systems (PEMS) for three distinct case studies involving traffic, gasoline fuel tanks and large combustion plants (LCP). The underlying theme of pollutant emissions exists in all three case studies whereby the gases that are monitored are NO₂, unburned hydrocarbons, and SO₂. The datasets are collected online via database libraries, and consequently data preprocessing and data division are done. Back-propagation neural networks (BPNN) are first used to model the emission, and then to compare, generalized regression neural networks (GRNN) are used. From the results it is shown that GRNN

models outperform BPNN algorithms for complex and nonlinear datasets, because of the underlying radial basis kernel transfer function. The RBF kernel has fewer numerical difficulties; one of it is that the kernel output is contained between 0 and 1; hence the solution provided by GRNN is stable, certain and localized.

CHUANBAO and FUWU (2011) Described an approach for replacing the engine out NO_x sensor with an artificial neural network (ANN) based NO_x perception. A multi-layer perception network was trained to estimate NO_x concentration from engine speed, load, exhaust temperature, and oxidation factor information. This supervised learning was conducted with measured engine data. The network was validated against measured data that was excluded from the training data set. The paper details application of this technique to a heavy duty diesel engine.

KHOSHHAL et. al. (2011) Investigated numerically the influence of the fuel temperature on NO_x formation by studying the CFD modeling of NO_x emission in an experimental furnace equipped with high temperature air combustion (HiTAC) system. The comparison between the predicted results and measured values have shown good agreement, which implies that the adopted combustion and NO_x formation models are suitable for predicting the characteristics of the flow, combustion, heat transfer, and NO_x emissions in the HiTAC chamber. Moreover the predicted results show that increase of the fuel temperature results in a higher fluid velocity, better fuel jet mixing with the combustion air, smaller flame and lower NO_x emission.

YAP and KARRI (2012) Developed a two-stage emissions predictive model by investigating common feedforward neural network models. The first stage model involves predicting engine parameters power and tractive forces and the predicted parameters are used as inputs to the second stage model to predict the vehicle emissions. The following gasses were predicted from the tailpipe emissions for a scooter application; CO, CO₂, HC and O₂. Three feedforward neural network models were investigated and compared in this study; backpropagation, optimization layer-by-layer and radial basis function networks. Based on the experimental setup, the neural network models were trained and tested to accurately predict the effect of the engine operating conditions on the emissions by varying the number of hidden nodes. The selected optimization layer-by-layer network proved to be the most accurate and reliable predictive tool with prediction errors of $\pm 5\%$.

GOBBATO et. al. (2012) Presented an experimental and computational analysis of both the isothermal and the reactive flow field inside a gas turbine combustor designed to be fed with natural gas and hydrogen. The study aims at evaluating the capability of a coarse grid CFD model, already validated in previous reactive calculations, in predicting the flow field and NO_x emissions. An experimental campaign was performed on an isothermal flow test rig to investigate the combustion air splitting and the penetration of both primary and dilution air jets. These experimental data are used to validate the isothermal computations. The impact of combustion on the calculated flow field and on air splitting is investigated as well. Finally, NO_x emission trend estimated by a post-processing technique is presented. The numerical NO_x concentrations at the combustor

discharge are compared with experimental measurements acquired during operation with different fuel burnt (natural gas or hydrogen) and different amount of steam injected.

GUOQIANG et. al. (2012) Proposed a new combination modeling method whose structure consists of three components: extreme learning machine (ELM), adaptive neuro-fuzzy inference system (ANFIS) and PS-ABC which is a modified hybrid artificial bee colony algorithm. The combination modeling method has been proposed in an attempt to obtain good approximations and generalization performances. In the whole model, ELM is used to build a global model, and ANFIS is applied to compensate the output errors of ELM model to improve the overall performance. In order to obtain a better generalization ability and stability model, PS-ABC is adopted to optimize input weights and biases of ELM. For stating the proposed model validity, it is applied to set up the mapping relation between the boiler efficiency and operational conditions of a 300 WM coal-fired boiler. Compared with other combination models, the proposed model shows better approximations and generalization performances.

Illiyas et. al. (2013) Addressed the problem of NO_x emission using a model of furnace of an industrial boiler, and proposed a neural network structure for high performance prediction of NO_x as well as O₂. The studied boiler is 160 MW, gas fired with natural gas, water-tube boiler, having two vertically aligned burners. The boiler model is a 3D problem that involves turbulence, combustion, radiation in addition to NO_x modeling. The 3D computational fluid dynamic model is developed using Fluent simulation

package. The model provides calculations of the 3D temperature distribution as well as the rate of formation of the NO_x pollutant, enabling a better understanding on how and where NO_x are produced. The boiler was simulated under various operating conditions. The generated data is then used for initial development and assessment of neural network soft sensors for emission prediction based on the conventional process variable measurements. The performance of the proposed soft sensor is then evaluated using actual data from an industrial boiler. The developed soft sensor achieves comparable accuracy to the continuous emission monitor analyzer, however, with substantial reduction in the cost of equipment and maintenance.

Yu and Zhu (2013) Developed NO_x emission characteristics and overall heat loss model for a 300MW coal-fired boiler by Back Propagation (BP) neural network, by which the functional relationship between outputs (NO_x emissions & overall heat loss of the boiler) and inputs (operational parameters of the boiler) of a coal-fired boiler can be predicted. A number of field test data from a full-scale operating 300MWe boiler were used to train and verify the BP model. The NO_x emissions & heat loss predicted by the BP neural network model showed good agreement with the measured. Then, BP model and the non-dominated sorting genetic algorithm II (NSGA-II) were combined to gain the optimal operating parameters which lead to lower NO_x emissions and overall heat loss boiler. The optimization results showed that hybrid algorithm by combining BP neural network with NSGA-II can be a good tool to solve the problem of multi-objective optimization of a coal-fired combustion, which can reduce NO_x emissions and overall heat loss effectively for the coal-fired boiler.

In summary, through reviewing the literature you can clearly observe that most of the PEMS applications are on coal-fired boilers and furnaces as coal is the highest waste producer among the other types of fuel. Then, the application was extended also to the other fuels as the environment regulations become more stringent. Most of the papers used FFBPNN for modeling the PEMS. Note that, there are only few papers about predicting the NO_x emissions from gas turbine power plants and most of them are based on CFD. In this work the PEMS will be modeled through employing ANFIS & FFBPNN.

Table 1 is summarizing the modeling approach and application of the literature papers:

Table 1 Literature Modeling Approach and Application.

#	AUTHORS	YEAR	ANN method	Application
1	Specht D.	1991	GRNN	General
2	Dong D. & Mcavoy T.	1995	NNPLS & NLPCA	Emission monitoring on data from process heaters
3	Kames J. & Keeler J.	1995	Pavilion software (combines NN, FL, & DS)	SO ₂ & NO _x emissions prediction on two cement kilns boilers
4	Reifman J. & Feldman E.	1998	FCRNN & MFFNN	NO _x emissions control on data from coal-fired power plants
5	Ikonen E., Najim K., & Kortela U.	2000	FNN/DLP	Predict stack emissions (NO _x , SO ₂ , & CO ₂) on data from fuel-fired combined cycle power plant *No details about the plant. *Limited data sets (24 sets with 1 hour increment) *2 inputs / 1 output

#	AUTHORS	YEAR	ANN method	Application
6	Azid I., Ripin Z., Aris M., Ahmad A., Seetharamu K., & Yusoff R.	2000	FFBPNN	Predict stack emissions (NO _x , SO ₂ , & CO ₂) on data from fuel-fired power plant
7	Steohen Kang Li	2000	CNN	NO _x emissions prediction on data from coal-fired power plant
8	Hao Z., Kefa C., & Jianbo M.	2001	FFBPNN	NO _x emissions prediction on data from coal-fired power plant
9	Chong A., Wilcox S., & Ward J.	2001	FFMLPNN	CO, NO _x , & O ₂ emissions prediction on data from coal fired boiler.
10	Ferretti & Piroddi	2001	???	NO _x emissions estimation prediction on data from thermal power plant
11	Tronci S., Baratti R., & Servida A.	2002	MFFNN	CO, NO _x , & O ₂ emissions prediction on data from pilot power plant furnace
12	Kesgin U	2003	GA & FFBPNN	Optimization of efficiency and NO _x emissions in a natural gas engine
13	Zhou H., Cen K., & Fan J.	2003	FFBPNN	NO _x emissions prediction on data from coal-fired power plant
14	Graziani S., Pitrone N., Xibilia M., & Barbalace N.	2004	FFMLPNN	Chimney NO _x emissions prediction on data from refinery

#	AUTHORS	YEAR	ANN method	Application
15	Ciccone A., Cinnamon C., & Niejadlik P.	2005	FFMLPNN	<p>NOx emissions prediction on four power generating facilities operating combined cycle natural gas fired Combustion Gas Turbines (CGT)</p> <p>1-North Bay: 25 MW CGT (DLN) *ANN: 6-14-9-1 *Inputs: Fuel flow / Compr. disch. temp. / Comp. disch. pressure / Mass flow / Load / Duct burner fuel gas.</p> <p>2-Kapuskasing: 25 MW CGT (DLN) *ANN: 6-14-4-1 *Inputs: Fuel flow / Compr. disch. temp. / Comp. disch. pressure / Air mass flow / Load / Duct burner fuel gas.</p> <p>3-Tunis: 31 MW CGT *ANN:13-24-11-1</p> <p>4-Nipigon: 22 MW CGT *ANN: 7-16-9-1</p>
16	Habib M., Elshafei M., & Dajani M.	2007	CFD	NOx emissions prediction on a model furnace of an industrial boiler utilizing fuel gas.
17	Rusinowski H. & Stanek W.	2007	FFPBNN	Fuel losses in steam boilers
18	Ligang Z., Shuijun Y., & Minggao Y.	2008	GRNN	NOx emissions prediction on data from coal-fired power plant
19	Shakil M., Elshafei M., Habib M., & Maekli F.	2008	FFBPNN/DRNN	NOx emissions prediction on data from industrial boiler

#	AUTHORS	YEAR	ANN method	Application
20	Fast M., Assadi m., & De S.	2009	FFBPNN	<p>Prediction of gas turbine performance on data from cogeneration unit.</p> <p>* 22 MW GT (Anti-icing)</p> <p>* 3 Inputs: Relative humidity / Ambient pressure / Ambient temperature.</p> <p>* 8 Outputs: Air mass flow / Compr. disch. temp. / Compr. disch. Pressure / Fuel flow / Turbin exhaust temp. / Load / CO2 / Generated heat.</p> <p>* Developed GUI: Offline simulation for training, online condition monitoring for early detection of fault and degradation, and sensor validation</p>
21	Smrekar J., Assadi M., Fast M., Kustrin I., & De S.	2009	FFBPNN	Steam properties prediction on data from coal-fired power plant boiler
22	Lei-Hua F., Wei-Hua G., & Feng Y.	2009	BPNN/LS-SVM	NOx emissions prediction on data from coal-fired power plant boiler
23	Zheng L., Jia H., Yu S., & Yo M.	2010	LS-SVM	NOx emissions prediction on data from coal-fired power plant
24	Fichet V., Kanniche M., Plion P., & Gicquel O.	2010	CRN (CFD)	NOx emissions prediction from a gas turbine power plant
25	Eddy C. & Haining G.	2010	CFD	NOx emissions prediction on data from six coal-fired boilers.

#	AUTHORS	YEAR	ANN method	Application
26	Bartolini C., Caresana F., Comodi G., Pelagalli L., Renzi M., & Vagni S.	2010	FFBPNN & ANFIS	NOx emissions prediction on data from Micro Gas Turbines (MGT); 100kW
27	Elangeshwaran P., Rosdiazli I., & Vijanth A.	2011	BPNN/GRNN	Emissions prediction on data set of a compilation of plant by plant for total emission of SO2, Nox, and dust.
28	Chuanbao Liu & Fuwu Yan	2011	GRNN	NOx emissions prediction on data from a diesel engine in passenger bus.
29	Khoshhal A., Rahimi M., & AlSairafi A.	2011	CFD	NOx emissions prediction on data from experimental furnace.
30	Gobbato P., Masi M., Toffolo A., & Tanzini G.	2012	CFD	NOx emissions prediction on a gas turbine combustor.
31	Guoqiang L., Peifeng N., Chao L., & Weiping Z.	2012	ELM/ANFIS/ABC	Efficiency estimation on data from a 300 MW coal-fired boiler.

CHAPTER 3

COGENERATION PLANT UNDER STUDY

3.1 Process description

The cogeneration plant under study is a gas turbine cogeneration system which is discussed and explained in section 1.2.2. It consists of the following process equipment and systems:

1. Two Combustion Gas Turbine Generators (CGTG).
2. Two Heat Recovery Steam Generators (HRSG) with supplementary firing duct burners.
3. Fuel gas system.
4. Steam & Feed water system.
5. Sampling system.
6. Chemical dosing system.
7. Make up water system.
8. Closed cooling water system.
9. Instrument & Service air system.
10. Service gas system.
11. Utility & Potable water system.
12. Waste water collection and transfer system.
13. Electrical System.

14. Emergency diesel generator (EDG).

15. Central control room (CCR).

The plant generates 311 MW gross power (155.5 MW X 2 CGTGs) and net steam capacity of 567 t/h (734 t/h with supplementary firing). The plant is equipped with NO_x analyzer which is the Continuous Emission Monitoring System (CEMS). The analyzer is insertion type measures the concentration of NO_x based on its Ultra Violet absorption spectra. Its measuring range is 0-150 ppmvd.

Our focus will be on the combustion system at which the NO_x is generated. The CGTGs are equipped with Dry Low NO_x (DLN) burners that significantly reduce the NO_x concentration to 12 ppmvd. However, during startup the NO_x concentration is high and it reaches 130 ppmvd. Note that, high emission operation during start up might take 30 minutes only but might extend to one day or more depending on the readiness of the downstream plant.

3.2 Combustion Gas Turbine Generator (CGTG)

The Combustion Gas Turbine Generators (CGTGs) consist mainly of a compressor, combustor, and turbine. Initially, a diffusion flame (non-premixed) flame was adapted in the CGTG combustors to achieve stable operation and durability. This method was combined with water and steam injection to lower the high NO_x emissions generated from such flame. In the recent years, the environmental regulations for lowering the NO_x

emissions have increased and this traditional way of NO_x reduction is replaced with the new technology in combustion "DLN" Dry Low NO_x. The DLN combustors employ lean, pre-mixed flame to achieve low NO_x levels.

The GE frame 7FA + e under study is a single shaft, high-performance, combined cycle gas turbine generator manufactured by General Electric with a design capacity of 155.5 MW. This gas turbine generator assembly as shown in Figure 6 consists of the following major sections Inlet Guide Vane (IGV) to control air-flowrate, 18-stages compressor, DLN-2.6 can-type combustors (14 each), 3-stages turbine, and exhaust to Heat Recovery Steam Generator (HRSG).

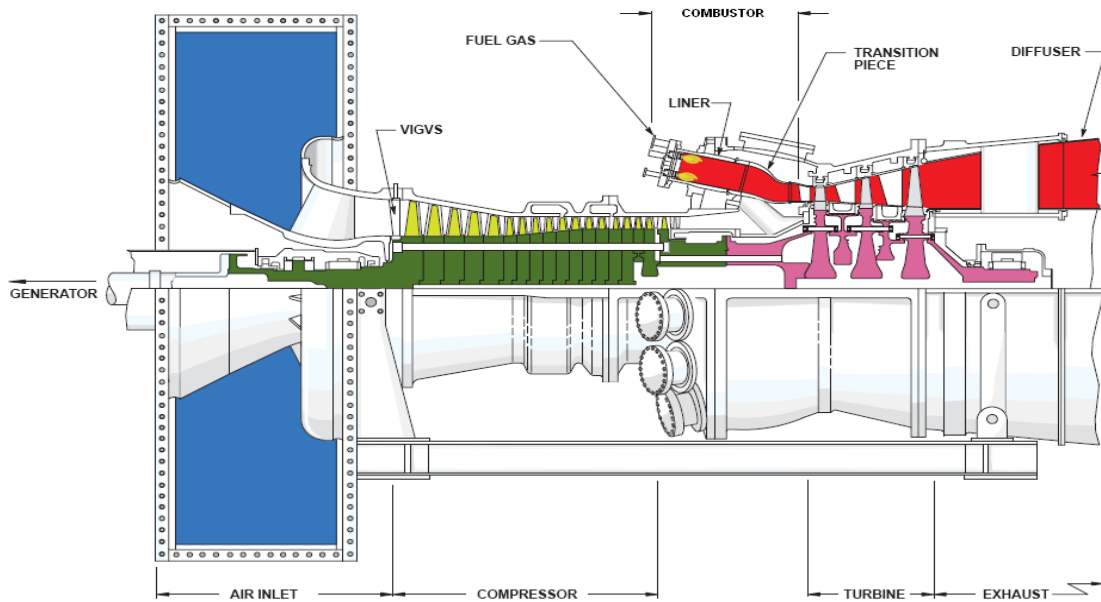


Figure 6 Gas turbine generator assembly

3.3 GE DLN-2.6 Combustion system

The combustion system is of the reverse-flow type with 14 combustion chambers (DLN-2.6) arranged around the periphery of the compressor discharge casing as shown on Figure 6. This system also includes the fuel nozzles, a spark plug ignition system, flame detectors, and crossfire tubes. Each DLN-2.6 combustion system has six fuel nozzles as shown in Figure 7. At these nozzles the gaseous fuel and air are fully pre-mixed.

The excess air in this lean combustion cools the flame and reduces the rate of thermal NO_x formation. Lean premixing of gaseous fuel and air prior to combustion can further reduce NO_x emissions. This is accomplished by minimizing localized fuel-rich pockets (and high temperatures) within the combustion zones.



Figure 7 DLN-2.6 Combustor fuel nozzles

In low emissions operation, 90% of the gas fuel is injected through radial gas injection spokes in the premixer, and combustion air is mixed with the fuel in tubes surrounding each of the six fuel nozzles as shown in Figure 8.

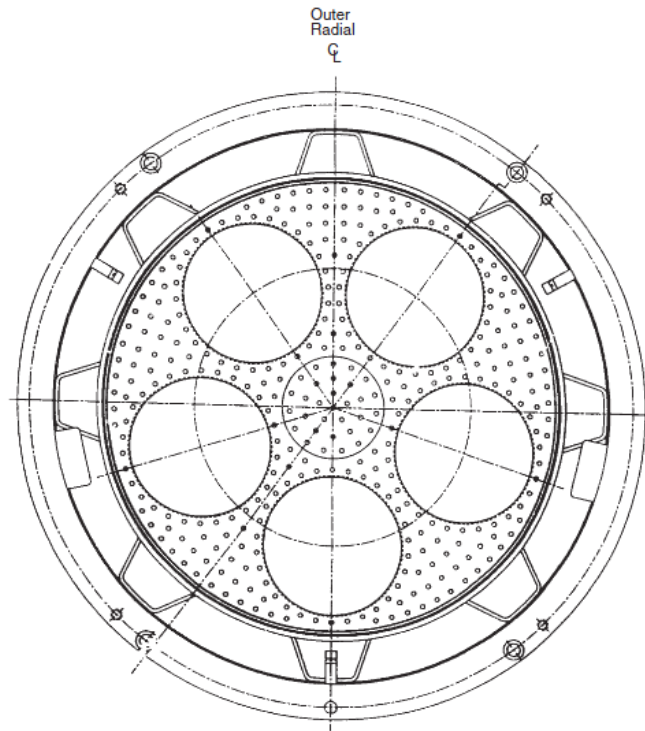


Figure 8 Cap assembly-view from downstream

Hot gases shown in Figure 9, generated from burning fuel in the combustion chambers, flow through the impingement cooled transition pieces to the turbine. High pressure air from the compressor discharge is directed around the transition pieces. Some of the air enters the holes in the impingement sleeve to cool the transition pieces and flows into the flow sleeve. The rest enters the annulus between the flow sleeve and the combustion liner through holes in the downstream end of the flow sleeve. This air enters the combustion zone through the cap assembly for proper fuel combustion. Fuel is supplied to each

combustion chamber through six nozzles designed to disperse and mix the fuel with the proper amount of combustion air.

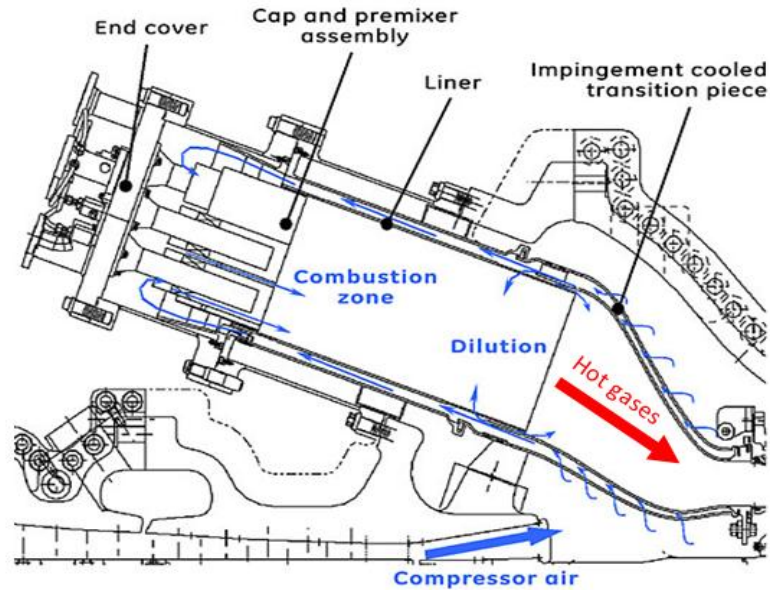


Figure 9 DLN-2.6 Combustor

Figure 10 shows a cross-section of a DLN-2 fuel nozzle. As noted, the nozzle has passages for diffusion gas, premixed gas, oil, and water. When mounted on the endcover, the diffusion passages of four of the fuel nozzles are fed from a common manifold, called the primary that is built into the endcover. The premixed passages of the same four nozzles are fed from another internal manifold called the secondary. The premixed passages of the remaining nozzle are supplied by the tertiary fuel system; the diffusion passage of that nozzle is always purged with compressor discharge air and passes no fuel.

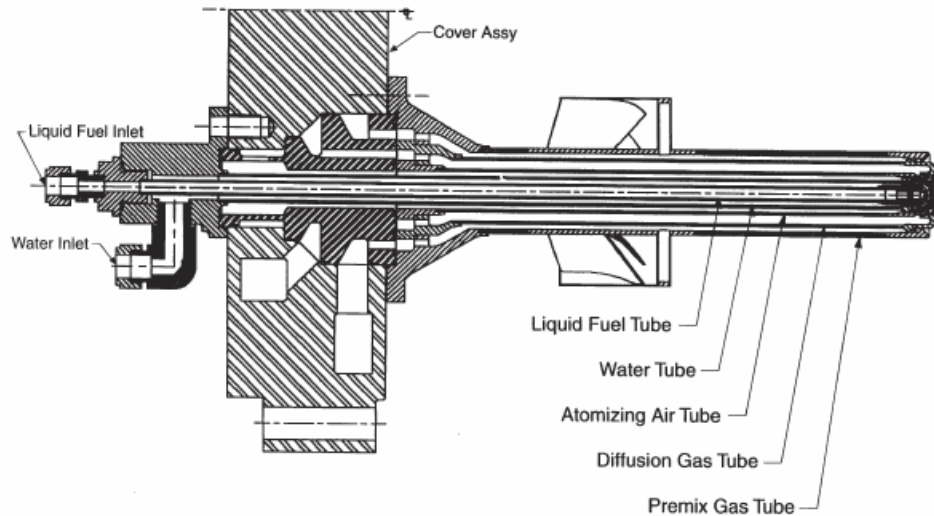


Figure 10 DLN-2 Fuel nozzle cross-section

The premixer tubes are part of the cap assembly. The fuel and air are thoroughly mixed, flow out of the five tubes at high velocity and enter the burning zone where lean, low-NOx combustion occurs. The vortex breakdown from the swirling flow exiting the premixers, along with the sudden expansion in the liner, are mechanisms for flame stabilization. Five nozzle/premixer tube assemblies are located on the head end of the combustor. A quaternary fuel manifold is located on the circumference of the combustion casing to bring the remaining fuel flow to casing injection pegs (15 each) located radially around the casing.

3.3.1 DLN-2 Fuel system

There are four fuel streams in DLN-2.6; Primary fuel, Secondary fuel, Tertiary fuel, and Quaternary fuel. Figure 11 shows the fuel nozzles installed on the combustion chamber end cover and the connections for the primary, secondary and tertiary fuel systems.

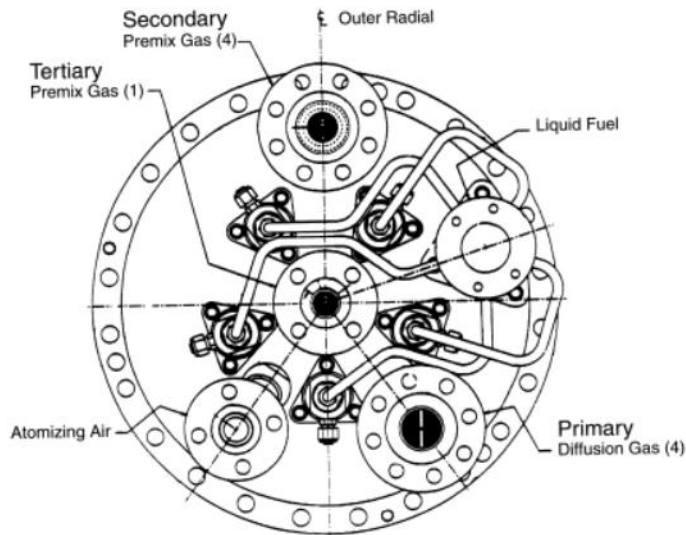


Figure 11 DLN-2 Combustor fuel streams

Primary fuel: fuel gas entering through the diffusion gas holes in the swirler assembly of each of the outboard four fuel nozzles.

Secondary fuel: premix fuel gas entering through the gas metering holes in the fuel gas injector spokes of each of the outboard four fuel nozzles.

Tertiary fuel: premix fuel gas delivered by the metering holes in the fuel gas injector spokes of the inboard fuel nozzle.

The quaternary system: injects a small amount of fuel through 15 each pegs around the casing into the airstream just up-stream from the fuel nozzle swirlers.

The DLN-2 control system regulates the fuel distribution to the primary, secondary, tertiary and quaternary fuel system. The fuel flow distribution to each combustion fuel system is a function of combustion reference temperature and IGV temperature control mode. Diffusion, piloted premix and premix flame are established by changing the distribution of fuel flow in the combustor.

The gas fuel system (Figure 17) consists of the gas fuel stop-ratio valve, primary gas control valve, secondary gas control valve premix splitter valve and quaternary gas control valve. The stop-ratio valve is designed to maintain a predetermined pressure at the control-valve inlet. The primary, secondary and quaternary gas control valves regulate the desired gas fuel flow delivered to the turbine in response to the fuel command from the SPEEDTRONIC™ controls.

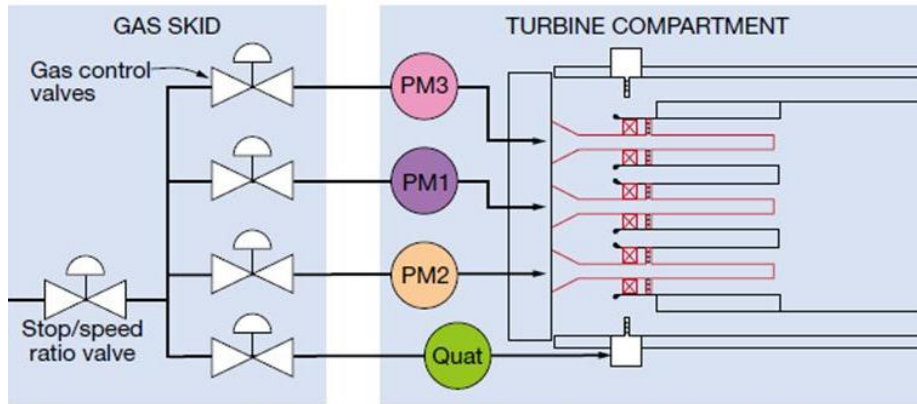


Figure 12 DLN-2.6 Fuel system control valves

3.3.2 DLN-2.6 Combustion modes

The DLN-2.6 combustion system can operate in several different modes. Figure 13 illustrates the fuel flow scheduling associated with DLN-2.6 operation. Fuel staging depends on combustion reference temperature and IGV temperature control operation mode.

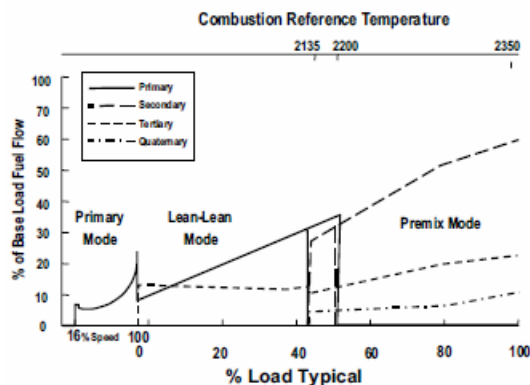


Figure 13 DLN-2.6 Fuel flow scheduling

Primary mode

Fuel flows only to the primary side of the four fuel nozzles and generating a diffusion flame. Primary mode is used from ignition to 81% corrected speed.

Lean-Lean mode

Fuel flows to the primary (diffusion) fuel nozzles and single tertiary (premixing) fuel nozzle. This mode is used from 81% corrected speed to a pre-selected combustion reference temperature. The percentage of primary fuel flow is modulated throughout the range of operation as a function of combustion reference temperature. If necessary, lean-lean mode can be operated throughout the entire load range of the turbine. Selecting “lean-lean base on” locks out premix operation and enables the machine to be taken to base load in lean-lean.

Premix transfer mode

Transition state between lean-lean and premix modes. Throughout this mode, the primary and secondary gas control valves modulate to their final position for the next mode. The premix splitter valve is also modulated to hold a constant tertiary flow split.

Piloted premix mode

Fuel is directed to the primary, secondary and tertiary fuel nozzles. This mode exists while operating with temperature control off as an intermediate mode between lean-lean and premix mode. This mode also exists as a default mode out of premix mode and, in the event that premix operating is not desired, piloted premix can be selected and operated to base load. Primary, secondary and tertiary fuel split are constant during this mode of operation.

Premix mode

Fuel is directed to the secondary, tertiary and quaternary fuel passages and premixed flame exists in the combustor. The minimum load for premixed operation is set by the combustion reference temperature and IGV position. It typically ranges from 50% with inlet bleed heat on to 65% with inlet bleed heat off. Mode transition from premix to piloted premix or piloted premix to premix, can occur whenever the combustion reference temperature is greater than 2200°F / 1204°C. Optimum emissions are generated in premix mode.

Tertiary Full Speed No Load (FSNL)

Initiated upon a breaker open event from any load $> 12.5\%$. Fuel is directed to the tertiary nozzle only and the unit operates in secondary FSNL mode for a minimum of 20 seconds, then transfers to lean-lean mode.

Each Gas Turbine (GT) has four Gas Control Valves (GCVs) as explained in section 2.3.1 and shown in Figure 12. These valves are numbered as PM1, PM2, PM3 & PM4 (PM is short form for “Pre-Mix”) as shown in Figure 14.

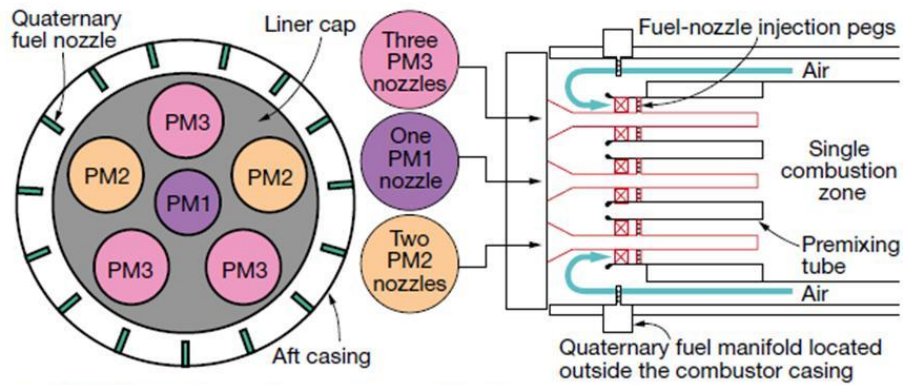


Figure 14 DLN-2.6 Fuel nozzles arrangement

These control valves will be opened or closed to sequentially ignite the six nozzles based on the load on the GT in a manner that maintains lean pre-mixed combustion and flame

stability. At the beginning, only PM1 will be in service, which is called Mode 1. Then, the modes will be changing as below:

Mode2	PM2
Mode3	PM1+PM2
Mode4	PM1+PM3
Mode5	PM2+PM3
Mode6	PM1+PM2+PM3
Mode6Q	PM1+PM2+PM3+PM4

If you observe, the number mentioned with Mode is the sum of the numbers indicated with PMs. For example, Mode3 will have PM1 and PM2. i.e., $1+2=3$. In the same way, Mode5 will have PM2 and PM3 in service. i.e. $2+3=5$. And the PM4 will be indicated with letter 'Q', as indicated in Mode6Q, as the PM4 is nothing but the control valve for Quaternary. Below is the loading sequence shown in Figure 15:

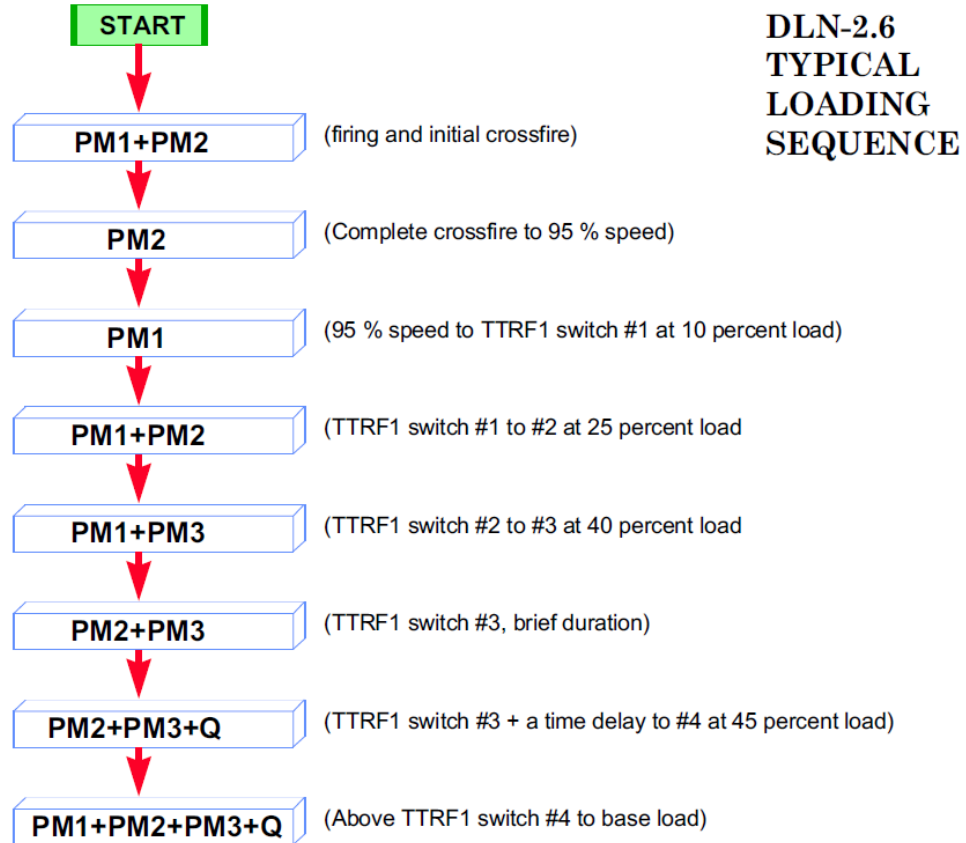


Figure 15 DLN-2.6 Loading sequence

3.3.3 DLN-2.6 Combustor NO_x emissions

There are two sources of NO_x emissions in the exhaust of a gas turbine. Most of the NO_x is generated by the fixation of atmospheric nitrogen in the flame, which is called thermal NO_x. Nitrogen oxides are also generated by the conversion of a fraction of any nitrogen chemically bound in the fuel (called fuel-bound nitrogen or FBN). Thermal NO_x is generated by a chemical reaction sequence called the Zeldovich Mechanism. This set of well-verified chemical reactions assumes that the generation of thermal NO_x is an

exponential function of the temperature of the flame and a linear function of the time which the hot gases are at flame temperature. The temperature profile through the CGTG is shown in Figure 16. The firing temperature what GE is using is at Section B, which is at First stage nozzle outlet. This temperature would be less by 38 °C from the Actual Combustion Temperature.

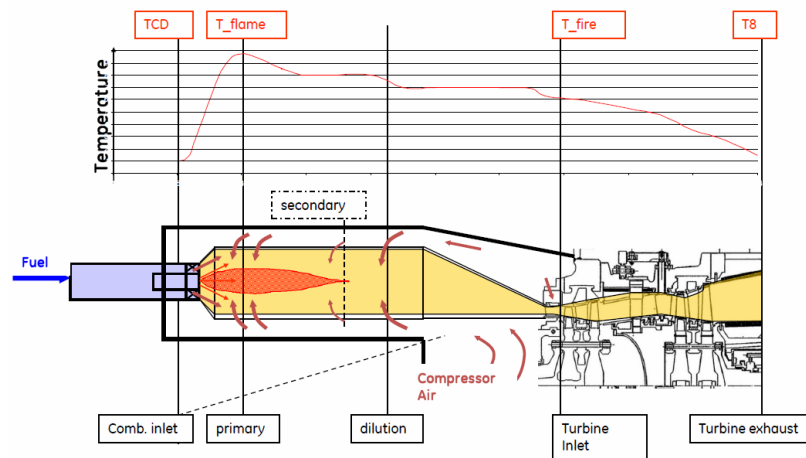


Figure 16 Temperature profile in CGTG

CHAPTER 4

ARTIFICIAL NEURAL NETWORKS

Artificial intelligence (AI) systems are widely accepted as a technology offering an alternative way to tackle complex and illdefined problems. They can learn from examples, are fault tolerant in the sense that they are able to handle noisy and incomplete data, are able to deal with non-linear problems, and once trained can perform prediction and generalization at high speed. They have been used in diverse applications in control, robotics, pattern recognition, forecasting, medicine, power systems, manufacturing, optimization, signal processing, and social/psychological sciences. They are particularly useful in system modeling such as in implementing complex mappings and system identification. AI systems comprise areas like, expert systems, artificial neural networks, genetic algorithms, fuzzy logic and various hybrid systems, which combine two or more techniques.

ANNs are collections of small individually interconnected processing units. Information is passed between these units along interconnections. An incoming connection has two values associated with it, an input value and a weight. The output of the unit is a function of the summed value. ANNs while implemented on computers are not programmed to perform specific tasks. Instead, they are trained with respect to data sets until they learn patterns used as inputs. Once they are trained, new patterns may be presented to them for prediction or classification. ANNs can automatically learn to recognize patterns in data

from real systems or from physical models, computer programs, or other sources. An ANN can handle many inputs and produce answers that are in a form suitable for designers.

AI systems are able to learn the key information patterns within a multi-dimensional information domain. In addition, many of the AI systems like, neural networks are fault tolerant, robust, and noise immune. Data from combustion processes being inherently noisy are good candidate problems to be handled with AI systems.

The concept of ANN analysis has been discovered nearly 50 years ago, but it is only in the last 20 years that applications software has been developed to handle practical problems. The history and theory of neural networks have been described in a large number of published literatures and will not be covered in this paper except for a very brief overview of how neural networks operate. (Kalogirou, 2003)

4.1 ANN Applications

ANNs are good for tasks involving incomplete data sets, fuzzy or incomplete information, and for highly complex and ill-defined problems, where humans usually decide on an intuitional basis. They can learn from examples, and are able to deal with non-linear problems. Furthermore, they exhibit robustness and fault tolerance. The tasks

that ANNs cannot handle effectively are those requiring high accuracy and precision as in logic and arithmetic. ANNs have been applied successfully in a number of application areas. Some of the most important ones are (Nannariello, 2001):

1. Function approximation. Mapping of a multiple input to a single output is established. Unlike most statistical techniques, this can be done with adaptive model-free estimation of parameters.

2. Pattern association and pattern recognition. This is a problem of pattern classification. ANNs can be effectively used to solve difficult problems in this field, like for instance in sound, image, or video recognition. This task can even be made without an a priori definition of the pattern. In such cases, the network learns to identify totally new patterns.

3. Associative memories. This is the problem of recalling a pattern when given only a subset clue. In such applications, the network structures used are usually complicated, composed of many interacting dynamical neurons.

4. Generation of new meaningful patterns. This general field of application is relatively new. Some claims are made that suitable neuronal structures can exhibit rudimentary elements of creativity.

ANNs have been applied successfully in a various fields of mathematics, engineering, medicine, economics, meteorology, psychology, neurology, and many others. Some of the most important ones are: in pattern, sound and speech recognition, in the analysis of electromyographs and other medical signatures, in the identification of military targets and in the identification of explosives in passenger suitcases. They have also being used in weather and market trends forecasting, in the prediction of mineral exploration sites, in electrical and thermal load prediction, in adaptive and robotic control and many others. Neural networks are also used for process control because they can build predictive models of the process from multi-dimensional data routinely collected from sensors.

4.2 ANN Characteristics

Neural networks obviate the need to use complex mathematically explicit formulas, computer models, and impractical and costly physical models. Some of the characteristics that support the success of ANNs and distinguish them from the conventional computational techniques are (Nannariello, 2001):

- The direct manner in which ANNs acquire information and knowledge about a given problem domain (learning interesting and possibly non-linear relationships) through the ‘training’ phase.
- Neural networks can work with numerical or analogue data that would be difficult to deal with by other means because of the form of the data or because there are so many variables.

- Neural network analysis can be conceived of as a ‘black box’ approach and the user does not require sophisticated mathematical knowledge.
- The compact form in which the acquired information and knowledge is stored within the trained network and the ease with which it can be accessed and used.
- Neural network solutions can be robust even in the presence of ‘noise’ in the input data.
- The high degree of accuracy reported when ANNs are used to generalize over a set of previously unseen data (not used in the ‘training’ process) from the problem domain.

While neural networks can be used to solve complex problems they do suffer from a number of shortcomings. The most important of them are:

- The data used to train neural nets should contain information, which ideally, is spread evenly throughout the entire range of the system.
- There is limited theory to assist in the design of neural networks.
- There is no guarantee of finding an acceptable solution to a problem.
- There are limited opportunities to rationalize the solutions provided.

4.3 Biological and artificial neurons

A biological neuron is shown in Figure 17. In brain, there is a flow of coded information (using electrochemical media, the so-called neurotransmitters) from the synapses towards

the axon. The axon of each neuron transmits information to a number of other neurons. The neuron receives information at the synapses from a large number of other neurons. It is estimated that each neuron may receive stimuli from as many as 10,000 other neurons. Groups of neurons are organized into sub-systems and the integration of these subsystems forms the brain. It is estimated that the human brain has got around 100 billion interconnected neurons.

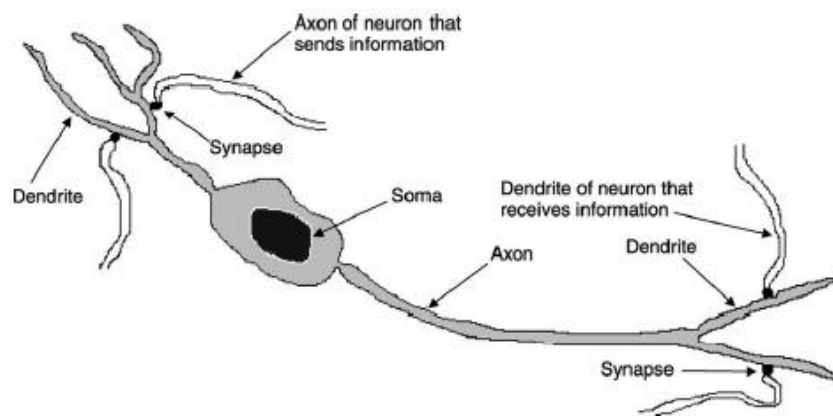


Figure 17 Biological neuron

Figure 18 shows a highly simplified model of an artificial neuron, which may be used to stimulate some important aspects of the real biological neuron. An ANN is a group of interconnected artificial neurons, interacting with one another in a concerted manner. In such a system, excitation is applied to the input of the network. Following some suitable operation, it results in a desired output. At the synapses, there is an accumulation of some potential, which in the case of the artificial neurons is modeled as a connection weight. These weights are continuously modified, based on suitable learning rules. (Kalogirou, 2003)

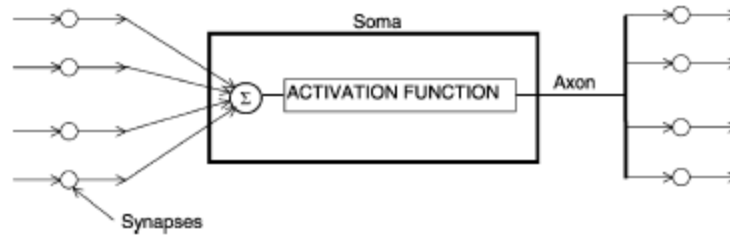


Figure 18 Artificial neuron

4.4 Feed Forward Back Propagation Neural Network (FFBPNN)

A schematic diagram of typical multi-layer feedforward neural network architecture is shown in Figure 19. The network usually consists of an input layer, some hidden layers and an output layer. In its simple form, each single neuron is connected to other neurons of a previous layer through adaptable synaptic weights. Knowledge is usually stored as a set of connection weights (presumably corresponding to synapse efficacy in biological neural systems). Training is the process of modifying the connection weights in some orderly fashion using a suitable learning method. The network uses a learning mode, in which an input is presented to the network along with the desired output and the weights are adjusted so that the network attempts to produce the desired output. The weights after training contain meaningful information whereas before training they are random and have no meaning.

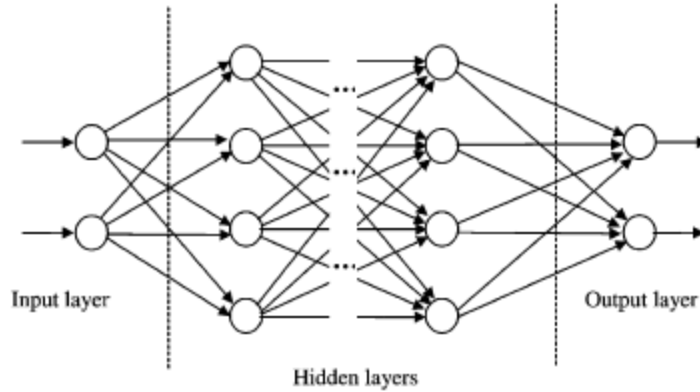


Figure 19 Multi-layer Feed Forward Neural Network

Figure 20, shows how information is processed through a single node. The node receives weighted activation of other nodes through its incoming connections. First, these are added up (summation). The result is then passed through an activation function; the outcome is the activation of the node. For each of the outgoing connections, this activation value is multiplied with the specific weight and transferred to the next node.

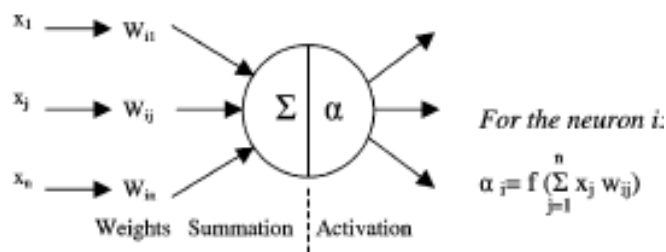


Figure 20 Information processing in a neural network

A training set is a group of matched input and output patterns used for training the network, usually by suitable adaptation of the synaptic weights. The outputs are the dependent variables that the network produces for the corresponding input. It is important

that all the information the network needs to learn is supplied to the network as a data set. When each pattern is read, the network uses the input data to produce an output, which is then compared to the training pattern, i.e. the correct or desired output. If there is a difference, the connection weights (usually but not always) are altered in such a direction that the error is decreased. After the network has run through all the input patterns, if the error is still greater than the maximum desired tolerance, the ANN runs again through all the input patterns repeatedly until all the errors are within the required tolerance. When the training reaches a satisfactory level, the network holds the weights constant and the trained network can be used to make decisions, identify patterns, or define associations in new input data sets not used to train it.

The most popular learning algorithms are the back propagation (BP) and its variants. The BP algorithm is one of the most powerful learning algorithms in neural networks. The training of all patterns of a training data set is called an epoch. The training set has to be a representative collection of input–output examples. BP training is a gradient descent algorithm. It tries to improve the performance of the neural network by reducing the total error by changing the weights along its gradient. The error is expressed by the root-mean-square value (RMS), which can be calculated by:

$$E = \frac{1}{2} \left[\sum_p \sum_i |t_{ip} - o_{ip}|^2 \right]^{1/2}$$

where E is the RMS error, t the network output (target), and o the desired output vectors over all pattern p: An error of zero would indicate that all the output patterns computed

by the ANN perfectly match the expected values and the network is well trained. In brief, BP training is performed by initially assigning random values to the weight terms (w_{ij}) in all nodes. Each time a training pattern is presented to the ANN, the activation for each node, α_{pi} ; is computed. After the output of the layer is computed the error term, δ_{pi} ; for each node is computed backwards through the network. This error term is the product of the error function, E ; and the derivative of the activation function and hence is a measure of the change in the network output produced by an incremental change in the node weight values. For the output layer nodes and for the case of the logistic-sigmoid activation, the error term is computed as:

$$\delta_{pi} = (t_{pi} - \alpha_{pi})\alpha_{pi}(1 - \alpha_{pi})$$

For a node in a hidden layer:

$$\delta_{pi} = \alpha_{pi}(1 - \alpha_{pi}) \sum_k \delta_{pk} w_{kj}$$

In the latter expression, the k subscript indicates a summation over all nodes in the downstream layer (the layer in the direction of the output layer). The j subscript indicates the weight position in each node. Finally, the d and a terms for each node are used to compute an incremental change to each weight term via:

$$\Delta w_{ij} = \varepsilon(\delta_{pi}\alpha_{pi}) + m w_{ij}(old)$$

The term η is referred to as the learning rate and determines the size of the weight adjustments during each training iteration. The term m is called momentum factor. It is applied to the weight change used in the previous training iteration, w_{ij} (old). Both of these constant terms are specified at the start of the training cycle and determine the speed and stability of the network.

In BP networks, the number of hidden neurons determines how well a problem can be learned. If too many are used, the network will tend to try to memorize the problem, and thus not generalize well later. If too few are used, the network will generalize well but may not have enough ‘power’ to learn the patterns well. Getting the right number of hidden neurons is a matter of trial and error, since there is no science to it. In general the number of hidden neurons (N) may be estimated by applying the following empirical formula

$$N = \frac{I + O}{2} + \sqrt{P_i}$$

where I is the number of input parameters, O is the number of output parameters and P_i is the number of training patterns available.

The feedforward with multiple hidden slabs are very powerful to detect different features of the input vectors when different activation functions are given to the hidden slabs. This architecture shown in Figure 21 has been used in a number of engineering problems for modeling and prediction with very good results.

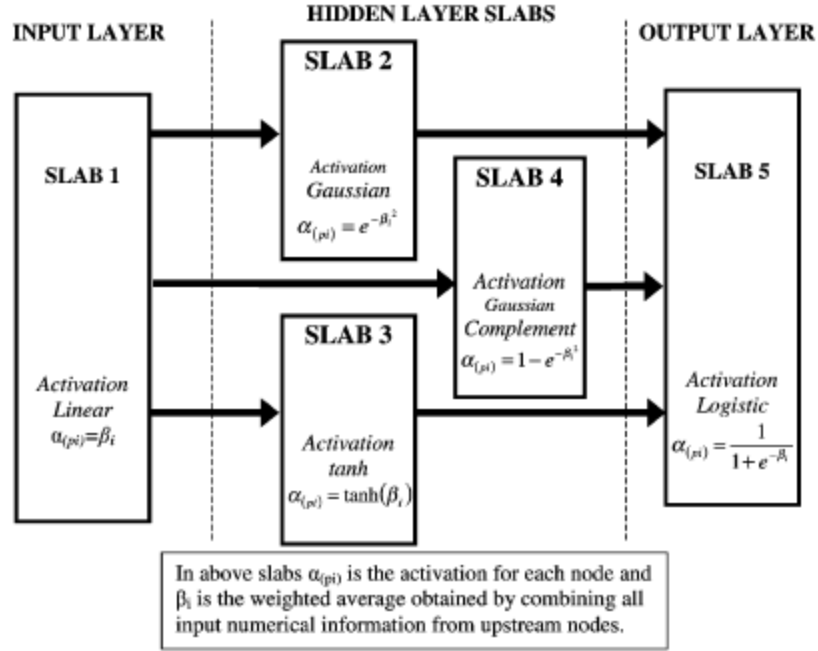


Figure 21 Feed Forward with multiple hidden slabs architecture

The information processing at each node site is performed by combining all input numerical information from upstream nodes in a weighted average of the form:

$$\beta_i = \sum_j w_{ij} \alpha_{pi} + b_1$$

where α_{pi} is the activation for each node and b_1 is a constant term referred to as the bias.

The final nodal output is computed via the activation function. This architecture has different activation functions in each slab. By referring to Figure 21, the input slab activation function is linear, i.e. $\alpha_{pi} = \beta_i$ (where β_i is the weighted average obtained by combining all input numerical information from upstream nodes), while the activations used in the other slabs are:

Gaussian for slab 2:

$$\alpha_{pi} = e^{-\beta_i^2}$$

Tanh for slab 3:

$$\alpha_{pi} = \tanh(\beta_i)$$

Gaussian complement for slab 4:

$$\alpha_{pi} = 1 - e^{-\beta_i^2}$$

Logistic for output slab:

$$\alpha_{pi} = \frac{1}{1 + e^{-\beta_i}}$$

Different activation functions are applied to hidden layer slabs in order to detect different features in a pattern processed through a network. The number of hidden neurons in the hidden layers may also be calculated. However, an increased number of hidden neurons may be used in order to get more ‘degrees of freedom’ and allow the network to store more complex patterns. This is usually done when the input data are highly non-linear. It is recommended in this architecture to use Gaussian function on one hidden slab to detect features in the mid-range of the data and Gaussian complement in another hidden slab to detect features from the upper and lower extremes of the data. Combining the two feature sets in the output layer may lead to a better prediction. (Kalogirou, 2003)

4.5 Adaptive Neuro Fuzzy Inference System (ANFIS)

The Adaptive Neuro-Fuzzy Inference System (ANFIS) technique was originally presented by Jang in 1993. ANFIS is a simple data learning technique that uses Fuzzy Logic to transform given inputs into a desired output through highly interconnected Neural Network processing elements and information connections, which are weighted to map the numerical inputs into an output. ANFIS combines the benefits of the two machine learning techniques (Fuzzy Logic and Neural Network) into a single technique. An ANFIS works by applying Neural Network learning methods to tune the parameters of a Fuzzy Inference System (FIS). There are several features that enable ANFIS to achieve great success (Jang, 1993), (Jang, 1995):

- It refines fuzzy IF-THEN rules to describe the behavior of a complex system;
- It does not require prior human expertise;
- It is easy to implement;
- It enables fast and accurate learning;
- It offers desired data set; greater choice of membership functions to use; strong generalization abilities; excellent explanation facilities through fuzzy rules; and
- It is easy to incorporate both linguistic and numeric knowledge for problem solving.

Different rules cannot share the same output membership function. The number of membership functions must be equal to the number of rules. To represent the ANFIS

architecture, two fuzzy IF-THEN rules based on a first order Sugeno model are considered:

Rule (1): *IF x is A₁ AND y is B₁, THEN*

$$f_1 = p_1x + q_1y + r_1$$

Rule (2): *IF x is A₂ AND y is B₂, THEN*

$$f_2 = p_2x + q_2y + r_2$$

Where:

- x and y are the inputs,
- A_i and B_i are the fuzzy sets,
- f_i are the outputs within the fuzzy region specified by the fuzzy rule, and
- p_i, q_i, and r_i are the design parameters that are determined during the training process.

The ANFIS architecture used to implement these two rules is shown in Figure 4. In this figure, a circle indicates a fixed node, whereas a square indicates an adaptive node. ANFIS has a five-layer architecture. Each layer is explained in detail below.

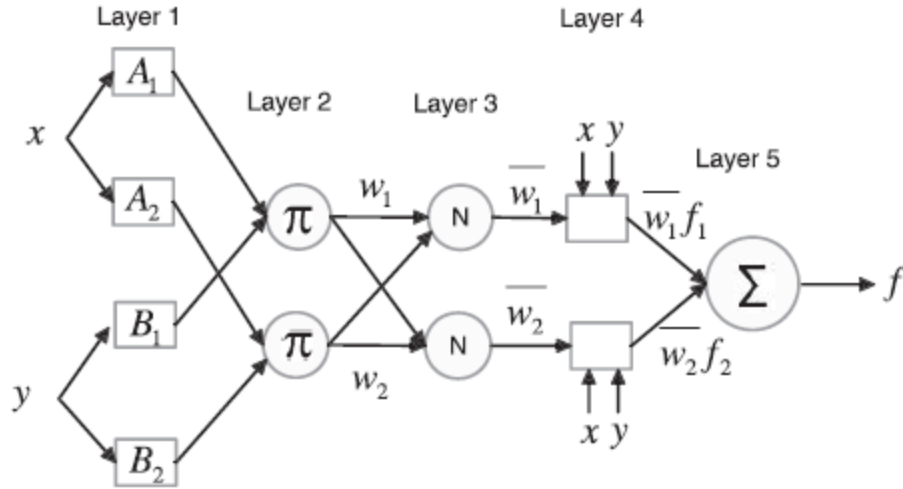


Figure 22 ANFIS architecture

In Layer 1, all the nodes are adaptive nodes. The outputs of Layer 1 are the fuzzy membership grade of the inputs, which are given by the following equations:

$$O_{1,i} = \mu A_i(x) ; i = 1, 2, \text{ and}$$

$$O_{1,i} = \mu B_{i-2}(y) ; i = 3, 4$$

Where x and y are the inputs to node i , and A_i and B_i are the linguistic labels (high, low, etc.) associated with this node function. $\mu A_i(x)$ and $\mu B_{i-2}(y)$ can adopt any fuzzy membership function. For example, if the bell-shaped membership function is employed, $\mu A_i(x)$ is given by

$$\mu A_i(x) = \frac{1}{1 + \left[\left(\frac{x - c_i}{a_i} \right)^2 \right]^{b_i}}, \quad i = 1, 2,$$

or the Gaussian membership function by

$$\mu A_i(x) = \exp \left[- \left(\frac{x - c_i}{a_i} \right)^2 \right], \quad i = 1, 2,$$

where a_i , b_i , and c_i are the parameters of the membership function.

In Layer 2, the nodes are fixed nodes. This layer involves fuzzy operators; it uses the **AND** operator to fuzzify the inputs. They are labeled with π , indicating that they perform as a simple multiplier. The output of this layer can be represented as

$$O_{2,i} = w_i = \mu A_i(x) * \mu B_i(y), \quad i = 1, 2,$$

These are the so-called firing strengths of the rules.

In Layer 3, the nodes are also fixed nodes labeled by N, to indicate that they play a normalization role to the firing strengths from the previous layer. The output of this layer can be represented as

$$O_{3,i} = \bar{w}_i = \frac{w_i}{w_1 + w_2}, \quad i = 1, 2,$$

Outputs of this layer are called normalized firing strengths.

In Layer 4, the nodes are adaptive. The output of each node in this layer is simply the product of the normalized firing strength and a first order polynomial (for a first order Sugeno model). The output of this layer is given by

$$O_{4,i} = \bar{w}_i f_i = \bar{w}_i (p_i x + q_i y + r_i), \quad i = 1, 2,$$

Where \bar{w} is the output of Layer 3, and p_i , q_i , and r_i are the consequent parameters.

In Layer 5, there is only one single fixed node labeled with Σ . This node performs the summation of all incoming signals. The overall output of the model is given by

$$O_{5,i} = \sum_i \bar{w}_i f_i = \frac{\sum_i w_i f_i}{\sum_i w_i}, \quad i = 1, 2$$

CHAPTER 5

NO_x EMISSION MODELING

5.1 Process data analysis

Initially 16 process data tags were selected, to test their influence on the NO_x formation which are detailed on Table 2:

Table 2 Process data ranges during start up.

DATA	START UP RANGE		UNIT
	MINIMUM	MAXIMUM	
COMPRESSOR INLET AIR FLOW	5.3	378.2	kg/s
COMPRESSOR DISCHARGE TEMPERATURE	45.8	414.3	°C
FUEL FLOW	1.8	8.1	Kg/s
AIR/FUEL	2.7	120.1	
FIRING TEMPERATURE	46.0	1313.9	°C
LHV	876.3	878.7	BTU/scf
N2	8.8	8.9	mole%
LOAD	0.4	145.6	MW
STEAM FLOW	0.0	290.7	tons/hr
HRSG STEAM TEMPERATURE	266.1	379.6	°C
HRSG STEAM PRESSURE	44.4	44.7	bar
NO _x	0.8	129.5	ppmvd
CO	1.1	792.5	ppm
O2	12.2	20.2	mole%
AMBIENT TEMPERATURE	29.9	42.2	°C
RELATIVE HUMIDITY	11.9	72.4	%

Then about 2000 data sets with 20 seconds increment were collected for these tags during the startup of the CGTG (0 to 50% load). The sensitivity of these tags and their influence on NO_x formation was studied and analyzed.

5.1.1 Sensitivity analysis

Figure 23 presents the time variations of the important operating variables namely; Load (MW), Firing temperature (°C), Compressor discharge temperature (°C), Steam flow (ton/h), and Compressor inlet air flow (kg/sec). These process variables are directly proportional and in harmony with the NO_x formation.

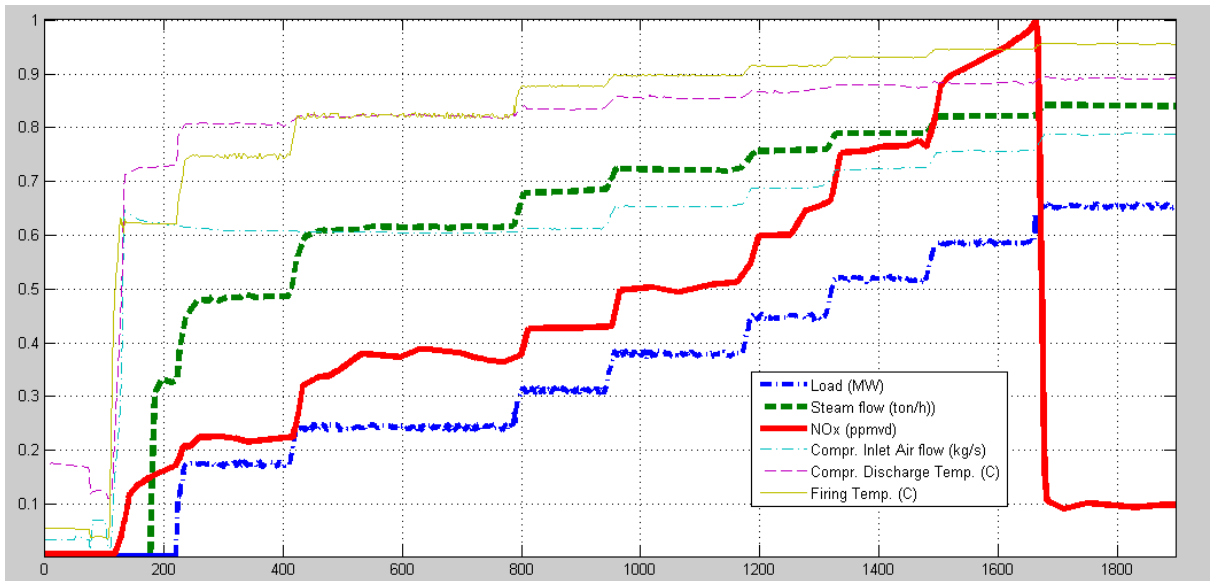


Figure 23 Process data in direct proportionality with NO_x formation

However, the Air to Fuel ratio is inversely proportional to the NO_x formation as shown in Figure 24:

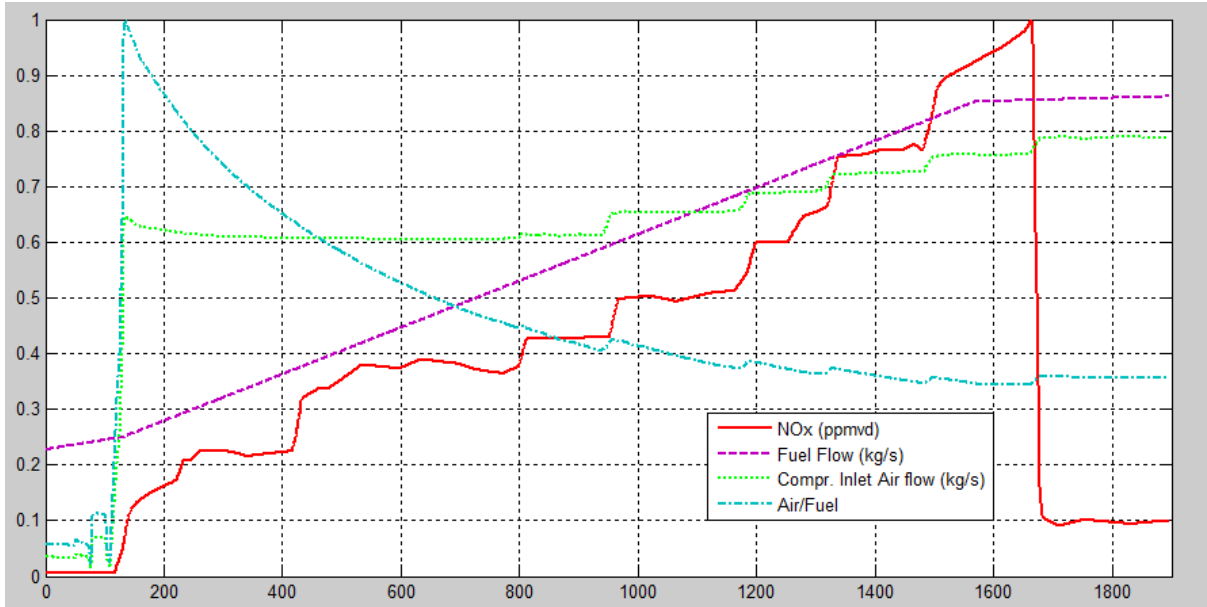


Figure 24 Inverse proportionality of Air/Fuel Ratio with NO_x formation

On the other hand, Figure 25 shows that LHV value, N₂ in fuel, the HRSG steam temperature, and HRSG steam pressure are almost constant without significant changes and have no clear influence on the NO_x formation. Hence, it will be excluded from the PEMS model.

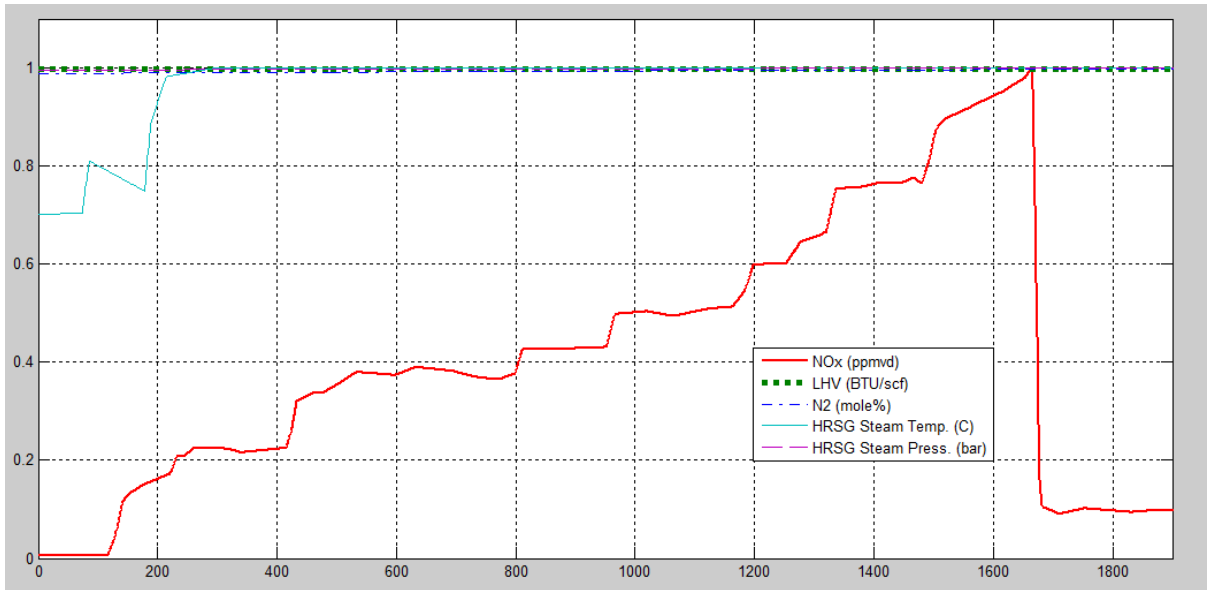


Figure 25 Constant process data with no clear influence on NO_x formation

Although, there is variation in the ambient temperature but there is no clear significant effect on the NO_x formation as shown in Figure 26. Also, the figure does not show clear correlation with the NO_x formation for the rest of the tags. But these tags (O₂, CO, and Relative humidity) are added to the PEMS model as they are theoretically contributing to the NO_x formation.

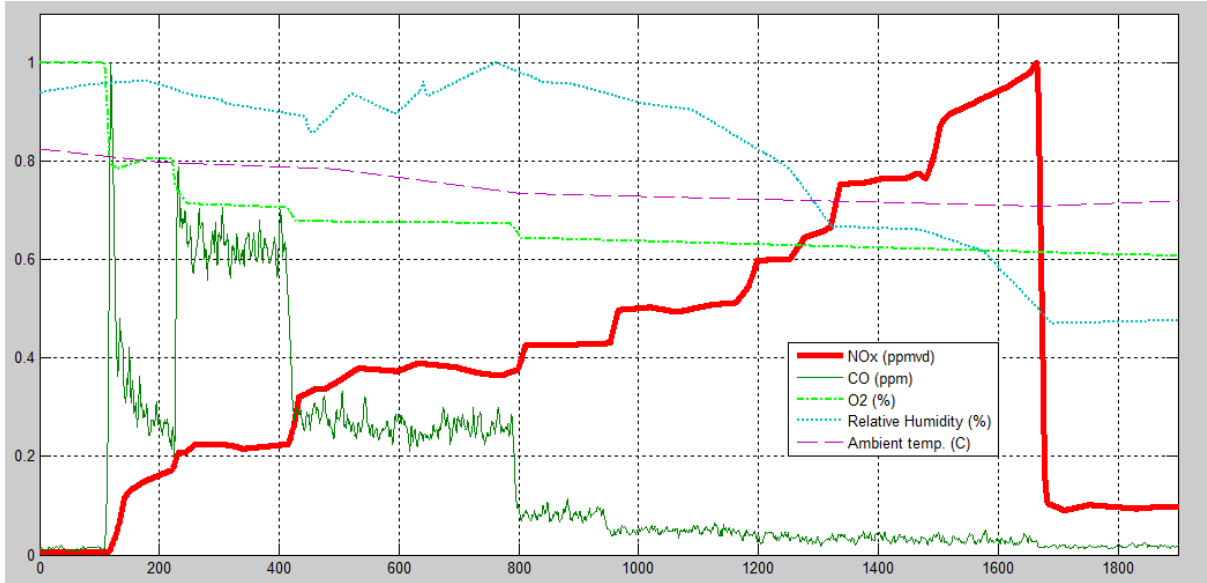


Figure 26 Process data with no clear correlation with NO_x

5.1.2 Process data correlation with NO_x

The correlation of the process data with NO_x were calculated using excel correlation tool. The excel correlation tool is based on Pearson Product-Moment Correlation which is the covariance of two variables divided by the product of their standard deviations. Below is the correlation equation (Pearson, 1895):

$$\rho_{xy} = \frac{Cov(X,Y)}{\sigma_x \sigma_y}$$

The strength of relationship is identified based on the coefficient "ρ" as explained in

Table 3:

Table 3 Strength of relationship corresponding to correlation coefficient ρ

Value of "ρ"	Strength of relationship
-1.0 to -0.5 or 1.0 to 0.5	Strong
-0.5 to -0.1 or 0.1 to 0.5	Weak
-0.1 to 0.1	None or really weak

Table 4, lists the calculated correlation coefficient for different process variables.

Table 4 Correlation coefficient for process variables

CORRELATION WITH		NOx (ppm)
LOAD	(MW)	0.978140044
Fuel flow	(kg/sec)	0.970637383
Relative Humidity	(%)	-0.868172776
Steam flow	(ton/h)	0.853315575
O2	(%)	-0.764797893
Firing temp	(°C)	0.739775129
Compr. Inlet air flow	(kg/sec)	0.725366018
Turbine exhaust temp	(°C)	0.652710826
Comp. disch. Temp	(°C)	0.647837055
CO	(ppm)	-0.541661133

Based on the modeling approach used in the literature review and the above correlation results, the following ten inputs were selected as inputs to the PEMS model:

1. Load (MW).

Used for modeling by (Azid, 2000), (Cicccone, 2005), (Rusinowski, 2007), (Ligang, 2008), (Smrekar, 2009), (Bartolini, 2010)

2. Fuel flow (kg/sec).

Used for modeling by (Ikonen, 2000), (Azid, 2000), (Steohen, 2000), (Hao, 2001), (Chong, 2001), (Zhou, 2003), (Cicccone, 2005), (Shakil, 2008)

3. Firing temperature (°C).

4. Compressor discharge temperature (°C).

Used for modeling by (Cicccone, 2005)

5. Steam flow (ton/h).

6. Air flow (kg/sec).

Used for modeling by (Ikonen, 2000), (Steohen, 2000), (Hao, 2001), (Chong, 2001), (Tronci, 2002), (Zhou, 2003), (Cicccone, 2005), (Ligang, 2008), (Shakil, 2008)

7. Air to fuel ratio.

Used for modeling by (Kesgin, 2003), (Shakil, 2008)

8. O₂ (%).

Used in modeling by (Hao, 2001), (Chong, 2001), (Zhou, 2003), (Rusinowski, 2007), (Ligang, 2008)

9. CO (%).

10. Relative humidity (%).

Used for modeling by (Fast, 2009)

5.2 ANFIS Modelling

The ANFIS modeling was started with ten inputs (load, steam flow, CO, O₂, fuel flow, compressor inlet air flow, air to fuel ratio, compressor discharge temperature, firing temperature, and relative humidity) but it was beyond the capability of the PC that indicated out of memory. The same message was received after reducing the inputs to nine; we dropped fuel flow and compressor inlet air flow as they are already represented by the air to fuel ratio. An excessive number of inputs not only impair the transparency of the underlying model, but also increase the complexity of computation necessary for building the model. Therefore, it is necessary to do input selection that finds the priority

of each candidate inputs and uses them accordingly. Specifically, the purposes of input selection include:

1. Removal of noise or irrelevant inputs.
2. Removal of inputs that depends on other inputs.
3. Make the underlying model more concise and transparent.
4. Reduce the time for model construction.

Now we will reduce the number of inputs for ANFIS modeling based on the above criteria and the data analysis results obtained through the trends and correlation coefficients. Whereas, the compressor discharge temperature and turbine exhaust temperature were dropped because they are dependent on the firing temperature. Also, we dropped fuel flow and compressor inlet air flow as they are already represented by the air to fuel ratio. Finally, the CO was dropped as it has weak correlation (-0.5417) with NO_x. Therefore, the ten inputs reduced to six as listed below:

1. Load.
2. Steam flow.
3. O₂.
4. Air to fuel ratio.
5. Firing temperature.
6. Relative humidity.

The ANFIS model was designed through employing several experiments on different models, each model with different design settings and epoch numbers. The performance

of each ANFIS model was evaluated based on the standard error produced. Then, the overall comparison has identified the best ANFIS model with the optimal settings that developed highest predictability and least standard error.

5.2.1 ANFIS model with six inputs (X*X*X*X*X*X)

The ANFIS modeling started initially with the simple form for six inputs with 2*2*2*2*2*2 combination of membership function numbers. Then the ANFI (2*2*2*2*2*2) model was tested at different epoch trials for each membership function type; namely Triangular, Trapezoidal, Generalized bell, Gaussian, 2-sided Gaussian, Pi (π), Difference Sigmoidal, and Product Sigmoidal. Note that, throughout the course of ANFIS modeling experiments it was identified that the Trapezoidal, 2-sided Gaussian, Difference Sigmoidal, and Product Sigmoidal membership functions are producing the least error among the other membership function types. Hence, the ANFIS modeling discussion will be focused on those functions only.

The basic ANFIS (2*2*2*2*2*2) model is assigning 2 membership functions for each of the four inputs, 12 functions altogether. The generated fuzzy inference system structure contains 64 fuzzy rules and 496 total number of parameters. Figure 27, shows that the best performance was achieved through applying the Trapezoidal membership function with single epoch which generated a minimum error of 0.019244.

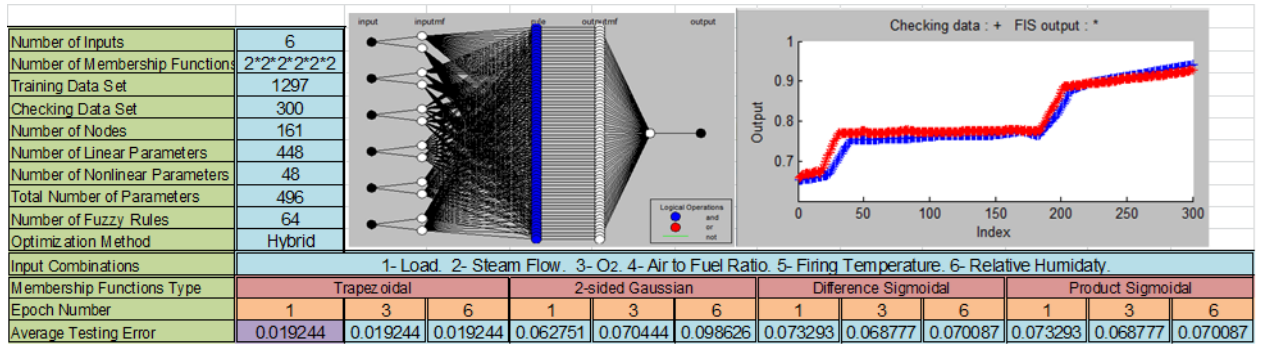


Figure 27 ANFIS (2*2*2*2*2) model

Now we will study the effect of increasing the number of membership functions assigned to the inputs. We designed new ANFIS (3*3*3*3*3*3) model as detailed on Figure 28, at which 3 membership functions were assigned for each input of the six inputs, 18 functions altogether. The generated fuzzy inference system structure contains 729 fuzzy rules and the total number of parameters is 5175 which is obviously too large and it is beyond the capability of the PC that indicated out of memory. Hence, the effect of increasing the number of membership functions assigned to the inputs can't be studied with six inputs.

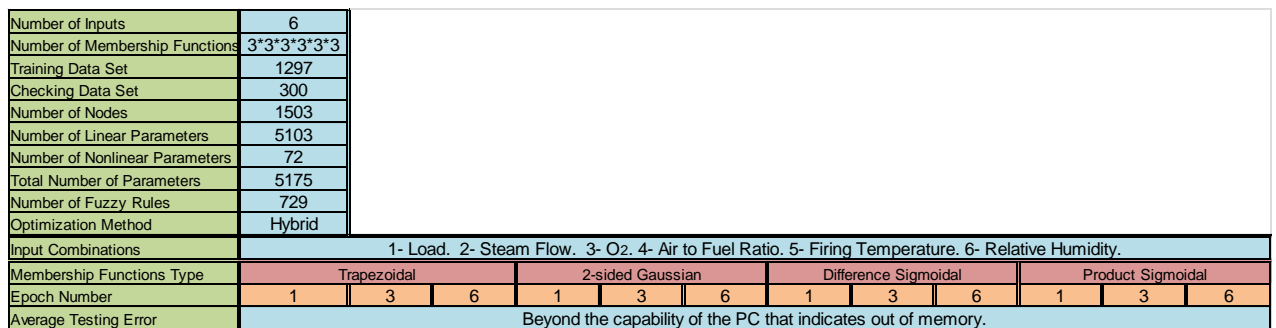


Figure 28 ANFIS (3*3*3*3*3*3) model.

Now we will try to improve the ANFIS (2*2*2*2*2*2) model through studying the effect of increasing the number of membership functions of one input at a time. This was applied on each individual input and on each trial the number of membership functions has been increased by one till the optimal results is sustained. The best results from all these trials were attained from ANFIS (2*2*2*2*12*2) model described in Figure 29 below. This model assigned 12 membership functions to input#5 (Firing Temperature), 22 functions altogether. The generated fuzzy inference system structure contains 384 fuzzy rules. The Trapezoidal membership function produced the best performance at epoch number 1 with minimum error of 0.039804. Note that, this error is higher than the error (0.019244) obtained from the basic ANFIS (2*2*2*2*2*2) model.

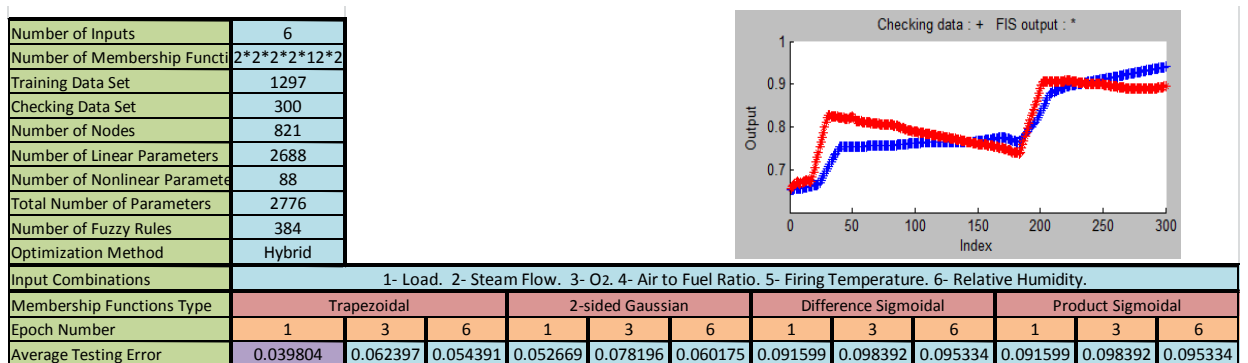


Figure 29 ANFIS (2*2*2*2*12*2) model.

Now we will try to improve the ANFIS (2*2*2*2*2*2) model through studying the effect of increasing the number of membership functions of two inputs at a time. This was applied alternatively on a combination of two inputs out of the six inputs; (X*X*2*2*2*2), (2*X*X*2*2*2*2), (2*2*X*X*2*2*2*2), (2*2*2*X*X*2*2*2*2), (2*2*2*2*X*X*2*2*2*2),

$(X^2 \times X^2 \times X^2)$, $(X^2 \times X^2 \times X^2)$, $(X^2 \times X^2 \times X^2)$, $(X^2 \times X^2 \times X^2 \times X)$, $(2 \times X^2 \times X^2 \times X)$,
 $(2 \times X^2 \times X^2 \times X)$, $(2 \times X^2 \times X^2 \times X)$, $(2 \times X^2 \times X^2 \times X)$, $(2 \times X^2 \times X^2 \times X)$, and
 $(2 \times X^2 \times X^2 \times X^2)$. Actually, we will test the developed fifteen ANFIS models through
 increasing the assigned membership functions for the predetermined pair of inputs by one
 till the optimal results is obtained for each model. Hence, the best model out of the
 fifteen models will be identified.

Throughout the course of training and testing of these models, it was identified that the
 ANFIS $(2 \times X^2 \times X^2 \times X^2)$ model is the best among the other combinations. In this model,
 the number of the membership functions for input#2 (Steam Flow) and input#5 (Firing
 Temperature) is increased by one. First we generated ANFIS $(2 \times 3 \times X^2 \times 3 \times X^2)$ model that
 contains 14 functions altogether, 144 fuzzy rules and 1064 total number of parameters as
 shown in Figure 30. For this structure, the Trapezoidal membership function produced
 the best performance among the others at epoch number 1 with minimum error of
 0.021058. Note that, this error is higher than the error (0.019244) obtained from the
 basic ANFIS $(2 \times X^2 \times X^2 \times X^2)$ model.

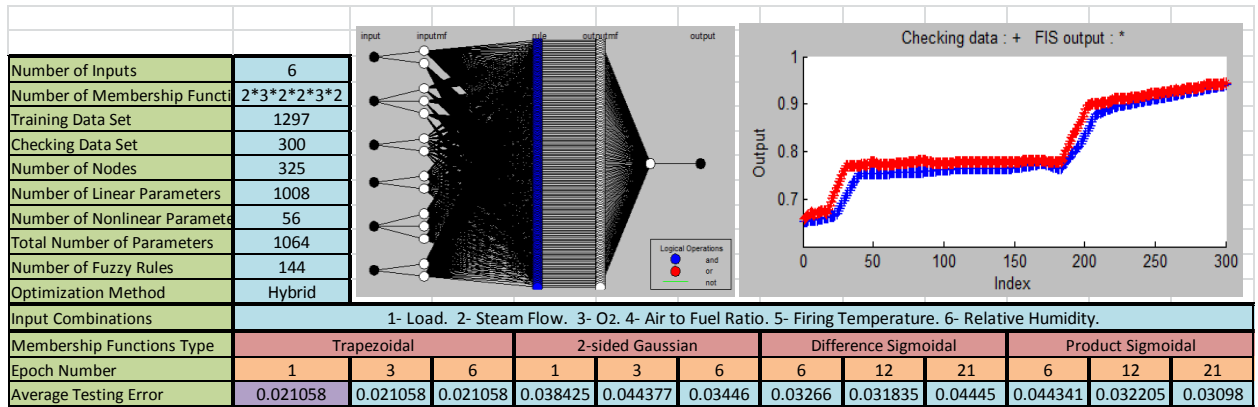


Figure 30 ANFIS (2*3*2*2*3*2) model.

Then we further increased the number of membership functions to four and generated ANFIS (2*4*2*2*4*2) model that contains 16 functions altogether, 256 fuzzy rules and 1856 total number of parameters as shown in Figure 31. For this structure, the Trapezoidal membership function produced the best performance among the others at epoch number 1 with minimum error of 0.033621. Note that, this error is higher than the error (0.021058) obtained from the ANFIS (2*3*2*2*3*2) model which is already higher than the basic ANFIS (2*2*2*2*2*2) model error.

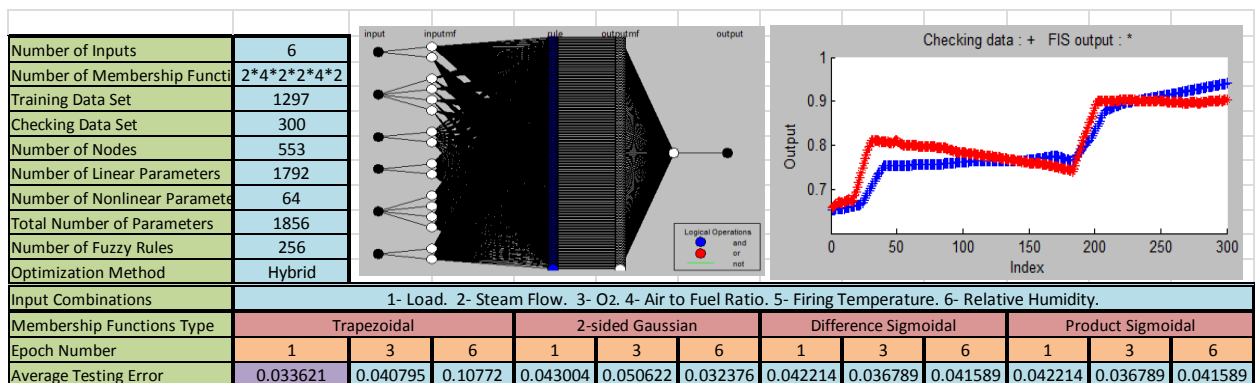


Figure 31 ANFIS (2*4*2*2*4*2) model.

Therefore, increasing the number of membership functions for the ANFIS (2*2*2*2*2*2) model for one input or more or even all will not necessarily improve the model predictability nor reduce the error. In fact, it will complicate the model, increase the computational time, and usually leads to model over fitting. In fact, the best performance for six inputs was obtained through the basic model ANFIS (2*2*2*2*2*2) with an error of 0.019244.

In the next section we will study the effect of reducing the number of ANFIS inputs to five on the ANFIS predictability.

5.2.2 ANFIS with five inputs (X*X*X*X*X):

Here we have to get rid of one input from the previous ANFIS structure. By referring to the trend , it was concluded that both O₂ and relative humidity have no clear correlation with NO_x unlike the air to fuel ratio that shows inverse proportionality with NO_x, and direct proportionality is shown by load, steam flow, and firing temperature. Hence, we will test new ANFIS models by removing O₂ or relative humidity alternatively from the inputs.

We will start with removing the relative humidity from the inputs. So, the five inputs will be load, steam flow, O₂, air/fuel ratio, and firing temperature. It is a good practice to start with the basic structure for Five inputs; ANFIS (2*2*2*2*2). This model is

assigning 2 membership functions to each of the five inputs, 10 functions altogether. The generated fuzzy inference system structure contains 32 fuzzy rules and 232 total number of parameters. Figure 32, shows that this ANFIS model performs best with a Trapezoidal membership function at epoch number 6 with minimum error of 0.01848 which is lower than the error (0.019244) generated by the previously identified best model for six inputs ANFIS (2*2*2*2*2*2). Therefore, decreasing the number of inputs not only improved the predictability but also decreased the complexity of computation necessary for building the model.

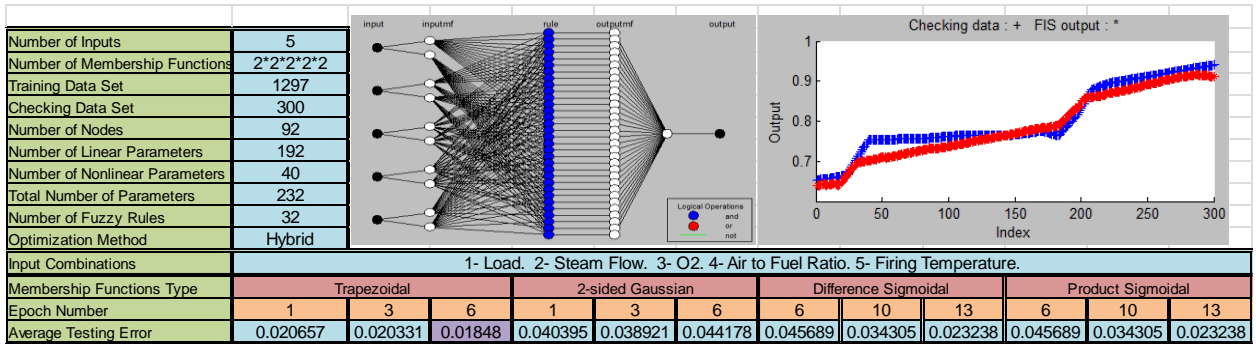


Figure 32 ANFIS (2*2*2*2*2) model with O2.

Now we will study the effect of increasing the number of membership functions assigned to the inputs. We designed new ANFIS (3*3*3*3*3) model as detailed on Figure 33, at which 3 membership functions were assigned for each input of the five inputs, 15 functions altogether. The generated fuzzy inference system structure contains 243 fuzzy rules and 1518 total number of parameters. The best performance attained by this structure is with Trapezoidal membership functions at epoch number 10 that produced an

average testing error of 0.030159. Note that, this error is higher than the one produced (0.01848) with the basic ANFIS (2*2*2*2*2) model.

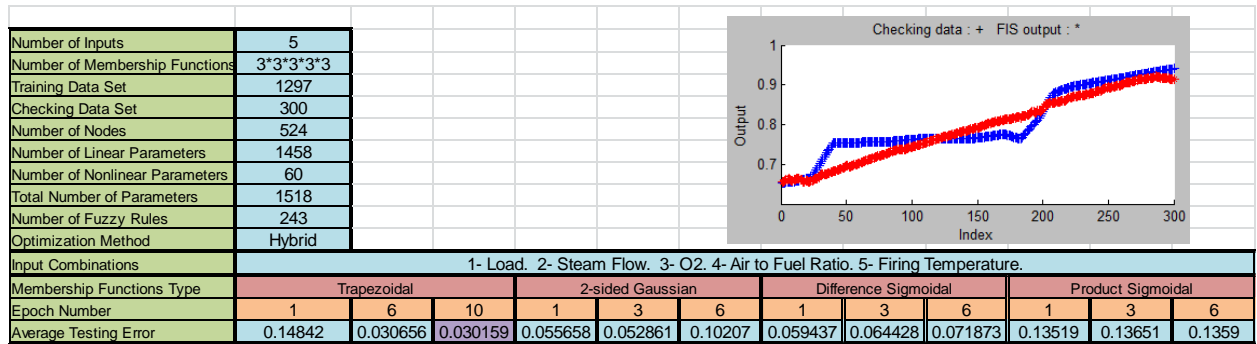


Figure 33 ANFIS (3*3*3*3*3) model with O2.

We further increased the number of membership functions to 4 and developed ANFIS (4*4*4*4*4) model which is assigning 4 membership functions to each input of the five inputs, 20 functions altogether. The generated fuzzy inference system structure contains $4^5 = 1024$ fuzzy rules which is large and beyond the capability of the PC and mat lab program that indicated out of memory. Hence, increasing the membership functions assigned to the inputs not necessarily will improve the model predictability nor reduce the error. In fact, it will complicate the model, increase the computational time, and usually leads to model overfitting.

Now we will try to improve the ANFIS (2*2*2*2*2) model through studying the effect of increasing the number of membership functions of one input at a time. This was

applied on each individual input and on each trial the number of membership functions has been increased by one till the optimal results is sustained. The best results from all these trials were attained from ANFIS (2*2*2*2*12) model described in Figure 34. This model assigned 12 membership functions to input#5 (Firing Temperature), 20 functions altogether. The generated fuzzy inference system structure contains 192 fuzzy rules and 1232 total number of parameters. The Difference Sigmoidal and Product Sigmoidal membership functions produced the best performance at epoch number 6 with minimum error of 0.019544. Note that, this error is higher than the error (0.01848) obtained from the basic ANFIS (2*2*2*2*2) model.

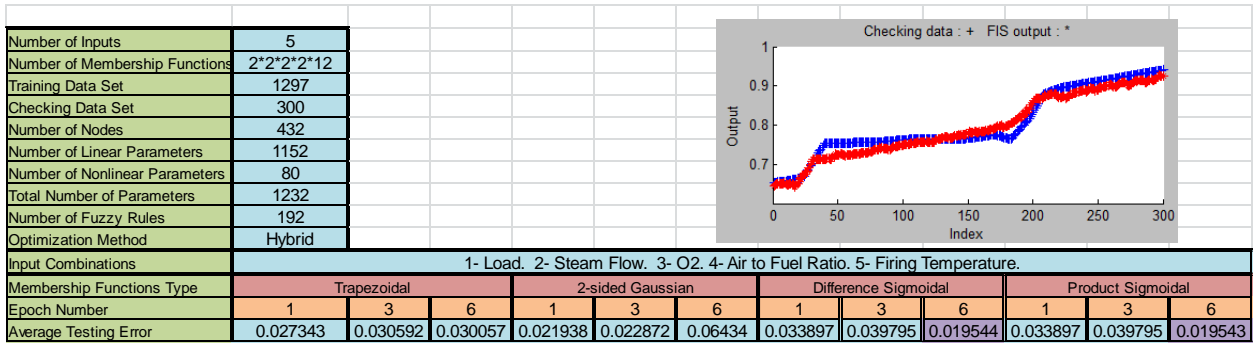


Figure 34 ANFIS (2*2*2*2*12) model with O2.

Now we will try to improve the ANFIS (2*2*2*2*2) model through studying the effect of increasing the number of membership functions of two inputs at a time. This was applied alternatively on a combination of two inputs out of the five inputs; (X*X*2*2*2), (X*2*X*2*2), (X*2*2*X*2), (X*2*2*2*X), (2*X*2*2*X), (2*2*X*2*X), (2*2*2*X*X), (2*X*X*2*2), (2*2*X*X*2), and (2*X*2*X*2). Actually, we will test

the developed ten ANFIS models through increasing the assigned membership functions for the predetermined pair of inputs by one till the optimal results is obtained for each model. Hence, the best model out of the ten models will be identified.

Throughout the course of training and testing of these models, it was identified that the ANFIS (2*X*2*2*X) model is the best among the other combinations. In this model, the number of the membership functions for input#2 (Steam Flow) and input#5 (Firing Temperature) is increased by one. First we generated ANFIS (2*3*2*2*3) model that contains 12 functions altogether, 72 fuzzy rules and 480 total number of parameters as shown in Figure 35. For this structure, the Trapezoidal membership function produced the best performance at epoch number 1 with minimum error of 0.018564. Note that, this error is higher than the error (0.01848) obtained from the basic ANFIS (2*2*2*2*2) model.

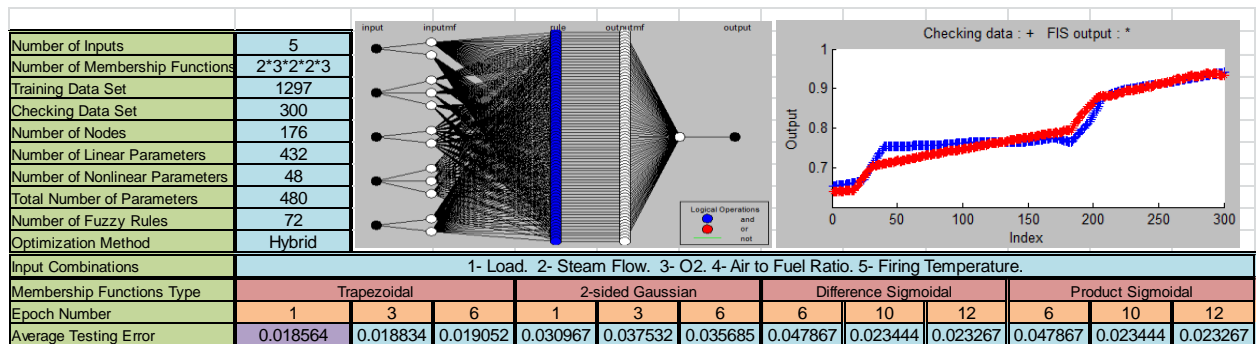


Figure 35 ANFIS (2*3*2*2*3) model with O2.

Then we further increased the number of membership functions to four and generated ANFIS (2*4*2*2*4) model that contains 14 functions altogether, 128 fuzzy rules and 824

total number of parameters as shown in Figure 36. For this structure, the Trapezoidal membership function produced the best performance among the others at epoch number 3 with minimum error of 0.019048. Note that, this error is higher than the error (0.018564) obtained from the ANFIS (2*3*2*2*3) model which is already higher than the basic ANFIS (2*2*2*2*2) model error.

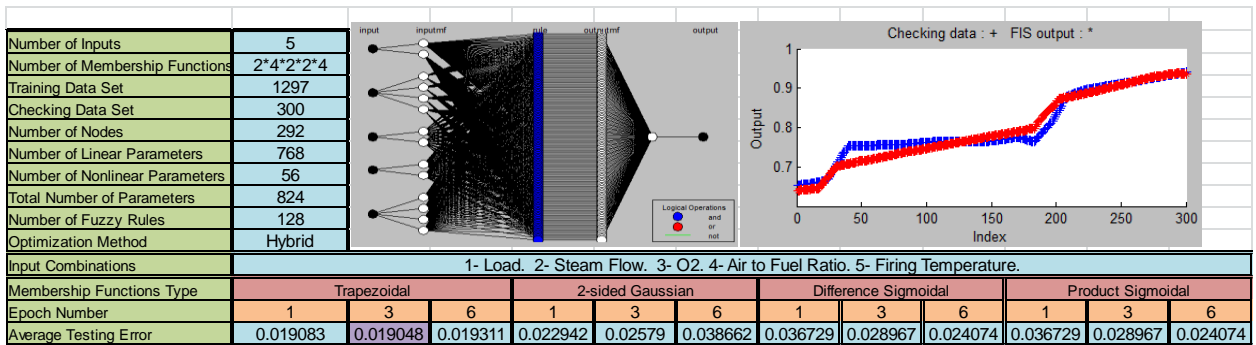


Figure 36 ANFIS (2*4*2*2*4) model with O2.

Therefore, increasing the number of membership functions for the ANFIS (2*2*2*2*2) model with O2 for one input or more or even all will not necessarily improve the model predictability nor reduce the error. In fact, it will complicate the model, increase the computational time, and usually leads to model over fitting. In fact, the best model for five inputs including O2 is the basic ANFIS (2*2*2*2*2) model with a generated error of 0.01848.

Similarly now we will test the ANFIS with five inputs including the relative humidity instead of O2. So, the five inputs will be load, steam flow, air/fuel ratio, firing temperature, and relative humidity. We started with the basic structure for Five inputs;

ANFIS (2*2*2*2*2). This model is assigning 2 membership functions to each of the five inputs, 10 functions altogether. The generated fuzzy inference system structure contains 32 fuzzy rules and 232 total number of parameters. Figure 37, shows that this ANFIS model performs best with a 2-Sided Gaussian membership function at epoch number 1 with minimum error of 0.0293 which is higher than the error (0.019244) generated by the previously identified best model for six inputs ANFIS (2*2*2*2*2*2). Therefore, the removal of O2 from the inputs degraded the performance of the ANFIS predictability.

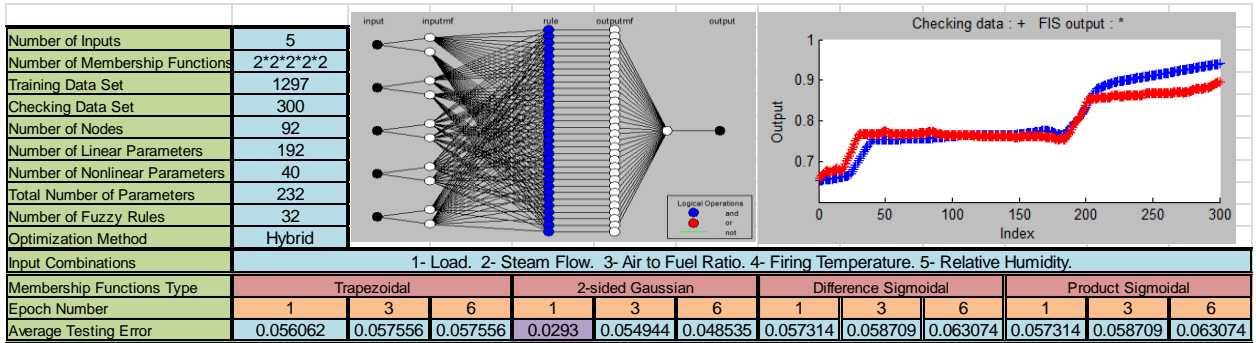


Figure 37 ANFIS (2*2*2*2*2) model with relative humidity.

Now we will study the effect of increasing the number of membership functions assigned to the inputs. We designed new ANFIS (3*3*3*3*3) model as detailed on Figure 38, at which 3 membership functions were assigned for each input of the four inputs, 15 functions altogether. The generated fuzzy inference system structure contains 243 fuzzy rules and 1518 total number of parameters. The best performance attained by this structure is with Difference Sigmoidal and Product Sigmoidal membership functions at epoch number 1 that produced an average testing error of 0.10372. Note that, this error is much higher than the one produced (0.0293) with the basic ANFIS (2*2*2*2*2) model.

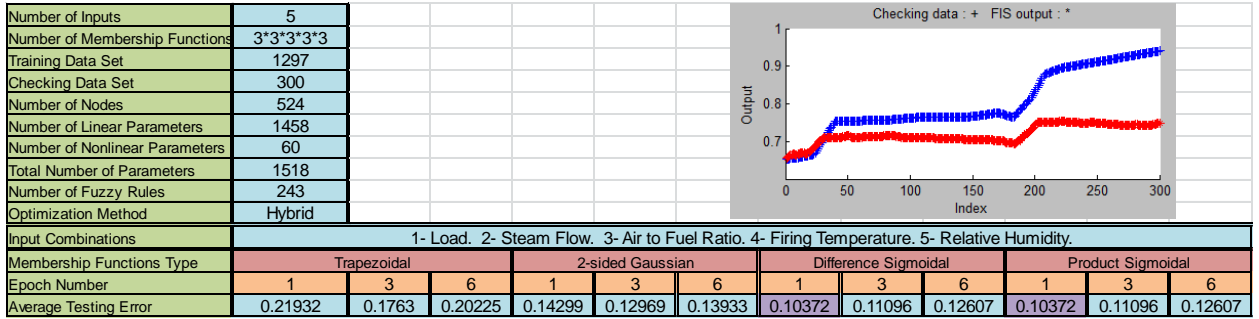


Figure 38 ANFIS (3*3*3*3*3) model with relative humidity.

We further increased the number of membership functions to 4 and developed ANFIS (4*4*4*4*4) model which is assigning 4 membership functions to each input of the five inputs, 20 functions altogether. The generated fuzzy inference system structure contains $4^5 = 1024$ fuzzy rules which is large and beyond the capability of the PC and mat lab program that indicated out of memory. Hence, increasing the membership functions assigned to the inputs not necessarily will improve the model predictability nor reduce the error. In fact, it will complicate the model, increase the computational time, and usually leads to model overfitting.

Now we will try to improve the ANFIS (2*2*2*2*2) model through studying the effect of increasing the number of membership functions of one input at a time. This was applied on each individual input and on each trial the number of membership functions has been increased by one till the optimal results is sustained. The best results from all these trials were attained from ANFIS (2*2*2*12*2) model described in Figure 39. This model assigned 12 membership functions to input#4 (Firing Temperature), 20 functions

altogether. The generated fuzzy inference system structure contains 192 fuzzy rules and 1232 total number of parameters. The Trapezoidal membership function produced the best performance among the others among the others at epoch number 1 with minimum error of 0.040684. Note that, this error is higher than the error (0.0293) obtained from the basic ANFIS (2*2*2*2*2) model.

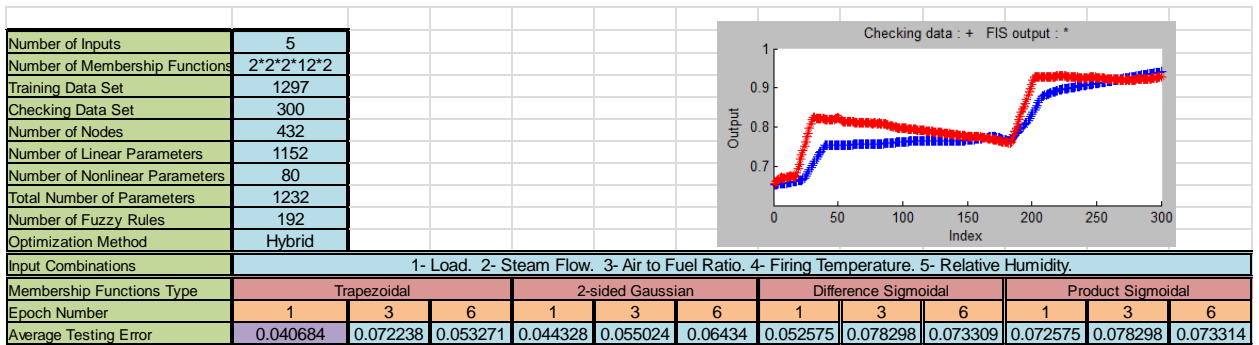


Figure 39 ANFIS (2*2*2*12*2) model with relative humidity.

Now we will try to improve the ANFIS (2*2*2*2*2) model through studying the effect of increasing the number of membership functions of two inputs at a time. This was applied alternatively on a combination of two inputs out of the five inputs; (X*X*2*2*2), (X*2*X*2*2), (X*2*2*X*2), (X*2*2*2*X), (2*X*2*2*X), (2*2*X*2*X), (2*2*2*X*X), (2*X*X*2*2) (2*2*X*X*2), and (2*X*2*X*2). Actually, we will test the developed ten ANFIS models through increasing the assigned membership functions for the predetermined pair of inputs by one till the optimal results is obtained for each model. Hence, the best model out of the ten models will be identified.

Throughout the course of training and testing of these models, it was identified that the ANFIS (2*X*2*X*2) model is the best among the other combinations. In this model, the number of the membership functions for input#2 (Steam Flow) and input#4 (Firing Temperature) is increased by one. First we generated ANFIS (2*3*2*3*2) model that contains 12 functions altogether, 72 fuzzy rules and 480 total number of parameters as shown in Figure 40. For this structure, the 2-Sided Gaussian membership function produced the best performance at epoch number 11 with minimum error of 0.026646. Note that, this error is higher than the error (0.0293) obtained from the basic ANFIS (2*2*2*2*2) model.

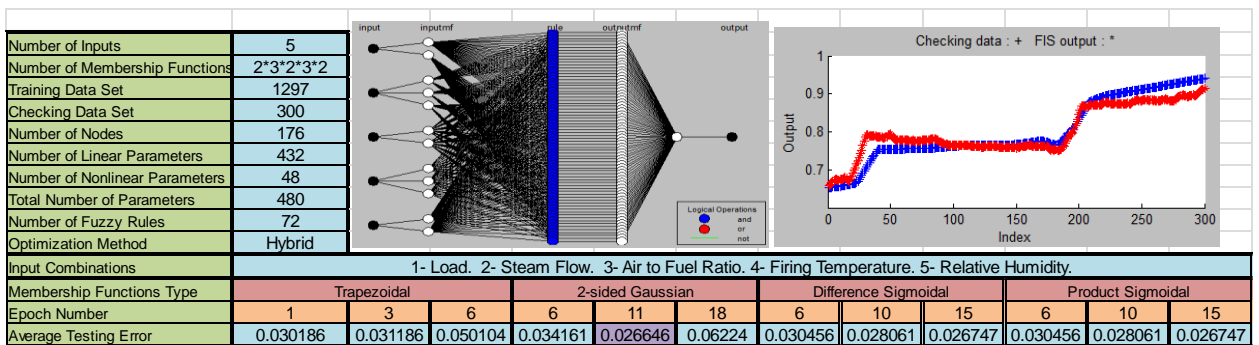


Figure 40 ANFIS (2*3*2*3*2) model with relative humidity.

Then we further increased the number of membership functions to four and generated ANFIS (2*4*2*4*2) model that contains 14 functions altogether, 128 fuzzy rules and 824 total number of parameters as shown in Figure 41. For this structure, the 2-Sided Gaussian membership function produced the best performance at epoch number 6 with minimum error of 0.02816. Note that, this error is higher than the error (0.026646) obtained from the ANFIS (2*3*2*3*2) model.

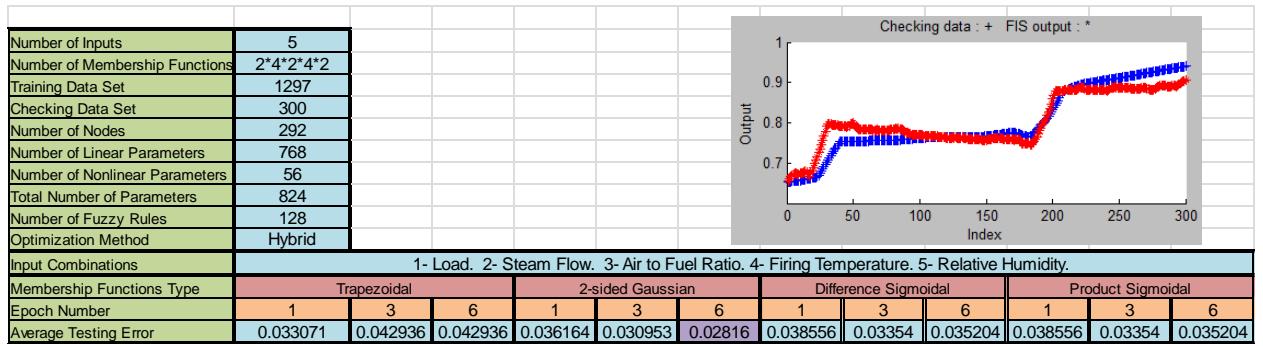


Figure 41 ANFIS (2*4*2*4*2) model with relative humidity.

Therefore, increasing the number of membership functions for the ANFIS (2*2*2*2*2) model for one input or more or even all will not necessarily improve the model predictability nor reduce the error. In fact, it will complicate the model, increase the computational time, and usually leads to model over fitting.

For five inputs including O2, the best ANFIS performance was achieved through the basic (2*2*2*2*2) model with an average error of 0.01848 which is lower than the error (0.019244) generated through the identified best model for six inputs (2*2*2*2*2*2). Hence, reducing the number of inputs might improve the predictability of the ANFIS.

For five inputs including relative humidity, the best ANFIS performance was achieved through (2*3*2*3*2) model with an average error of 0.026646 which is higher than the error (0.019244) generated through the identified best model for six inputs (2*2*2*2*2*2). Therefore, the proper selection of inputs contributes with higher

influence on the ANFIS performance than reducing the number of inputs. Note that, the relative humidity has negative impact on the model performance. Next we will further test the effect of reducing the number of inputs on the ANFIS performance by reducing the number of inputs to four.

5.2.3 ANFIS with four inputs (X*X*X*X):

Here we will get rid of O₂ and relative humidity as they have no clear correlation with NO_x as shown in the trends discussed in the data analysis section. Hence, we will test new ANFIS models by removing O₂ and relative humidity from the inputs.

We will start with the basic ANFIS (2*2*2*2) model which is assigning 2 membership functions for each of the four inputs, 8 functions altogether. The generated fuzzy inference system structure contains 16 fuzzy rules and 112 total number of parameters. Figure 42, shows that this ANFIS model performs best with the Difference Sigmoidal and Product Sigmoidal at epoch number 28 with minimum error of 0.01841 which is lower than the error (0.01848) generated through the identified best model for five inputs (2*2*2*2*2). Hence, decreasing the number of inputs further from six to four improved the predictability of the ANFIS model and simplified its structure.

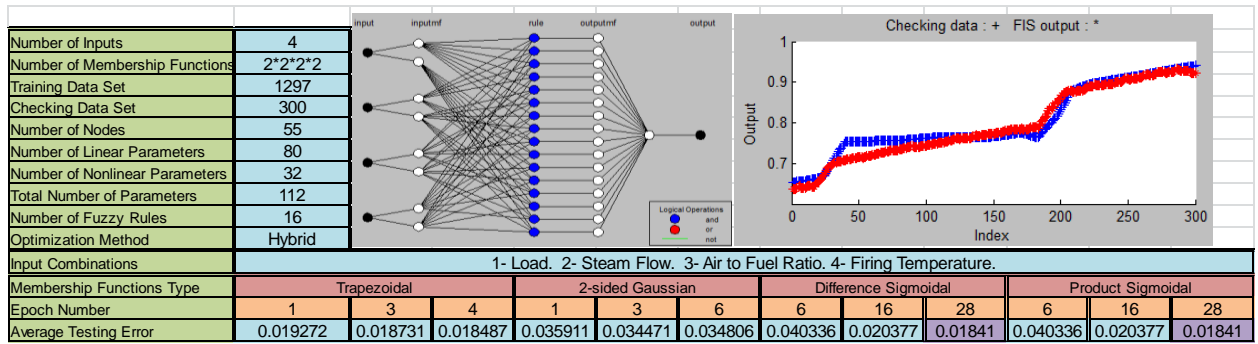


Figure 42 ANFIS (2*2*2*2) model.

Now we will study the effect of increasing the number of membership functions assigned to the inputs. We designed new ANFIS (3*3*3*3) model as detailed on Figure 43, at which 3 membership functions were assigned for each input of the four inputs, 12 functions altogether. The generated fuzzy inference system structure contains 81 fuzzy rules and 453 total number of parameters. The best performance attained by this structure is with 2-Sided Gaussian membership function at epoch number 3 that produced an average testing error of 0.028749. Note that, this error is higher than the error (0.018473) generated by ANFIS (2*2*2*2) model.

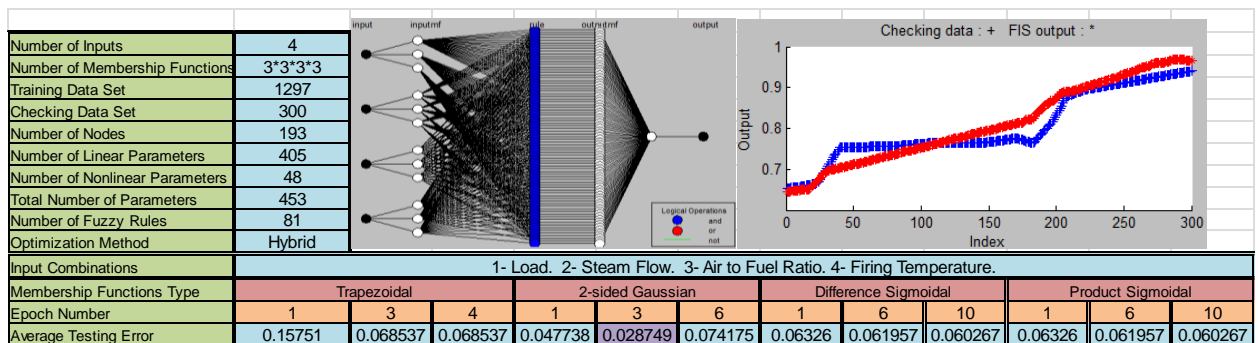


Figure 43 ANFIS (3*3*3*3) model.

We further increased the number of membership functions to 4 and developed ANFIS (4*4*4*4) model which is detailed on Figure 44, at which 4 membership functions were assigned for each input of the four inputs, 16 functions altogether. The generated fuzzy inference system structure contains 256 fuzzy rules and 1344 total number of parameters. The best performance attained by this structure is with Difference Sigmoidal and Product Sigmoidal membership functions at epoch number 1 that produced an average testing error of 0.019568. Note that, this error is still higher than the one produced (0.018473) with the ANFIS (2*2*2*2) model.

Therefore, increasing the number of membership functions assigned to the inputs not necessarily will improve the model predictability nor reduce the error. In fact, it will complicate the model, increase the computational time, and usually leads to model overfitting.

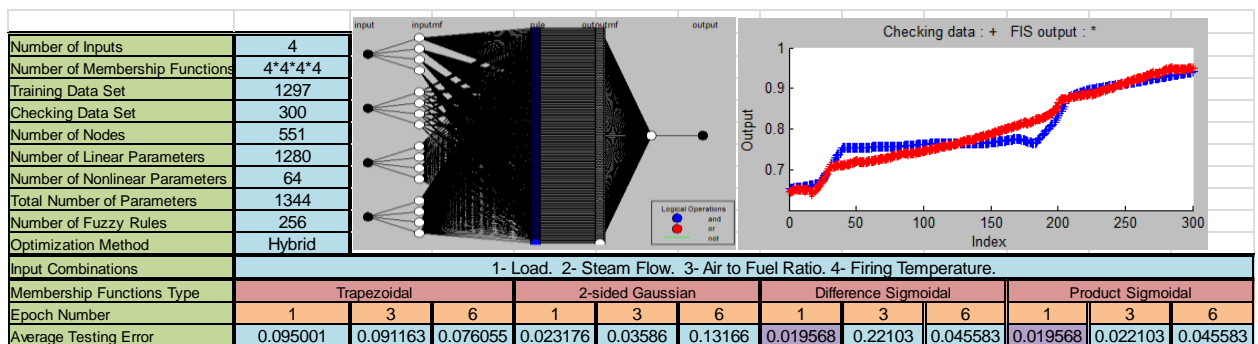


Figure 44 ANFIS (4*4*4*4) model.

Now we will try to improve the ANFIS (2*2*2*2) model through studying the effect of increasing the number of membership functions of one input at a time. This was applied

on each individual input and on each trial the number of membership functions has been increased by one till the optimal results is sustained. The best results from all these trials were attained from ANFIS (2*2*2*12) model described in Figure 45. This model assigned 12 membership functions to input#4 (Firing Temperature), 18 functions altogether. The generated fuzzy inference system structure contains 96 fuzzy rules and 552 total number of parameters. The 2-Sided Gaussian membership function produced the best performance at epoch number 2 with minimum error of 0.017271. Note that, this error is lower than the error (0.018473) obtained from ANFIS (2*2*2*2) model.

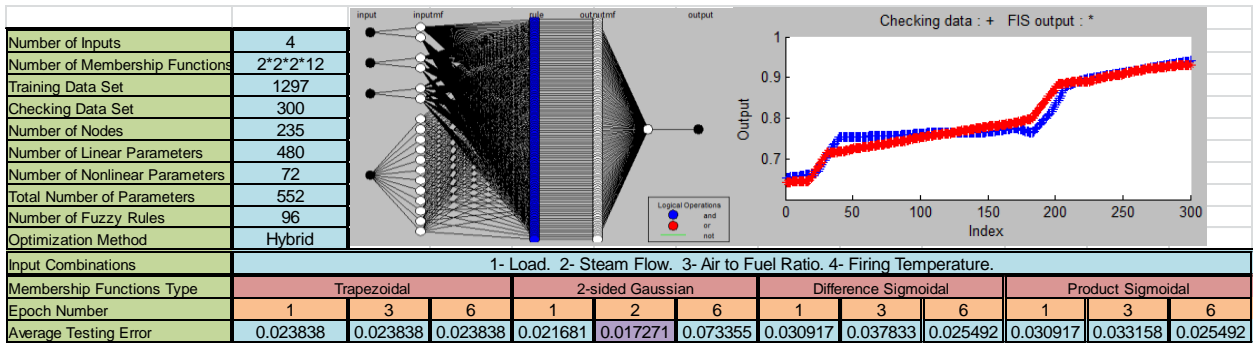


Figure 45 ANFIS (2*2*2*12) model.

Now we will try to improve the ANFIS (2*2*2*2) model through studying the effect of increasing the number of membership functions of two inputs at a time. This was applied alternatively on a combination of two inputs out of the four inputs; (X*X*2*2), (X*2*X*2), (X*2*2*X), (2*X*X*2), (2*2*X*X), and (2*X*2*X). Actually, we will test the developed six ANFIS models through increasing the assigned membership functions for the predetermined pair of inputs by one till the optimal results is obtained for each model. Hence, the best model out of the six models will be identified.

Throughout the course of training and testing of these models, it was identified that the ANFIS (2*8*2*8) model is the best among the other combinations. This model which is detailed on Figure 46, is assigning 2 membership functions to input#1 (Load) and input#3 (Air to Fuel Ratio) and assigning 8 membership functions to input#2 (Steam Flow) and input#4 (Firing Temperature), 20 functions altogether. The generated fuzzy inference system structure contains 256 fuzzy rules and 1360 total number of parameters. The best results obtained for this model is through using Difference Sigmoidal and Product Sigmoidal at epoch number 2 with an average error of 0.017642. Note that, the ANFIS (2*2*2*12) model has produced lower error (0.017271). Therefore, increasing the number of membership functions for two inputs will not necessarily improve the model predictability nor reduce the error. In fact, it will complicate the model, increase the computational time, and usually leads to model overfitting.

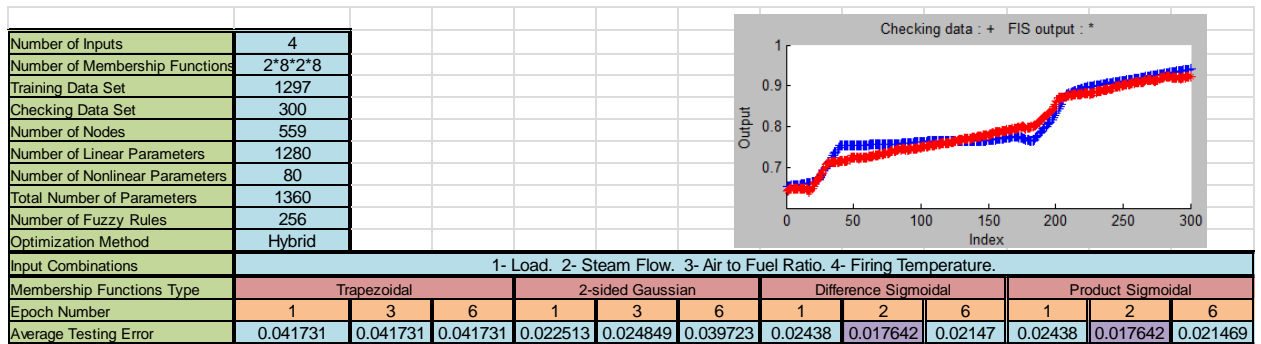


Figure 46 ANFIS (2*8*2*8) model.

5.3 FFBPNN Modelling

The FFBPNN model will be developed to estimate the NO_x emissions in ppm by applying ten inputs as determined in the correlation section. These inputs are Load (MW), Steam Flow (ton/hr), Firing Temperature (°C), Air/Fuel Ratio, CO (ppm), O₂ (%), Fuel Flow (kg/s), Compressor Inlet Air Flow (Kg/s), Relative Humidity (%), and Compressor Discharge Temperature (°C). We employed 1650 real process data sets; about 1150 sets used for training, 250 sets used for validation, and 250 sets used for testing. The training function used is Levenberg-Marquardt.

The FFBPNN model was designed through employing several experiments on different models, each model with different number of hidden neurons. The performance of each FFBPNN model was evaluated at different epoch number based on the Mean Square Error (MSE) produced. Then, the overall comparison has identified the best FFBPNN model with the optimal number of hidden neurons and epoch number at which highest predictability and least MSE error is achieved.

5.3.1 FFBPNN with ten inputs

The FFBPNN modeling started initially with 10 hidden neurons and the best performance was achieved at epoch number 199. The performance was evaluated based on the MSE

error; it was 1.02465E-05 for training, 1.41131E-05 for validation, and 1.96918E-05 for testing. Then, the experiments continued by increasing the number of hidden neurons by one and test it at different number of epochs by comparing the MSE errors. Table 5, summarize the results for some experiments that shows that FFBPNN model with 42 hidden neurons (10-42-1) produced the best performance at epoch number 209 with MSE error of 6.41128E-06 during training, 9.00293E-06 during validation, and 7.18072E-06 during testing. Note that, the experiments were extended till 50 hidden neurons through which the performance of the models was lower than the one obtained through 42 hidden neurons. Therefore, increasing the number of hidden neurons of the FFBPNN model will improve the predictability of the model to certain extent and then if it is increased more it will be degraded due to overfitting.

Table 5 FFBPNN (10 inputs) modeling results.

Number of Inputs	10											
Number of Outputs	1											
Training Data Set	1168											
Validation Data Set	251											
Testing Data Set	251											
Training Function	Levenberg-Marquardt											
Output	Nox											
Inputs	1-Load. 2-Steam Flow. 3-Firing Temp. 4-Air/Ratio. 5-CO. 6-O2. 7-Fuel Flow. 8-Compr. Inlet Air Flow. 9-Relative Humidity. 10-Compr. Disch. Temp.											
# of Hidden Neurons	10	15	21	25	30	35	40	42	45	46	50	
Number of Epoch	199	364	337	274	152	180	129	209	305	394	267	
Time (s)	11	28	28	26	17	23	19	32	51	68	51	
Training	MSE	1.02465E-05	7.13057E-06	8.58867E-06	1.02415E-05	7.42338E-06	9.36768E-06	1.50418E-05	6.41128E-06	5.71278E-06	5.21947E-06	8.29231E-06
	Regression	1	1	1	1	1	1	1	1	1	1	1
Validation	MSE	1.41131E-05	9.64638E-06	1.34782E-05	1.64806E-05	1.66146E-05	2.04539E-05	1.91810E-05	9.00293E-06	1.12297E-05	7.16617E-06	1.08544E-05
	Regression	1	1	1	1	1	1	1	1	1	1	1
Testing	MSE	1.96918E-05	1.27657E-05	1.60803E-05	1.67403E-05	1.16697E-05	1.39868E-05	1.34248E-05	7.18072E-06	9.50054E-06	2.37352E-05	1.41622E-05
	Regression	1	1	1	1	1	1	1	1	1	1	1

Table 6, summarize the test results at different epoch numbers for the obtained best FFBPNN model with 42 hidden neurons. From the data in the table, we can conclude that it is not necessarily increasing the number of epochs will improve the predictability of the model nor reduce the MSE error.

Table 6 FFBPNN (10-42-1) modeling results

Number of Inputs	10											
Number of Outputs	1											
Training Data Set	1327											
Validation Data Set	285											
Testing Data Set	285											
Training Function	Levenberg-Marquardt											
Output	Nox											
Inputs	1-Load. 2-Steam Flow. 3-Firing Temp. 4-Air/Ratio. 5-CO. 6-O2. 7-Fuel Flow. 8-Compr. Inlet Air Flow. 9-Relative Humidity. 10-Compr. Disch. Temp.											
# of Hidden Neurons	42											
Number of Epoch	14	30	55	88	150	181	209	243	264	319	347	
Time (s)	2	4	8	13	23	28	32	37	41	50	53	
Training	MSE	8.25296E-05	2.27942E-05	2.01309E-05	1.44816E-05	1.26458E-05	8.25582E-06	6.41128E-06	6.73475E-06	7.08455E-06	6.82360E-06	5.43989E-06
	Regression	1	1	1	1	1	2	1	1	1	1	1
Validation	MSE	4.15426E-05	2.46499E-05	1.61459E-04	1.57613E-05	1.61035E-05	1.01808E-05	9.00293E-06	1.64339E-05	2.51457E-05	2.34209E-05	7.13885E-06
	Regression	1	1	1	1	1	2	1	1	1	1	1
Testing	MSE	1.28877E-04	2.99434E-05	1.00641E-04	3.86615E-05	1.49490E-05	1.08453E-05	7.18072E-06	1.92859E-05	2.77855E-05	1.55926E-05	2.09211E-05
	Regression	1	1	1	1	1	2	1	1	1	1	1

Figure 47, shows the performance of the FFBPNN model at different epochs number. And it was identified that the best validation performance achieved at epoch number 203. Note that, the training will be automatically stopped when the validation error increased for six consecutive iterations which occurred at epoch number 209.

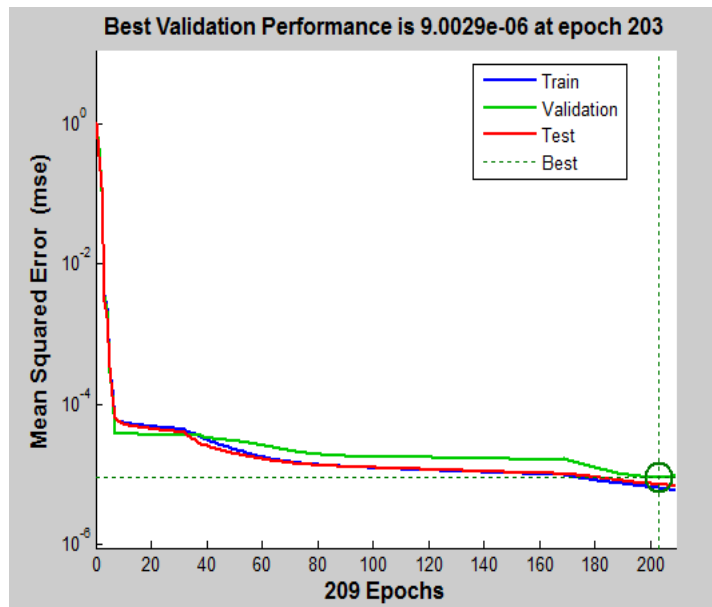


Figure 47 FFBPNN (10-42-1) Performance at different epochs number.

Figure 48, shows the spread of error on the data sets (training, validation, and testing) and its frequency. Also, it will indicate if there are any outliers in the data.

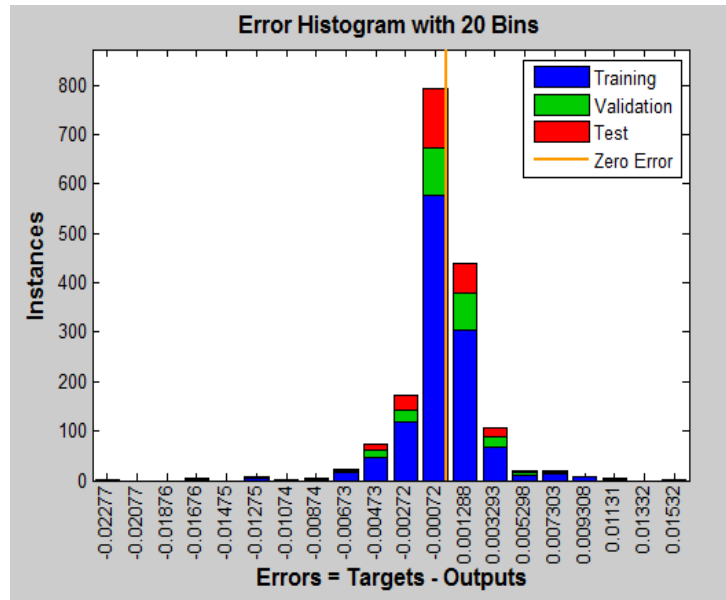


Figure 48 FFBPNN (10-42-1) Error Histogram.

Figure 49, displays the FFBPNN model output with respect to targets for training, validation, and test sets. In fact, it shows a perfect fit as all of the data sets falls along the 45 degree line, where the network outputs equal to the targets.

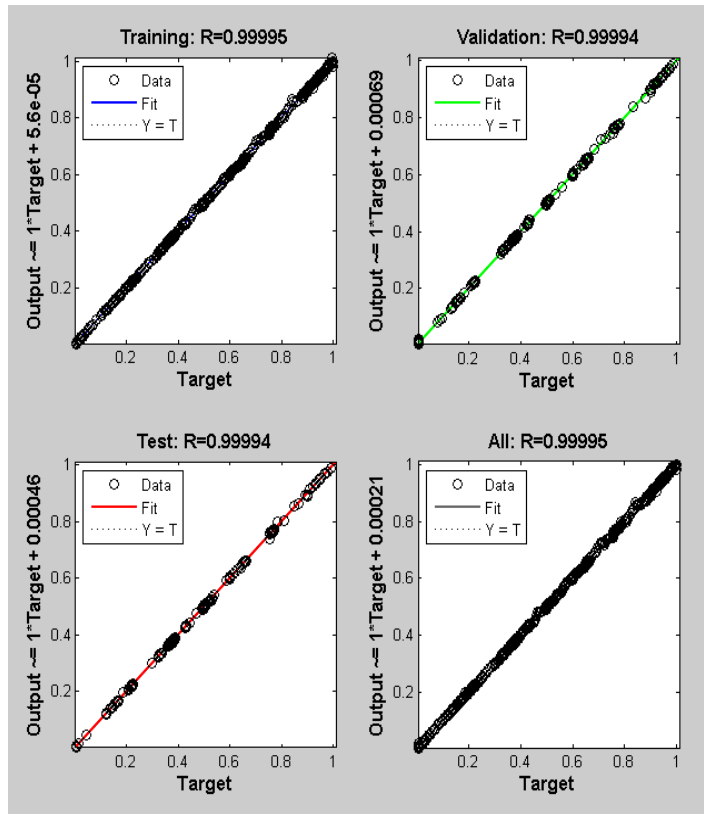


Figure 49 FFBPNN (10-42-1) Regression test.

5.3.2 FFBPNN with six inputs

Here we will test the effect of reducing the number of inputs from 10 to 6 inputs. The six inputs were selected as discussed in the ANFIS modeling section. So, the six inputs will be load, steam flow, firing temperature, air/fuel ratio, O₂, and relative humidity.

The FFBPNN modeling started initially with 10 hidden neurons and the best performance was achieved at epoch number 62. The performance was evaluated based on the MSE

error; it was E6.00469-05 for training, 4.68002E-05 for validation, and 8.19357E-05 for testing. Then, the experiments continued by increasing the number of hidden neurons by one and test it at different number of epochs by comparing the MSE errors. Table 8, summarize the results for some experiments that shows that FFBPNN model with 42 hidden neurons (6-42-1) produced the best performance at epoch number 285 with MSE error of 8.68282E-06 during training, 1.05235E-05 during validation, and 1.03641E-05 during testing. Note that, the experiments were extended till 50 hidden neurons through which the performance of the models was lower than the one obtained through 42 hidden neurons. Therefore, increasing the number of hidden neurons of the FFBPNN model will improve the predictability of the model to certain extent and then if it is increased more it will be degraded due to overfitting.

Table 7 FFBPNN (6 inputs) modeling results

Number of Inputs	6											
Number of Outputs	1											
Training Data Set	1168											
Validation Data Set	251											
Testing Data Set	251											
Training Function	Levenberg-Marquardt											
Output	Nox											
Inputs	1-Load. 2-Steam Flow. 3-Firing Temp. 4-Air/Ratio. 5-O2. 6-Relative Humidity.											
# of Hidden Neurons	10	15	20	25	30	35	37	40	42	45	50	
Number of Epoch	62	135	103	715	178	578	253	480	285	508	102	
Time (s)	3	8	6	52	14	52	23	47	31	54	11	
Training	MSE	6.00469E-05	4.95170E-05	4.00669E-05	1.83246E-05	3.17926E-05	1.14269E-05	1.90600E-05	1.86170E-05	8.68282E-06	1.40447E-05	6.94499E-05
	Regression	1	1	1	1	1	1	1	1	1	1	1
Validation	MSE	4.68002E-05	8.46156E-05	4.00480E-05	1.92923E-05	3.35030E-05	1.72799E-05	1.92439E-05	1.81473E-05	1.05235E-05	1.63410E-05	3.76672E-05
	Regression	1	1	1	1	1	1	1	1	1	1	1
Testing	MSE	8.19357E-05	6.29630E-05	5.09618E-05	2.95962E-05	4.50950E-05	6.11428E-05	2.11932E-05	2.67832E-05	1.03641E-05	2.78441E-05	5.32162E-05
	Regression	1	1	1	1	1	1	1	1	1	1	1

Table 8, summarize the test results at different epoch numbers for the obtained best FFBPNN model with 42 hidden neurons. From the data in the table, we can conclude

that it is not necessarily increasing the number of epochs will improve the predictability of the model nor reduce the MSE error.

Table 8 FFBPNN (6-42-1) modeling results

Number of Inputs	6										
Number of Outputs	1										
Training Data Set	1168										
Validation Data Set	251										
Testing Data Set	251										
Training Function	Levenberg-Marquardt										
Output	Nox										
Inputs	1-Load. 2-Steam Flow. 3-Firing Temp. 4-Air/Ratio. 5-O2. 6-Relative Humidity.										
# of Hidden Neurons	42										
Number of Epoch	15	28	49	79	124	147	227	285	383	702	
Time (s)	1	3	5	8	13	16	23	31	42	52	
Training	MSE	7.88614E-05	4.42128E-05	5.64249E-05	4.81335E-05	1.41622E-05	1.41289E-05	1.20763E-06	8.68282E-06	9.90038E-06	7.92187E-06
	Regression	1	1	1	1	1	1	1	1	1	1
Validation	MSE	3.49700E-05	2.32920E-05	3.49768E-05	3.46466E-05	1.55414E-05	1.34938E-05	2.14011E-05	1.05235E-05	1.51720E-05	1.68911E-05
	Regression	1	1	1	1	1	1	1	1	1	1
Testing	MSE	4.18662E-05	2.51446E-04	7.06476E-05	1.58480E-04	2.48284E-05	2.01317E-05	1.24612E-05	1.03641E-05	1.94914E-05	1.80636E+05
	Regression	1	1	1	1	1	1	1	1	1	1

Note that, the error generated by the network has increased as an effect of reducing the number of inputs to six. Whereas, the MSE error figures were 6.41128E-06 for training, 9.00293E-06 for validation, and 7.18072E-06 for test data sets with 10 inputs. This has no effect on the FFBPNN model performance as it will be explained in details.

Figure 50, shows the performance of the FFBPNN model at different epochs number. And it was identified that the best validation performance achieved at epoch number 279. Note that, the training will be automatically stopped when the validation error increased for six consecutive iterations which occurred at epoch number 285.

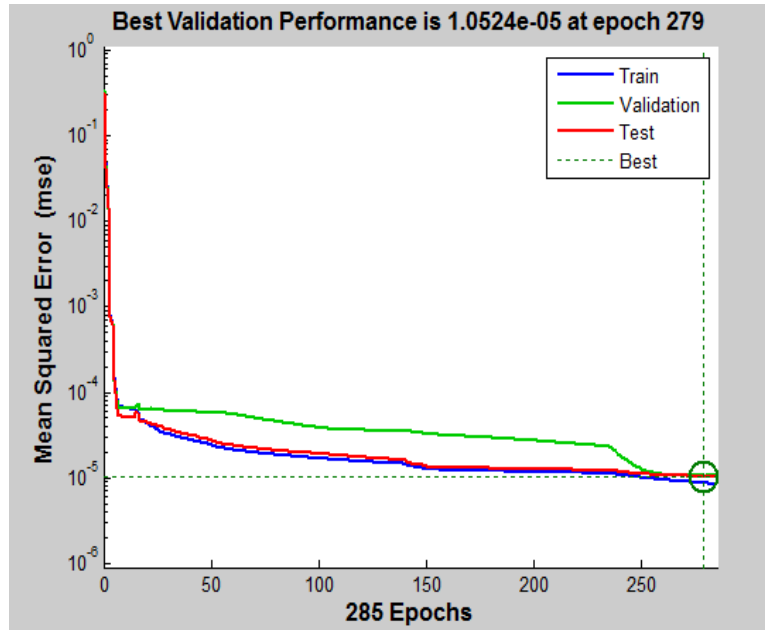


Figure 50 FFBPNN (6-42-1) Performance at different epochs number.

Figure 51, shows the spread of error on the data sets (training, validation, and testing) and its frequency. Also, it will indicate if there are any outliers in the data.

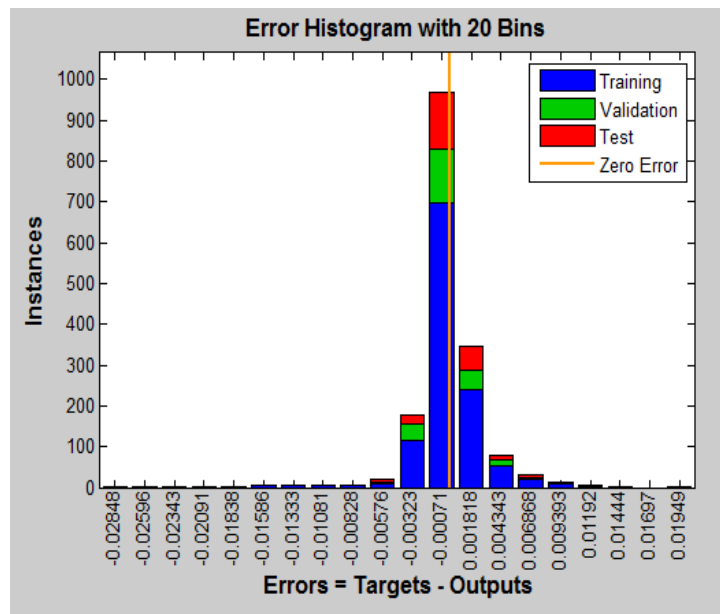


Figure 51 FFBPNN (6-42-1) Error Histogram

Figure 52, displays the FFBPNN model output with respect to targets for training, validation, and test sets. In fact, it shows a perfect fit as all of the data sets falls along the 45 degree line, where the network outputs equal to the targets.

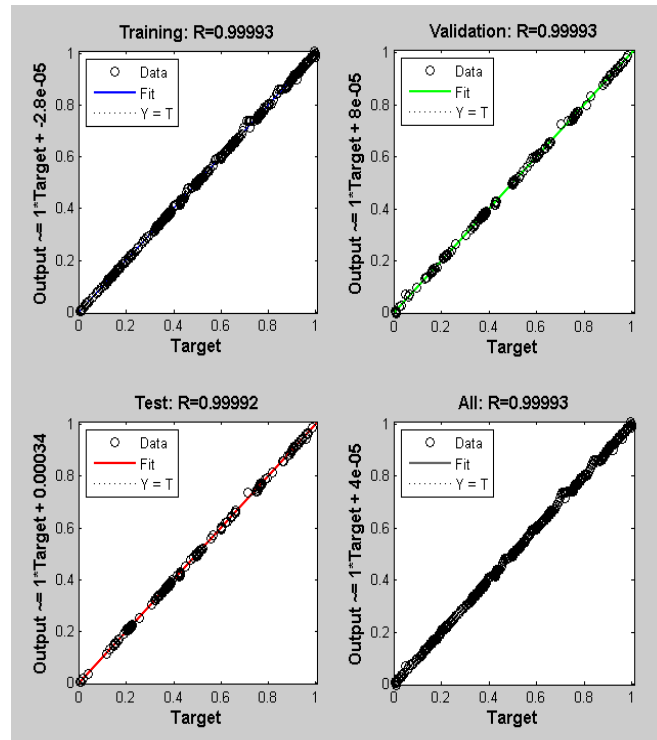


Figure 52 FFBPNN (6-42-1) Regression test.

5.3.3 FFBPNN with five inputs

Here we will test the effect of reducing the number of inputs to 5 inputs. These five inputs are load, steam flow, firing temperature, air/fuel ratio, and O2.

The FFBPNN modeling started initially with 10 hidden neurons and the experiments continued by increasing the number of hidden neurons by one and test it at different number of epochs by comparing the MSE errors. Table 9, summarize the results for some experiments that shows that FFBPNN model with 26 hidden neurons produced the best performance at epoch number 408 with MSE error of 1.39550E-05 during training, 1.68351E-05 during validation, and 1.40703E-05 during testing. Note that, the experiments were extended till 50 hidden neurons through which the performance of the models was lower than the one obtained through 26 hidden neurons. Therefore, increasing the number of hidden neurons of the FFBPNN model will improve the predictability of the model to certain extent and then if it is increased further it will be degraded due to overfitting.

Table 9 FFBPNN (5 inputs) modeling results

Number of Inputs	5											
Number of Outputs	1											
Training Data Set	1168											
Validation Data Set	251											
Testing Data Set	251											
Training Function	Levenberg-Marquardt											
Output	Nox											
Inputs	1-Load. 2-Steam Flow. 3-Firing Temp. 4-Air/Ratio. 5-O2.											
# of Hidden Neurons	10	15	20	23	25	26	30	35	38	44	50	
Number of Epoch	567	423	240	412	424	408	168	127	356	192	408	
Time (s)	40	33	20	31	33	32	13	11	32	19	46	
Training	MSE	4.81321E-05	2.23387E-05	2.13876E-05	1.59504E-05	2.10691E-05	1.39550E-05	2.39399E-05	2.92468E-05	1.85602E-05	2.68353E-05	2.42241E-05
	Regression	1	1	1	1	1	1	1	1	1	1	1
Validation	MSE	4.32047E-05	2.47006E-05	2.88771E-05	2.23225E-05	1.59333E-05	1.68351E-05	4.74704E-05	4.57172E-05	1.91742E-05	2.49979E-05	3.01892E-05
	Regression	1	1	1	1	1	1	1	1	1	1	1
Testing	MSE	1.91759E-04	2.54932E-05	3.23957E-05	2.41197E-05	3.56177E-05	1.40703E-05	2.46295E-05	4.05324E-05	2.47198E-05	3.21904E-05	4.04615E-05
	Regression	1	1	1	1	1	1	1	1	1	1	1

Table 10, summarize the test results at different epoch numbers for the obtained best FFBPNN model with 26 hidden neurons. From the data in the table, we can conclude

that it is not necessarily increasing the number of epochs will improve the predictability of the model nor reduce the MSE error.

Table 10 FFBPNN (5-26-1) modeling results

Number of Inputs	5											
Number of Outputs	1											
Training Data Set	1168											
Validation Data Set	251											
Testing Data Set	251											
Training Function	Levenberg-Marquardt											
Output	Nox											
Inputs	1-Load. 2-Steam Flow. 3-Firing Temp. 4-Air/Ratio. 5-O2.											
# of Hidden Neurons	26											
Number of Epoch	13	22	37	47	64	73	86	149	218	270	408	
Time (s)	1	1	2	3	4	5	6	11	15	19	32	
Training	MSE	1.20857E-04	7.08338E-05	1.10163E-04	9.58456E-05	5.03909E-05	3.70135E-05	5.17786E-05	4.06549E-05	2.99877E-05	2.03805E-05	1.39550E-05
	Regression	1	1	1	1	1	1	1	1	1	1	1
Validation	MSE	2.40135E-04	8.25497E-05	5.60614E-05	5.29365E-05	5.48290E-05	9.60989E-05	3.89467E+05	5.22905E-05	5.40899E-05	4.91949E-05	1.68351E-05
	Regression	1	1	1	1	1	1	1	1	1	1	1
Testing	MSE	7.80445E-05	4.42150E-04	7.65049E-05	1.41740E-04	3.12766E-04	5.63260E-05	3.79554E+05	5.30453E-05	6.69341E-05	7.18287E-05	1.40703E-05
	Regression	1	1	1	1	1	1	1	1	1	1	1

Note that, the error generated by the network has increased slightly as an effect of reducing the number of inputs to five. Whereas, the MSE error figures were 8.68282E-06 for training, 1.05235E-05 for validation, and 1.03641E-05 for test data sets with 6 inputs. This has no effect on the FFBPNN model performance as it will be explained in details.

Figure 53, shows the performance of the FFBPNN model at different epochs number. And it was identified that the best validation performance achieved at epoch number 402. Note that, the training will be automatically stopped when the validation error increased for six consecutive iterations which occurred at epoch number 408.

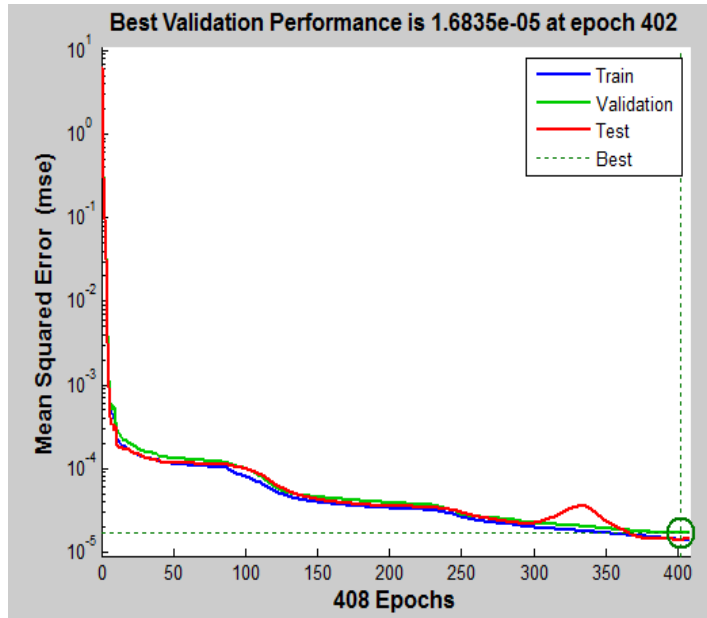


Figure 53 FFBPNN (5-26-1) Performance at different epochs number

Figure 54, shows the spread of error on the data sets (training, validation, and testing) and its frequency. Also, it will indicate if there are any outliers in the data.

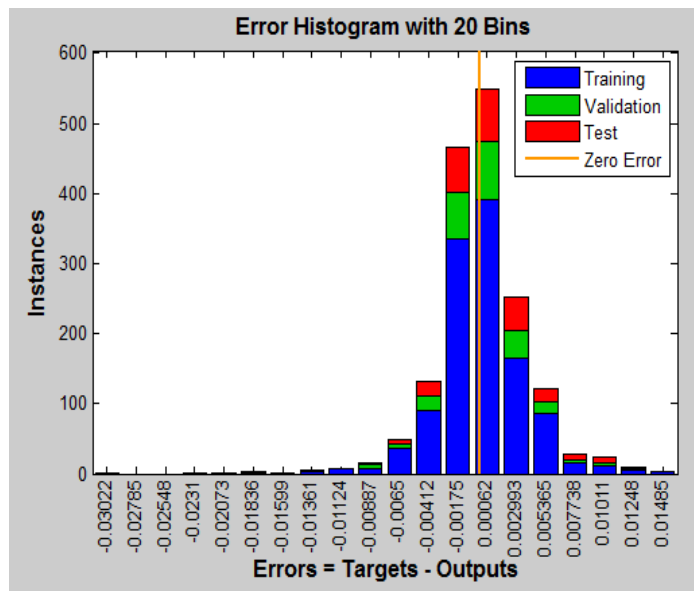


Figure 54 FFBPNN (5-26-1) Error Histogram

Figure 55, displays the FFBPNN model output with respect to targets for training, validation, and test sets. In fact, it shows a perfect fit as all of the data sets falls along the 45 degree line, where the network outputs equal to the targets.

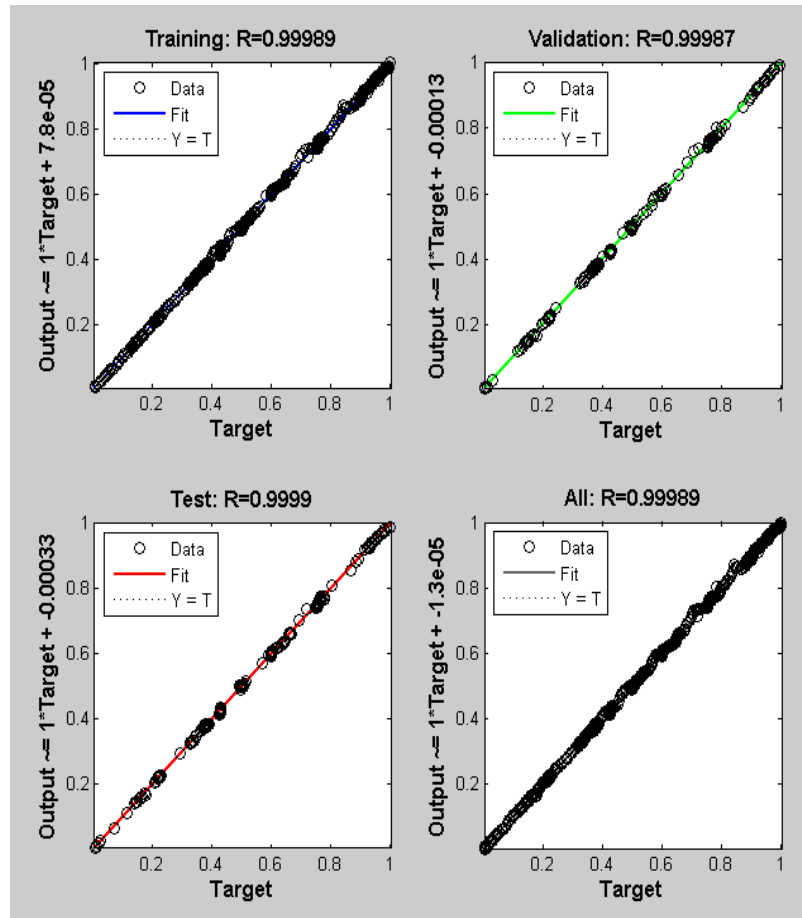


Figure 55 FFBPNN (5-26-1) Regression test

5.3.4 FFBPNN with four inputs

Here we will further reduced the number of inputs to four and study the effect on the performance. These four inputs are load, steam flow, firing temperature, and air/fuel ratio.

The FFBPNN modeling started initially with 10 hidden neurons and the experiments continued by increasing the number of hidden neurons by one and test it at different number of epochs by comparing the MSE errors. Table 11, summarize the results for some experiments that shows that FFBPNN model with 45 hidden neurons (4-45-1) produced the best performance at epoch number 743 with MSE error of 1.59912E-05 during training, 1.79788E-05 during validation, and 2.36345E-05 during testing. Note that, the experiments were extended till 50 hidden neurons through which the performance of the models was lower than the one obtained through 26 hidden neurons. Therefore, increasing the number of hidden neurons of the FFBPNN model will improve the predictability of the model to certain extent and then if it is increased further it will be degraded due to overfitting.

Table 11 FFBPNN (4 inputs) modeling results

Number of Inputs	4											
Number of Outputs	1											
Training Data Set	1168											
Validation Data Set	251											
Testing Data Set	251											
Training Function	Levenberg-Marquardt											
Output	Nox											
Inputs	1-Load. 2-Steam Flow. 3-Firing Temp. 4-Air/Ratio.											
# of Hidden Neurons	10	15	20	25	26	30	35	37	40	45	50	
Number of Epoch	108	197	90	306	635	730	487	570	551	743	759	
Time (s)	5	11	5	21	44	53	40	48	48	70	82	
Training	MSE	6.55236E-05	5.57972E-05	5.00539E-05	4.67836E-05	1.81611E-05	1.33665E-05	1.44448E-05	1.64131E-05	2.03926E-05	1.59912E-05	2.69794E-05
	Regression	1	1	1	1	1	1	1	1	1	1	1
Validation	MSE	7.37558E-05	4.70475E-05	5.19379E-05	3.98462E-05	2.70413E-05	2.35397E-05	1.53056E-05	1.91742E-05	2.46235E-05	1.79788E-05	3.25968E-05
	Regression	1	1	1	1	1	1	1	1	1	1	1
Testing	MSE	8.39653E-05	8.89236E-05	7.40498E-05	4.81743E-05	1.95561E-05	2.92109E-05	5.27026E-05	2.47198E-05	2.83207E-05	2.36345E-05	5.09799E-05
	Regression	1	1	1	1	1	1	1	1	1	1	1

Table 12, summarize the test results at different epoch numbers for the obtained best FFBPNN model with 45 hidden neurons. From the data in the table, we can conclude

that it is not necessarily increasing the number of epochs will improve the predictability of the model nor reduce the MSE error.

Table 12 FFBPNN (4-45-1) modeling results

Number of Inputs	4											
Number of Outputs	1											
Training Data Set	1168											
Validation Data Set	251											
Testing Data Set	251											
Training Function	Levenberg-Marquardt											
Output	Nox											
Inputs	1-Load. 2-Steam Flow. 3-Firing Temp. 4-Air/Ratio.											
# of Hidden Neurons	45											
Number of Epoch	18	31	51	134	198	278	354	429	454	500	743	
Time (s)	1	3	5	13	20	28	35	43	45	50	70	
Training	MSE	9.47212E-05	9.92558E-05	6.64225E-05	5.03553E-05	4.15858E-05	3.26050E-05	1.55885E-05	1.99351E-05	1.31099E-05	2.64590E-05	1.59912E-05
	Regression	1	1	1	1	1	1	1	1	1	1	1
Validation	MSE	4.02218E-04	2.25772E-05	8.77928E-05	5.39398E-05	4.80080E-05	2.82941E-05	1.94245E-05	3.16734E-05	1.61255E-05	3.88343E-05	1.79788E-05
	Regression	1	1	1	1	1	1	1	1	1	1	1
Testing	MSE	1.96651E-04	8.58076E-05	4.31987E-05	5.06364E-05	4.16048E-05	4.27139E-05	6.02900E-04	7.61322E-05	3.13150E-05	5.50933E-05	2.36345E-05
	Regression	1	1	1	1	1	1	1	1	1	1	1

Note that, the error generated by the network has increased slightly as an effect of reducing the number of inputs to four. Whereas, the MSE error figures were 1.395512E-05 for training, 1.79788E-05 for validation, and 1.40703E-05 for test data sets with 5 inputs. This has no effect on the FFBPNN model performance as it will be explained in details.

Figure 56, shows the performance of the FFBPNN model at different epochs number. And it was identified that the best validation performance achieved at epoch number 402. Note that, the training will be automatically stopped when the validation error increased for six consecutive iterations which occurred at epoch number 408.

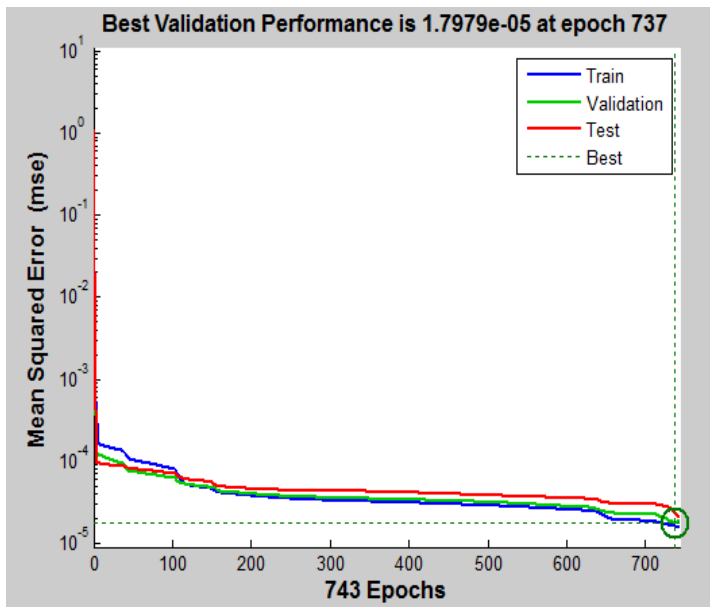


Figure 56 FFBPNN (4-45-1) Performance at different epochs number

Figure 57, shows the spread of error on the data sets (training, validation, and testing) and its frequency. Also, it will indicate if there are any outliers in the data.

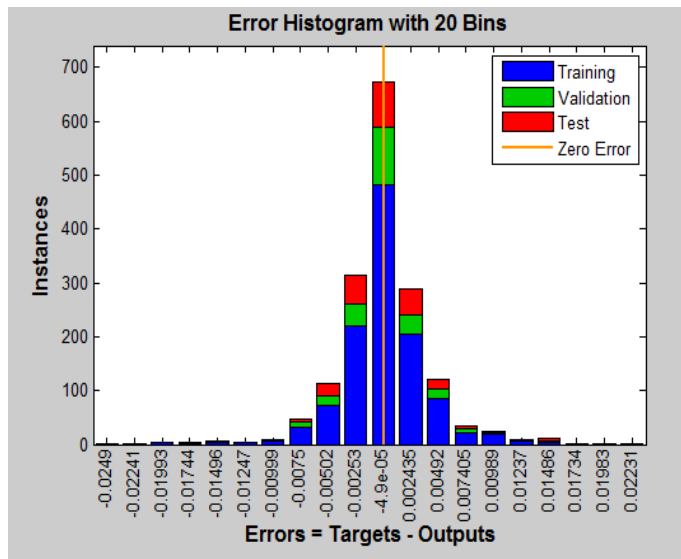


Figure 57 FFBPNN (4-45-1) Error Histogram

Figure 58, displays the FFBPNN model output with respect to targets for training, validation, and test sets. In fact, it shows a perfect fit as all of the data sets falls along the 45 degree line, where the network outputs equal to the targets.

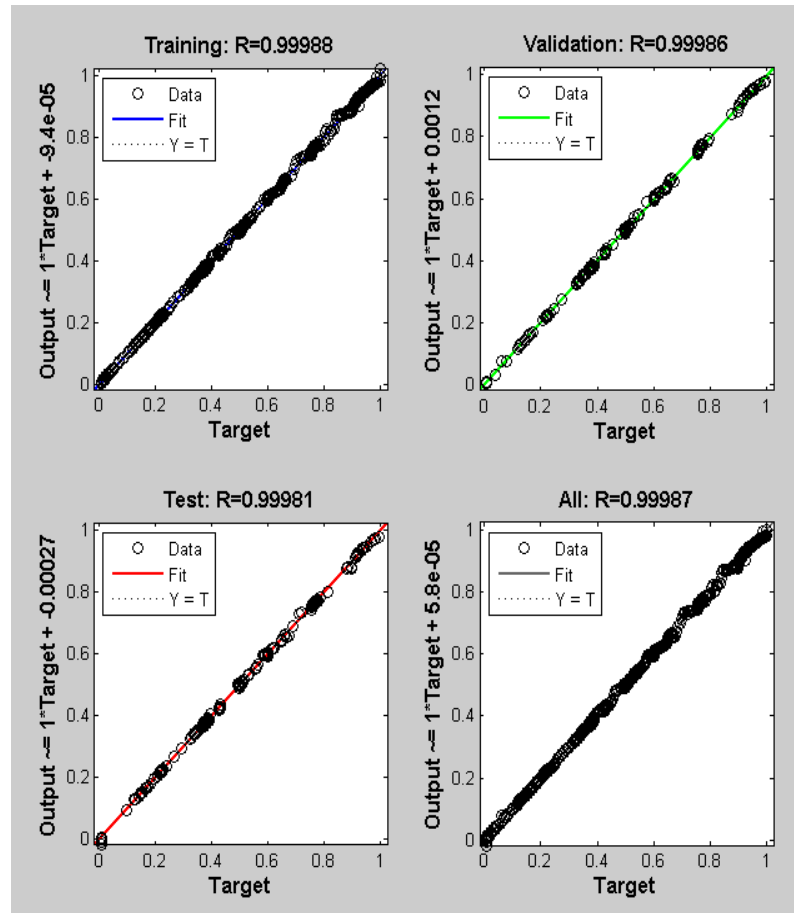


Figure 58 FFBPNN (4-45-1) Regression test

5.4 Results and Discussion

The results of the entire course of experiments conducted on different ANFIS models (6 inputs, 5 inputs, and 4 inputs tested under 4 different functions and each function at different epoch numbers) are summarized in Table 13.

Table 13 ANFIS modeling for Designing NO_x PEMS

Number of Inputs	Number of Membership Functions	Type Of Membership Function	Number of Fuzzy Rules	Total Number of Parameters	Number of Epochs	Average Testing Error
6	2*2*2*2*2	Trapezoidal	64	496	1	1.9244E-02
	3*3*3*3*3		729	5175		
	2*2*2*2*12*2	Trapezoidal	384	2776	1	3.9804E-02
	2*3*2*2*3*2	Trapezoidal	144	1064	1	2.1058E-02
	2*4*2*2*4*2	Trapezoidal	256	1856	1	3.3621E-02
5	2*2*2*2*2	Trapezoidal	32	232	6	1.8480E-02
	3*3*3*3*3	Trapezoidal	243	1518	10	3.0159E-02
	2*2*2*2*12*2	Difference Sigmoidal Product Sigmoidal	192	1232	1	1.9544E-02
	2*3*2*2*3	Trapezoidal	72	480	1	1.8564E-02
	2*4*2*2*4	Trapezoidal	128	824	3	1.9048E-02
4	2*2*2*2	Difference Sigmoidal Product Sigmoidal	16	112	28	1.8410E-02
	3*3*3*3	2-Sided Gaussian	81	453	3	2.8749E-02
	4*4*4*4	Difference Sigmoidal Product Sigmoidal	256	1344	1	1.9568E-02
	2*2*2*12	2-Sided Gaussian	96	552	2	1.7271E-02
	2*8*2*8	Difference Sigmoidal Product Sigmoidal	256	1360	3	1.7642E-02

The performance of the best ANFIS models with different number of inputs are compared against the target output in Figure 59.

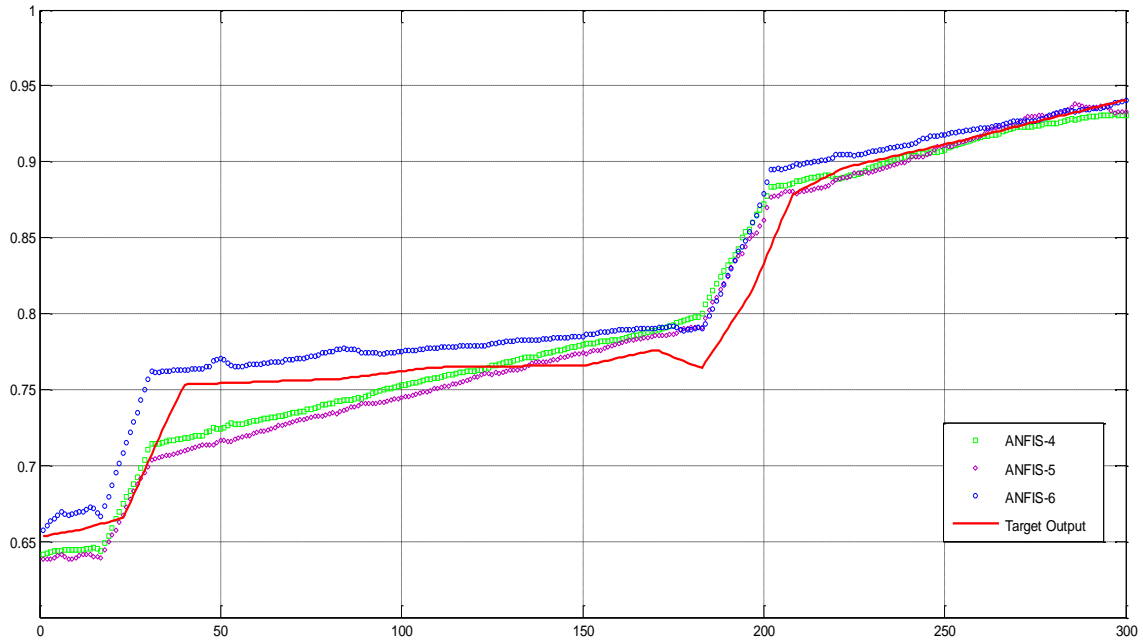


Figure 59 ANFIS models performance in reference to target output

From the above we have concluded the following:

1. Reducing the number of ANFIS inputs will improve the predictability of the model, simplify its structure by making it more concise and transparent, and reduce the computational time.

2. The proper selection of inputs is the main contributing factor with higher influence on the ANFIS performance than reducing the number of inputs. Whereas, including irrelevant inputs with weak correlation with NO_x, and inputs that depends on other inputs will degrade the ANFIS performance, complicate the structure, and increase the computational time.

Note that, the compressor discharge temperature and turbine exhaust temperature were dropped because they are dependent on the firing temperature. Also, we dropped fuel flow and compressor inlet air flow as they are already represented by the air to fuel ratio. The CO was dropped as it has weak correlation (-0.54) with NO_x. On the other hand, although the correlation with NO_x of O₂ (-0.77) and relative humidity (-0.87) is strong but it was identified from the experiments that dropping these from the inputs improved the ANFIS predictability. Note that, it was observed from the trends in the data analysis section that both O₂ and relative humidity showed no clear correlation with NO_x.

3. For designing PEMS predicting NO_x emissions from CGTG, it was identified that the optimal ANFIS model design was achieved through applying four inputs (load, steam flow, firing temperature, and air to fuel ratio).
4. The simple ANFIS structure with only two membership functions provided the best performance compared to higher number of membership functions as found for ANFIS (2*2*2*2*2*2) and ANFIS (2*2*2*2*2) as described in Table 13.
5. For four inputs, the simple ANFIS (2*2*2*2) model has developed close performance to the best model obtained which is ANFIS (2*2*2*12). It was identified in this model that the firing temperature has high influence on the NO_x prediction which is in compliance with the theory. Whereas, increasing the

number of its assigned membership functions to 12, reduced the predictability error from 0.01841 to 0.017271 as shown in Table 13.

The results of the entire course of experiments conducted on different FFBPNN models (10 inputs, 6 inputs, 5 inputs, and 4 inputs tested under different number of hidden neurons and epoch numbers) are summarized in Table 14.

Table 14 FFBPANN modeling for Designing NOx PEMS

Number of Inputs	Number of Hidden Neurons	Number of Epochs	Computational time (s)	Mean Square Error		
				Training	Validation	Testing
10	42	209	32	6.41128E-06	9.00293E-06	7.18072E-06
6	42	285	31	8.68282E-06	1.05235E-05	1.03641E-05
5	26	408	32	1.39550E-05	1.68351E-05	1.40703E-05
4	45	743	70	1.59912E-05	1.79788E-05	2.36345E-05

The performance of the best ANFIS models with different number of inputs are compared against the target output in Figure 60.

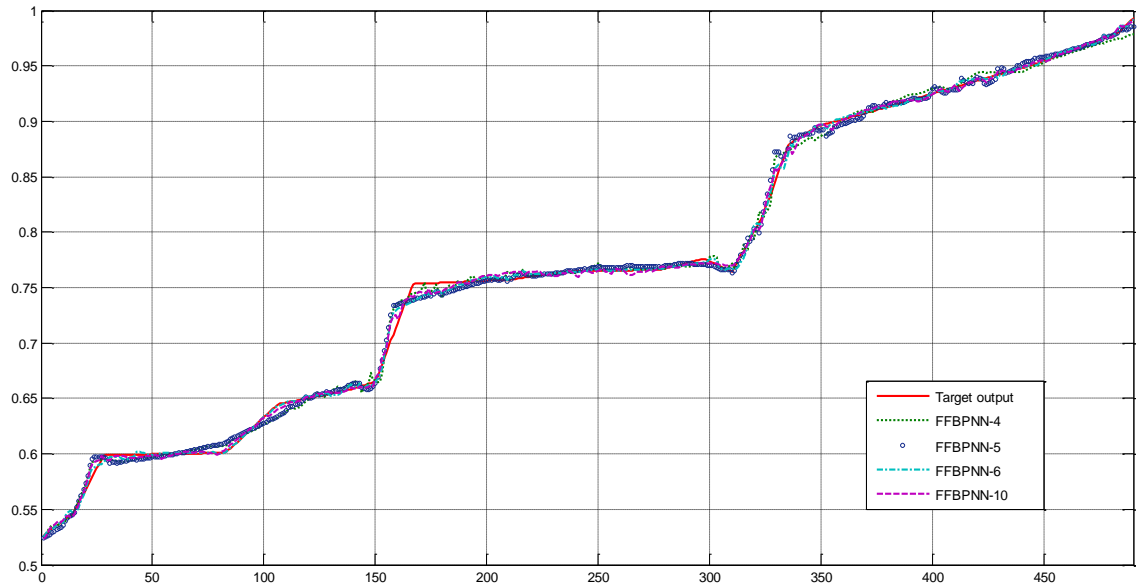


Figure 60 FFBPNN models performance in reference to target output

From the above we have concluded the following:

1. Reducing the number of FFBPNN inputs has no significant effect on the performance but it will increase the number of epochs required to develop the model as detailed on Table 14. Note that, there is no significant effect on the computational time resulted due to the increase of epochs.
2. The FFBPNN can easily adjust itself during training and adapt structures producing good performance with the provided data regardless of their number, their correlation strength with NO_x , and weather they are dependent inputs or not.

3. The FFBPNN models developed with 10, 6, 5, and 4 inputs generated lower errors as compared to the models developed by ANFIS as detailed on Table 15 and following regression Figures (59-65).

The performance of both FFBPNN and ANFIS models were discussed in details and compared on the above discussion. The modelling of both FFBPNN and ANFIS techniques are compared in Table 16, in terms of accuracy, modelling efforts, limitation on number of outputs, performance sensitivity to number and type of inputs, indication of highly influencing inputs, and modelling approach.

Table 15 Performance Comparison between FFBPNN & ANFIS models

Inputs	NN Type	FFBPNN	ANFIS
Four	Structure	45 Hidden neurons	2*2*2*12 membership functions
	Regression Test	0.99983	0.99901
	Maximum Absolute Error (MAE)	4.92 ppmvd	9.8 ppmvd
	Mean Square Error (MSE)	0.003 ppmvd	2.24 ppmvd
Five	Structure	26 Hidden neurons	2*2*2*2*2 membership functions
	Regression Test	0.99992	0.99908
	Maximum Absolute Error (MAE)	4.93 ppmvd	8.73 ppmvd
	Mean Square Error (MSE)	0.0014 ppmvd	2.4 ppmvd
Six	Structure	42 Hidden neurons	2*2*2*2*2*2 membership functions
	Regression Test	0.99994	0.99433
	Maximum Absolute Error (MAE)	6.29 ppmvd	15.53 ppmvd
	Mean Square Error (MSE)	0.001 ppmvd	2.49 ppmvd
Ten	Structure	42 Hidden neurons	Very complicated structure beyond the PC and Matlab capability.
	Regression Test	0.99993	
	Maximum Absolute Error (MAE)	4.17 ppmvd	
	Mean Square Error (MSE)	0.0011 ppmvd	

Table 16 Comparison between FFBPNN & ANFIS modeling

	FFBPNN	ANFIS
ACCURACY	Excellent	Fair
MODELING EFFORTS	Moderate	Major
NUMBER OF OUTPUTS	No limitation	Only one
PERFORMANCE SENSITIVITY TO NUMBER & TYPE OF INPUTS	Negligible impact	Major impact
INDEICATION OF HIGHLY INFLUENCING INPUTS	No	Yes
MODELING APPROACH	Trial & error (# hidden neurons, # epoch, & inputs)	Trial & error (Type of membership function, # membership functions, # epoch, & inputs)

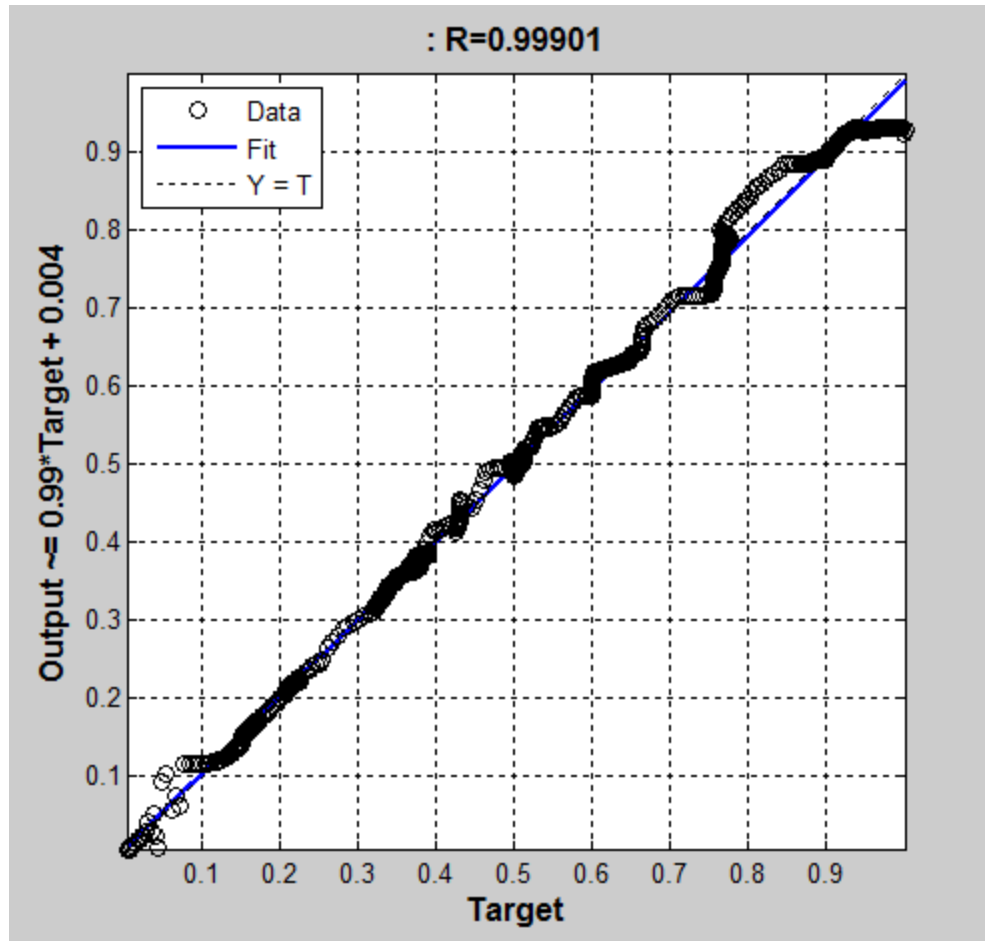


Figure 61 ANFIS (4 inputs-2*2*2*12) Regression test.

```
abs_error4=abs(Target_reg-anfis4_output);
```

```
>> [max_abs_error4, maxpt]=max(abs_error4)
```

```
max_abs_error4 =
```

```
0.0756
```

```
maxpt =
```

```
1663
```

```
>> MSE4=mean(abs_error4.^2)
```

MSE4 =

1.3886e-04

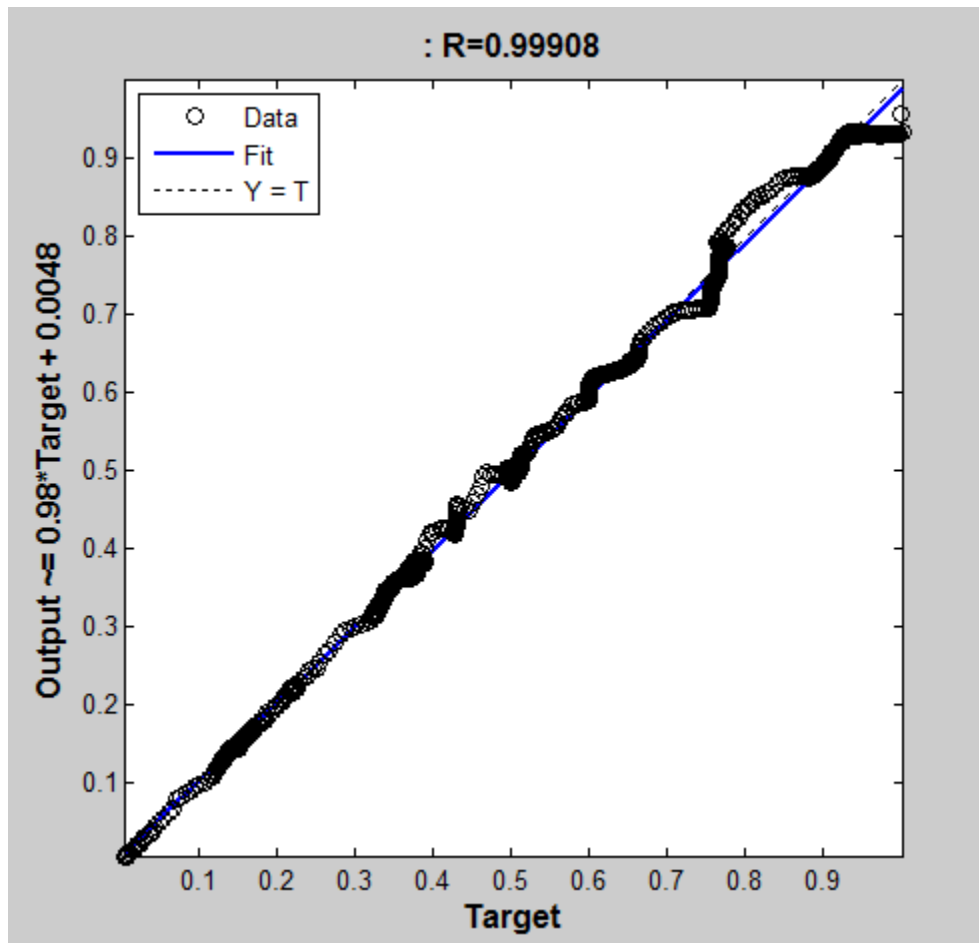


Figure 62 ANFIS (5 inputs-2*2*2*2) Regression test.

```
>> abs_error5=abs(Target_reg-anfis5_output);
```

```
>> [max_abs_error5, maxpt]=max(abs_error5)
```

max_abs_error5 =

0.0674

maxpt =

1664

```
>> MSE5=mean(abs_error5.^2)
```

MSE5 =

1.3851e-04

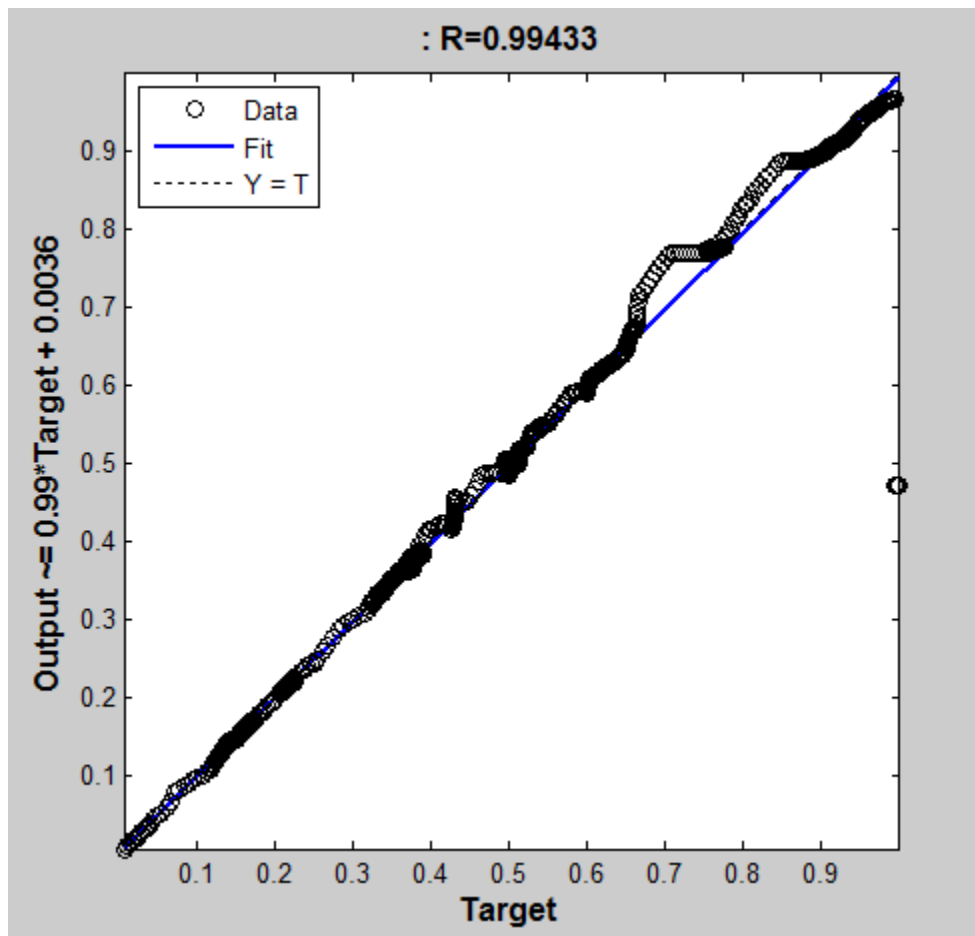


Figure 63 ANFIS (6 inputs-2*2*2*2*2) Regression test.

```
>> abs_error6=abs(Target_reg-anfis6_output);
```

```
>> [max_abs_error6, maxpt]=max(abs_error6)
```

```
max_abs_error6 =
```

```
0.5266
```

```
maxpt =
```

```
1664
```

```
>> MSE6=mean(abs_error6.^2)
```

```
MSE6 =
```

```
7.3785e-04
```

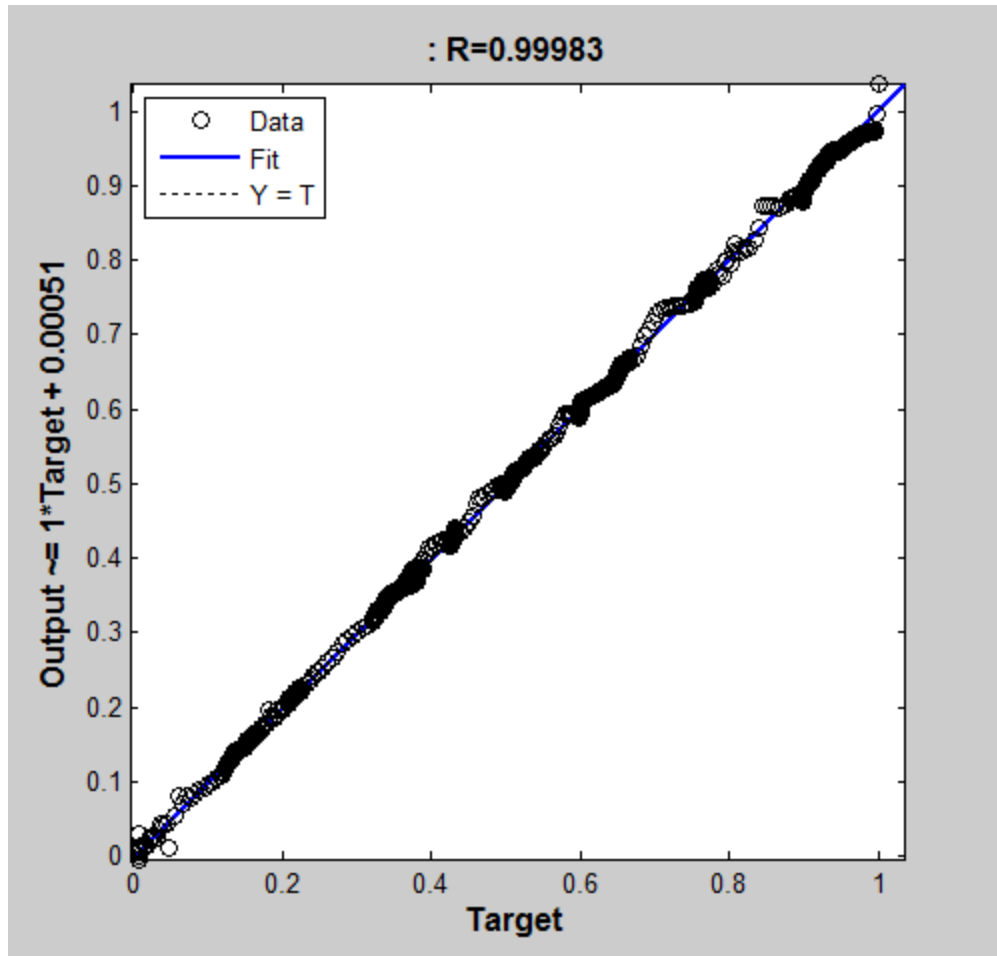


Figure 64 FFBPNN (4-45-1) Regression test.

```
>> abs_error4=abs(Target_reg-FFBPNN4_output);
```

```
>> [max_abs_error4, maxpt]=max(abs_error4)
```

```
max_abs_error4 =
```

```
0.0380
```

```
maxpt =
```

```
130
```

```
>> MSE4=mean(abs_error4.^2)
```

MSE4 =

2.1905e-05

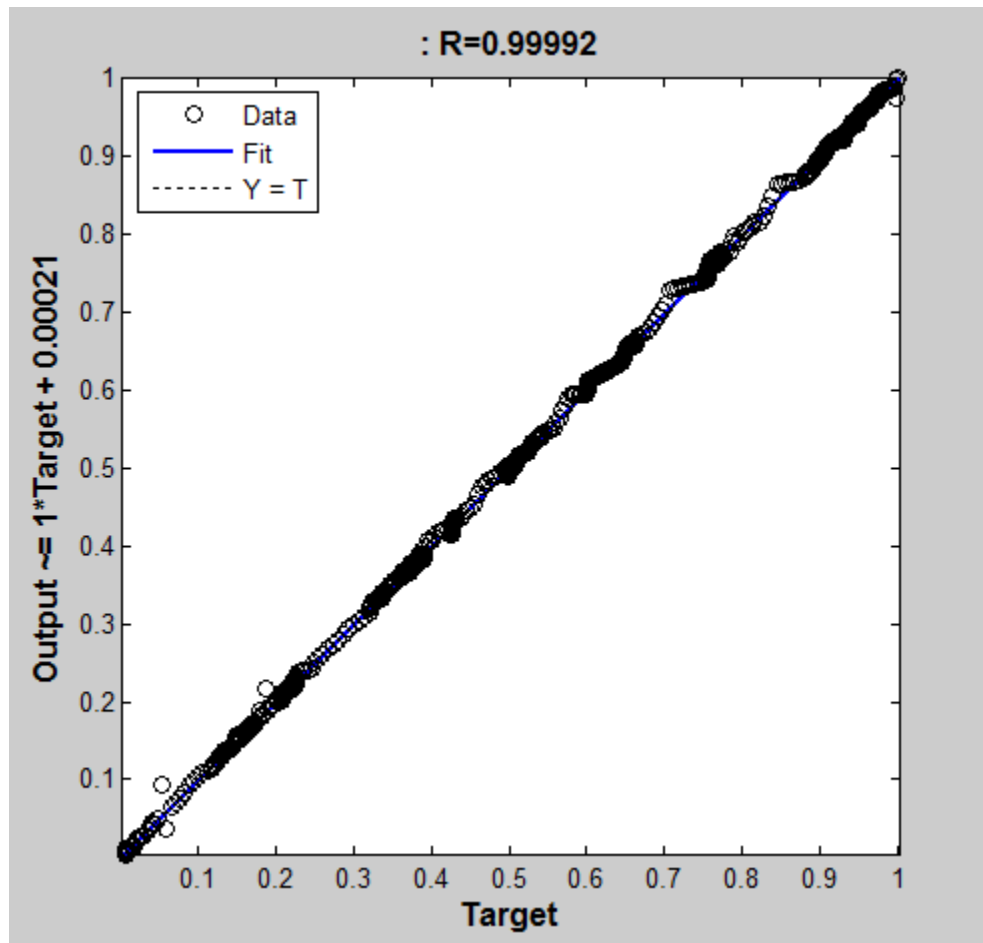


Figure 65 FFBPNN (5-26-1) Regression test.

```
>> abs_error5=abs(Target_reg-FFBPNN5_output);
```

```
>> [max_abs_error5, maxpt]=max(abs_error5)
```

max_abs_error5 =

0.0381

maxpt =

131

```
>> MSE5=mean(abs_error5.^2)
```

MSE5 =

1.0906e-05

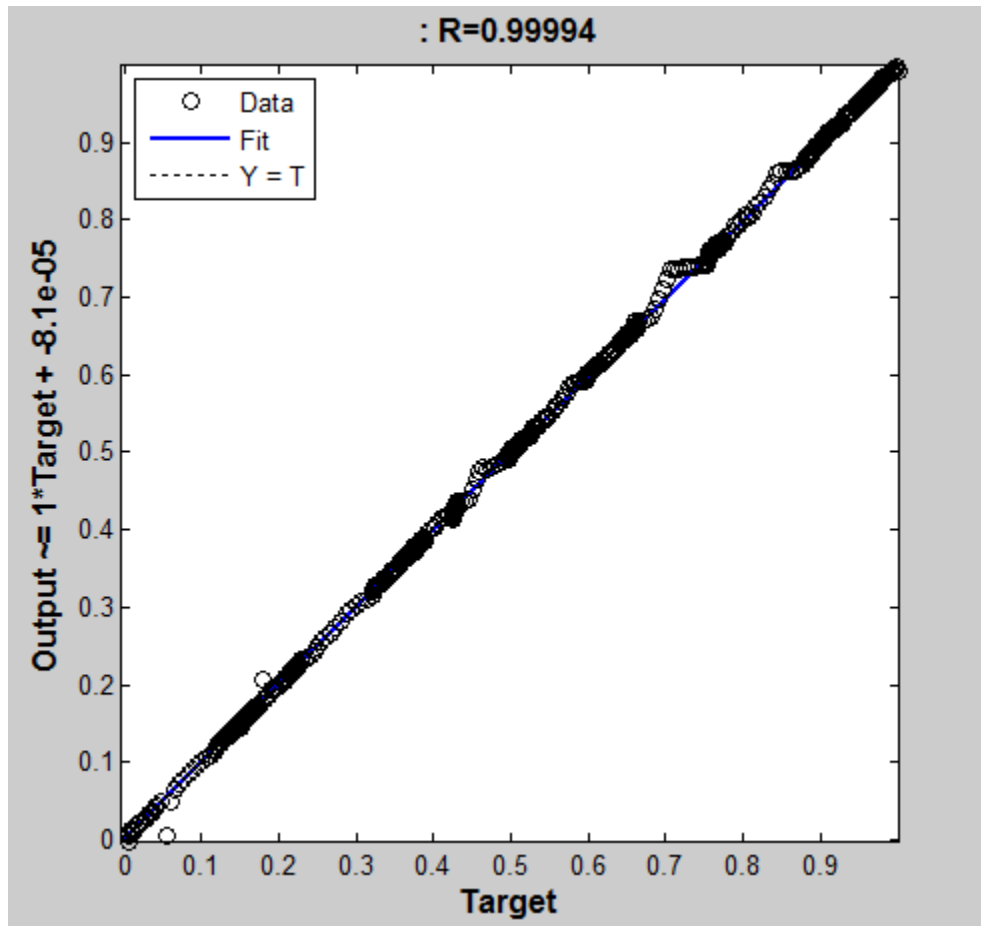


Figure 66 FFBPNN (6-42-1) Regression test.

```
>> abs_error6=abs(Target_reg-FFBPNN6_output);
```

```
>> [max_abs_error6, maxpt]=max(abs_error6)
```

```
max_abs_error6 =
```

```
0.0486
```

```
maxpt =
```

```
131
```

```
>> MSE6=mean(abs_error6.^2)
```

```
MSE6 =
```

```
7.6531e-06
```

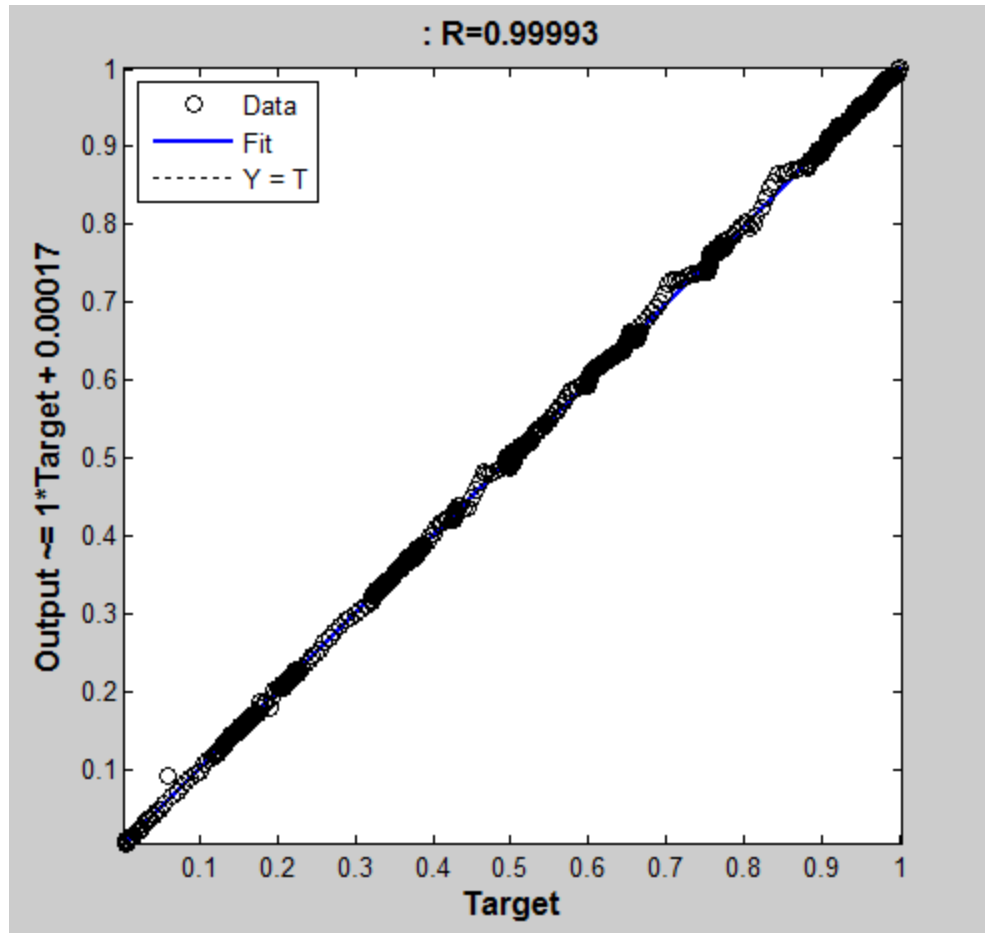



Figure 67 FFBPNN (10-42-1) Regression test.

```
>> abs_error10=abs(Target_reg-FFBPNN10_output);
```

```
>> [max_abs_error10, maxpt]=max(abs_error10)
```

```
max_abs_error10 =
```

```
0.0322
```

```
maxpt =
```

```
132
```

```
>> MSE10=mean(abs_error10.^2)
```

```
MSE10 =
```

```
8.6909e-06
```

CHAPTER 6

CONCLUSION

In this thesis we developed NO_x soft analyzer (PEMS) for heavy duty CGTG (155.5 MW) during start up based on real industrial process data. Two approaches in NN were tested to develop and decide the final model based on the obtained performance. Extensive analysis and study of the ANFIS system performance were conducted in reference to the number of inputs, type of inputs, number of membership function, type of membership function, and number of training epoch. Also, FFBPNN system went through similar study in reference to the number of inputs, type of inputs, number of hidden neurouns, and number of training epoch

Then, we discussed and compared the modeling of both FFBPNN & ANFIS systems and their obtained results. Throughout the entire course of experiments it was found that the FFBPNN model outperforms the ANFIS model. Also, it was found increasing the number of inputs to ANFIS model will degrade its performance in addition to complicating the model structure and increasing the computational time. However, in FFBPNN model, the performance enhanced slightly as an effect of increasing number of inputs. Based on that, it was concluded that FFBPNN model with four inputs (Load, Steam flow, Firing temperature, and A/F) shall be selected as the final PEMS model with the consideration of decreasing the number of inputs decreases the points of failure of the model. Note that, these inputs are individual field instruments and subject to failure and

drifts. Therefore, it is recommended to reduce the number of inputs to minimum and only primary inputs shall be included. In fact, this model will depend on five instruments not four as air to fuel ration is actually a two instruments data combined as one input.

The NO_x formation in DLN-2.6 combustors during startup and low loads (< 50%) is still high and shall be closely monitored and minimized. As future work, this model could be extended by collecting more data to cover the emissions at 50% to base load with and without supplementary firing. The suggested additional inputs will be supplementary firing temperature, 6Q combustion mode switch "0 or 1", and supplementary firing switch "0 or 1".

References

- Azid I., Ripin Z., Aris M., Ahmad A., Seetharamu K., Yusoff R** (2000), "Predicting Combined-Cycle Natural Gas Power Plant Emissions by Using Artificial Neural Networks". IEEE 2000; III:512-517.
- Bartolini C., Caresana F., Comodi G., Pelagalli L., Renzi M., & Vagni S.** (2011), "Application of artificial neural networks to micro gas turbines". ELSEVIER; Energy Conversion and Management 2011; 52:781-788.
- Boyce M.**, Gas Turbine Engineering Handbook. 2nd edition. Houston: Gulf Professional Publishing; 2002.
- Chong A., Wilcox S., & Ward J.** (2001), "Prediction of gaseous emissions from a chain grate stoker boiler using neural networks of ARX structure". IEEE; Proceedings of Science, Measurement and Technology 2001; 148 (3): 95-102.
- Ciccone A., Cinnamon C., & Niejadlik P.** (2005), "Artificial Neural Network-Based Predictive Emission Monitoring System for NOx Emissions". IAGT; 05-IAGT-2.4: 1-24.
- Chuanbau Liu Y & Fuwu Y.** (2011), "Radical Basis Function Neural Network-Based NOx Soft Sensor Technique". IEEE 2011; 1152-1156.
- Davis L. & Black S.** (2010), "Dry Low NOx Combustion Systems for GE Heavy-Duty Gas Turbines". GE Power Systems; GER-3568G (10/00): 1-22.
- Dong D. & McAvoy T.** (1995), "Emission Monitoring Using Multivariate Soft Sensors". American Control Conference; 761-765.
- Dvorak R., Chlapek P., Jecha D., Puchyr R., & Stehlik P.** (2010), "New approach to common removal of dioxins and NOx as a contribution to environmental protection". ELSEVIER; Journal of Cleaner Production 2010; 18:881-888.
- Eddy C. & Haining G.** (2010), "Estimation of NOx emissions from coal-fired utility boilers". ELSEVIER; Fuel 2010; 89: 2977-2984.
- Elangeshwaran P., Rosdiazli I., Vijanth A.** (2011), "Development of Predictive Emission Models for Various Applications using ANN". IEEE 2011; pp. 144-148.
- Energy Efficiency Office**, Introduction to Large-scale Combined Heat and Power Good Practice Guide No. 43. UK; 1992.

Environmental Protection Agency, 2011, <http://www.epa.gov/air/nitrogenoxides/> (04 Apr 2011).

Farquad M., Ravi V., & Raju S. (2010), "Support vector regression based hybrid rule extraction methods for forecasting". ELSEVIER; Expert Systems with Applications 2010; 37: 5577-5589.

Fast M., Assadi M., & De S. (2009), "Development and multi-utility of an ANN model for an industrial gas turbine". ELSEVIER; Applied Energy 2009; 86: 9-17.

Fenimore, C.P., "Formation of Nitric Oxide in Premixed Hydrocarbon Flames," Proceedings of the 13th Symposium (International) on Combustion, pp. 373-380, The Combustion Institute, Pittsburg, PA, 1971.

Ferretti G, Piroddi L. (2001), "Estimation of NO_x emissions in thermal power plants using artificial neural networks". Journal of Engineering for Gas Turbines & Power; ASME 2001; 123(2): 465-471.

Fichet V., Kanniche M., Plion P., & Gicquel O (2010), "A reactor network model for predicting NO_x emissions in gas turbines". ELSEVIER; Fuel 2010; 89:2202-2210.

Gobbato P., Masi M., Toffolo A., Lazzaretto A., & Tanzini G. (2012), "Calculation of the flow field and NO_x emissions of a gas turbine combustor by a coarse computational fluid dynamics model". ELSEVIER; Energy 2012; 45: 445-455.

Graziani S., Pitrone N., Xibilia M., & Barbalace N. (2004), "Improving monitoring of NO_x emissions in refineries". IEEE; Instrumentation and Measurement Technology Conference 2004; 594-597.

Guoqiang L., Peifeng N., Chao L., & Weiping Z. (2012), "Enhanced combination modeling method for combustion efficiency in coal-fired boilers". ELSEVIER; Applied Soft Computing 2012; 12: 3132-3140.

Habib M, Elshafei M, Dajani M. (2007), "Influence of combustion parameters on NO_x production in an industrial boiler". Science Direct; Computers & Fluids 2008; 37: 12-23.

Habib M., Elshafei M., & Dajani M. (2007), "Influence of combustion parameters on NO_x production in an industrial boiler". ELSEVIER; Computers & Fluids 2008; 37:12-23.

Haykin S., Neural networks: a comprehensive foundation. New York: Macmillan; 1994.

Hung, W.S. and Langenbacher, F., "PEMS: Monitoring NO_x Emissions From Gas Turbines," ASME Paper 95-GT-415, 1995.

Ikonen E., Najim K., & Kortela U. (2000), “Neuro-fuzzy modelling of power plant flue-gas emissions”. ELSEVIER; Engineering Applications of Artificial Intelligence 2000; 13: 705-717.

Jang J., “ANFIS: Adaptive-Network-Based Fuzzy Inference System,” IEEE Trans. Systems, Man, and Cybernetics, vol. 23, no. 3, pp. 665-684, May/June 1993.

Jang J. and Sun C., “Neuro-Fuzzy Modeling and Control,” Proc. IEEE, vol. 83, no. 3, pp. 378-406, Mar. 1995.

Kalogirou S. (2003), “Artificial intelligence for the modeling and control of combustion processes: a review”. Science Direct; Progress in Energy and Combustion Science 2003; 29: 515-566.

Kamas J. & Keeler J. (1995), “Predictive Emissions Monitoring Systems: A Low-Cost Alternative for Emissions Monitoring”. IEEE; 1995; 497-509.

Kang Li S. (2000), “A Cascaded Neural Network and Its Application to Modelling Power Plant Pollutant Emission”. IEEE; 3rd World Congress on Intelligent Control and Automation 2000; 992-997.

Kesgin U. (2003), “Genetic algorithm and artificial neural network for engine optimization of efficiency and NOx emission”. ELSEVIER; Fuel 2004; 83: 885-895.

Khaqan A. (2011), “PEMS: The Low-Cost Alternative to Emissions Monitoring”. Chemical Engineering 2011; April:28-31.

Khoshhal A., Rahimi M., & Alsairafi A. (2011), “CFD study on influence of fuel temperature on NOx emission in a HiTAC furnace”. ELSEVIER; International Communication in Heat and Mass Transfer 2011; 38: 1421-1427.

Lei-hua F., Wei-hua G., & Feng Y. (2009), “Soft-Sensor Modeling on NOx Emission of Power Station Boilers Based on Least Squares Support Vector Machines”. IEEE; 2nd International Conference on intelligent Computation Technology & Automation 2009; 462-466.

Ligang Z, Shuijun Y, Minggao Y. (2008), “Monitoring NOx Emissions from Coal-Fired Boilers using Generalized Regression Neural Network”. IEEE 2008; 43:1916-1919.

Nannariello J, Frike FR. Introduction to neural network analysis and its applications to building services engineering. Building Serv Engng Res Technol 2001;22(1): 58–68.

National Institute of Environmental Health Sciences, 2011, <http://www.niehs.nih.gov/> (04 Apr 2011)

- Reifman J. & Feldman E.** (1998), "Identification and control of NO emissions using neural networks". J. Air Waste Management Association, 1998; 48, (5), 408-417.
- Rusinowski H. & Stanek W.** (2007), "Neural modelling of steam boilers". ELSEVIER; Energy Conversion & Management 2007; 48:2802-2809.
- Shakil M., Elshafei M., Habib M., & Maleki F.** (2008), "Soft sensor for NO_x and O₂ using dynamic neural networks". ELSEVIER; Computers and Electrical Engineering 2009; 35:578-586.
- Smrekar J., Assadi M., Fast M., Kustrin I., & De S.** (2009), "Development of artificial neural network model for a coal-fired boiler using real plant data". ELSEVIER; Energy 2009; 34: 144-152.
- Specht D.** (1991), "A General Regression Neural Network". IEEE; Transactions on Neural Networks 1991; 2(No.6): 568-576.
- Toof, J.L.,** "A Model for the Prediction of Thermal, Prompt, and Fuel NO_x Emissions from Combustion Turbines," ASME Paper 85-GT-29, 1985.
- Tronci S., Baratti R., Servida A.** (2002), "Monitoring pollutant emissions in a 4.8 MW power plant through neural network". ELSEVIER; Neurocomputing 2002; 43:3-15.
- Turns, S.R.,** An Introduction to Combustion – 2nd Edition, McGraw Hill, New York, NY, 2000.
- Yap W. & Karri V.** (2012), "Emissions predictive modeling by investigating various neural network models". ELSEVIER; Expert Systems with Applications 2012; 39:2421-2426.
- Zheng L., Jia H., Yu S., & Yo M.** (2010), "Prediction of NO_x Concentration from Coal Combustion Using LS-SVR". IEEE; 2010.
- Zhou H., Cen K., & Fan J.** (2003), "Modeling and optimization of the NO_x emission characteristics of a tangentially fired boiler with artificial neural networks". ELSEVIER; Energy 2004; 2:167-183.
- Zhou H., Cen K., & Jianbo M.** (2001), "Combining neural network and genetic algorithms to optimize low NO_x pulverized coal combustion". ELSEVIER; Fuel 2001; 80: 2163-2169.

Vitae |

Name : Ali Abdullah Al-Malak

Nationality : Saudi

Date of Birth : 1/30/1976

Email : ali.malak.1@aramco.com

Address : P.O. Box 6073/Dhahran 31311/KSA

Academic Background : BS (with Dean List) from KFUPM University, KSA, in Applied Mechanical Engineering in 1998. Participated in the 6th Symposium on Industrial Systems and Control (SISC 2010) at KFUPM with paper presentation "Industrial Wireless Networks: Wireless HART & ISA 100.11.a"

Work Experience : Accumulated a unique blend of 15 years of industrial experience at different Aramco plants and involved in several upgrade projects. Currently, working with Ju'aymah NGL Fractionation Department since 2006. My area of interest includes process analyzers, flare gas flow measurements, PEMS, wireless, and solar systems.